

# REPORT DOCUMENTATION PAGE

Public reporting burden for this collection of information is estimated to average 1 hour per response, including gathering and maintaining the data needed, and completing and reviewing the collection of information. Send collection of information, including suggestions for reducing this burden, to Washington Headquarters Service, Davis Highway, Suite 1204, Arlington, VA 22202-4302, and to the Office of Management and Budget, Paper

AFRL-SR-BL-TR-00-

ces,  
this  
son

1. AGENCY USE ONLY (Leave blank)		2. REPORT DATE July 31, 2000	3. REPORT NUMBER 0457 05/15/94 - 05/14/98
4. TITLE AND SUBTITLE Photochemical Degradation Of Hazardous Chemicals In Natural Water And Soil			5. FUNDING NUMBERS F49620-94-0296
6. AUTHOR(S) Dr. John P. Hassett			
7. PERFORMING ORGANIZATION NAME(S) AND ADDRESS(ES) State University Of New York - Rsch Fnd. 1400 Washington Avenue/P.O. Box 9 Albany NY 12201			8. PERFORMING ORGANIZATION REPORT NUMBER
9. SPONSORING/MONITORING AGENCY NAME(S) AND ADDRESS(ES) Air Force Office Of Scientific Research/NA 110 Duncan Avenue, Room B115 Bolling AFB, DC 20332-8080			10. SPONSORING/MONITORING AGENCY REPORT NUMBER
11. SUPPLEMENTARY NOTES			
12a. DISTRIBUTION AVAILABILITY STATEMENT  "UNLIMITED"			12b. DISTRIBUTION CODE
13. ABSTRACT (Maximum 200 words) The aquatic photochemistry of two high-energy compounds was investigated as a part of a larger study of their environmental fate. Ammonium dinitramide (ADN) absorbs light < 400nm and degrades rapidly upon exposure to sunlight. Half-lives for the photolysis of ADN at the surface of a body of water were calculated as six minutes for a location in Syracuse, NY. However, much of the light that degrades ADN directly is absorbed in the top layer of water; the half-life at a depth of 2m was calculated as 15 years. A model of the absorption of light passing through the water column in combination with quantum yields was used in order to compare predicted and observed rates in Onondaga Lake, with good agreement. Dark solutions of ADN were stable indefinitely and indirect photolysis did not provide a significant decay mechanism. Although quadricyclane did not photolyze in distilled water, it degraded if natural dissolved organic matter (DOM) was also present. This phenomenon was ascribed to the reaction of quadricyclane with hydroperoxy (HO <sub>2</sub> ) and its conjugate base, superoxide (O <sub>2</sub> <sup>-</sup> ). The kinetics of this reaction were tested through the use of an alternative HO <sub>2</sub> /e <sup>-</sup> generator, xanthine-xanthine oxidase and a probe, ferricytochrome C. Using quadricyclane as a probe, the pH dependence of the production rate of HO <sub>2</sub> /e <sup>-</sup> was determined for a commercial humic solution. Results indicated that the predominant mechanism of formation of HO <sub>2</sub> /e <sup>-</sup> was electron transfer from an excited DOM moiety to oxygen and not the reaction of oxygen with hydrated electrons, photoejected by excited DOM.			
14. SUBJECT TERMS Photochemistry Of Hazardous Chemical In Natural Water			15. NUMBER OF PAGES 129
			16. PRICE CODE
17. SECURITY CLASSIFICATION OF REPORT	18. SECURITY CLASSIFICATION OF THIS PAGE	19. SECURITY CLASSIFICATION OF ABSTRACT	20. LIMITATION OF ABSTRACT

DTIC QUALITY INSPECTED 4

Standard Form 298 (Rev. 2-89) (EG)  
Prescribed by ANSI Std. Z39.18  
Designed using Perform Pro, WHS/DIOR, Oct 94

Final Technical Report

**Photochemistry of Hazardous Chemicals in Natural Water**

grants F49620-94-0296 and F49620-97-1-0355

to

US Air Force Office of Scientific Research

by

John P. Hassett  
Michelle M. Beretvas  
Chemistry Department  
SUNY College of Environmental Science and Forestry  
1 Forestry Drive  
Syracuse, NY 13210  
[jphasset@syr.edu](mailto:jphasset@syr.edu)  
(315) 470-6827

July 31, 2000

## Table of Contents

Table of Contents.....	ii
List of Figures.....	iv
List of Tables .....	vii
Abstract.....	viii
Chapter 1. <b>Introduction.....</b>	1
<b>Background.....</b>	4
References.....	30
Chapter 2. <b>Modeling the Photolysis of Ammonium Dinitramide</b>	
<b>in Natural Waters.....</b>	34
Abstract.....	34
Introduction.....	34
Materials and Methods.....	37
Results and Discussion.....	41
References.....	52
Chapter 3. <b>Determining the Rate constant for the Reaction of</b>	
<b>Quadricyclane with <math>\text{HOO/O}_2^-</math> .....</b>	55
Abstract.....	55
Introduction.....	56
Materials and Methods.....	62
Results and Discussion.....	64
References.....	80
Chapter 4. <b>Production rates of <math>\text{HOO/O}_2^-</math> in Aldrich Humic Solutions.....</b>	83
Abstract.....	83
Introduction.....	83
Materials and Methods.....	89
Results and Discussion.....	90
References.....	103
Chapter 5. <b>Comparison of Production Rates of <math>\text{HOO/O}_2^-</math> in four water</b>	
<b>samples using quadricyclane as a probe.....</b>	106
Abstract.....	106
Introduction.....	107
Materials and Methods.....	110
Results and Discussion.....	111
References.....	124

Conclusions.....	126
Appendices.....	128

## List of Figures

### Chapter 1.     **Introduction**

- Figure 1.1 (a) Representative resonance structures of the dinitramide ion, (b) structure of quadricyclane.....3

### Chapter 2.     **Modeling the Photolysis of Ammonium Dinitramide in Natural Waters**

- Figure 2.1 System for exposing samples to sunlight at depth in a lake. The supports are aluminium rods with clips to hold the screw-cap culture tubes.....40

- Figure 2.2 (a) Absorption spectrum of ADN  
 (b) Quantum yield for ADN photolysis  
 (c) Solar irradiance measured at noon on September 25, 1998 in Syracuse, NY  
 (d) Predicted photolysis rate constants for at the surface, using irradiance data from (c).....43

- Figure 2.3 Modeled irradiance at different depths in Onondaga Lake for surface irradiance given in Figure 2 (c).....45

- Figure 2.4 Predicted (●) and observed (○) concentrations of ADN remaining after six hour irradiation in Onondaga Lake on September 25, 1998. Error bars are 95% confidence intervals.....47

- Figure 2.5 Ratio of  $[ADN]_{obs}$  to  $[ADN]_{pred}$  for different depths in Onondaga Lake on four sampling days: (◇) 8/15/97, (□) 9/26/97, (△) 10/17/97, (○) 9/25/98.....48

### Chapter 3.     **Determining the Rate constant for the Reaction of Quadricyclane with $HOO/O_2^-$**

- Figure 3.1 The degradation of quadricyclane in an irradiated humic solution, pH 5.56 .....66  
 (▲) Zero order kinetics: [quadricyclane] vs. time,

(○) First order kinetics:  $\ln \frac{[\text{quadricyclane}]_0}{[\text{quadricyclane}]}$  vs. time

Figure 3.2 Reduction of ferricytochrome C by  $\text{HOO/O}_2^-$  at pH 7.02 in xanthine- xanthine oxidase with (□) and without (●) quadricyclane present; the curves represent the best fit to the data by non-linear regression.....69

Figure 3.3 Simulation of [quadricyclane] and  $[\text{HOO/O}_2^-]$  during enzymatic production at pH 7.02 using model with best-fit value of  $k_Q$ , the rate constant of the reaction of quadricyclane with  $\text{HOO/O}_2^-$ .....71

Figure 3.4 Variation of observed, rate constant for the reaction of quadricyclane with  $\text{HOO/O}_2^-$   $k_Q$  in enzymatic experiments. The curve represents the fit to a model that describes the variation in  $k_Q$  due to the ionization fractions of  $\text{HOO}$  and  $\text{O}_2^-$ .....73

Figure 3.5 Reduction of ferricytochrome C ( $\text{cyt}_{\text{ox}}$ ) to ferrocytochrome C ( $\text{cyt}_{\text{red}}$ ) in irradiated MilliQ water.....75

#### Chapter 4.     **Production rates of $\text{HOO/O}_2^-$ in Aldrich Humic Solutions**

Figure 4.1 Effect of quadricyclane concentration on rate of reaction of  $\text{HOO/O}_2^-$  at pH 5 (○) and pH 8 (●).....92

Figure 4.2 Variation of production of  $\text{HOO/O}_2^-$  by irradiated Aldrich humic solutions with pH..... 97

Figure 4.3 Absorbance spectra of Aldrich humic solutions ( $[\text{DOC}] = 8.5 \text{ mgL}^{-1}$ ) at pHs 3 – 11, taken in a 1 cm quartz cell..... 98

Figure 4.4 Production rate of  $\text{HOO/O}_2^-$  at pH 5.5 (○) and pH 12 (●) with varying concentrations of chloroethanol.....101

#### Chapter 5.     **Comparison of Production Rates of $\text{HOO/O}_2^-$ in four water samples using quadricyclane as a probe**

Figure 5.1 Absorbance spectra of Onondaga Lake, Cayuga Lake, Lake Ontario, an  $8.5 \text{ mgL}^{-1}$  [DOC] Aldrich humic solution. The spectra are taken in 10cm quartz cells.....113

Figure 5.2 Plots of apparent quantum yield of $\text{HOO}^{\cdot}\text{O}_2^{\cdot}$ production from irradiated samples of:	
(a) Aldrich humic solution.....	117
(b) Onondaga Lake water.....	117
(c) Cayuga Lake water.....	117
(d) Lake Ontario water.....	117

Figure 5.3 Degradation of quadricyclane in ( $\Delta$ ) Aldrich, ( $\diamond$ ) Onondaga, ( $\square$ ) Cayuga, ( $\circ$ ) Ontario water during a rooftop irradiation in the summer of 1998.....	121
---	-----

Figure 5.4 Wavelength dependence of modeled production rates of $\text{HOO}^{\cdot}\text{O}_2^{\cdot}$ for ( $\diamond$ ) Onondaga, ( $\square$ ) Cayuga, ( $\circ$ ) Ontario water using solar radiation data for summer noontime sun in Syracuse, NY.....	123
---	-----

## List of Tables

### Chapter 2.     **Modeling the Photolysis of Ammonium Dinitramide in Natural Waters**

Table 2.1 Quantum yields ( $\phi_\lambda$ ) for degradation of ADN at 285nm at four  
different temperatures in MilliQ water and humic solutions.....49

Table 2.2 Absorbances of ADN ( $A_\lambda$ ) and Aldrich humic acid ( $H_\lambda$ ) solutions  
with measured quantum yields of ADN. For the quantum yields,  
values are 95% confidence intervals.....51

### Chapter 3.     **Determining the Rate constant for the Reaction of Quadricyclane with $\text{HOO/O}_2^-$**

Table 1. Production rates of  $\text{HOO/O}_2^-$  using xanthine-xanthine oxidase at  
different pHs and relevant rate constants:  $k_{\text{dis}}$ , the rate constant for  
the dismutation of  $\text{HOO/O}_2^-$  (12),  $k_{\text{cyt}}$ , the rate constant for the  
reduction of ferricytochrome C with  $\text{HOO/O}_2^-$  (20,21), and  $k_Q$ , the  
calculated rate constant for the reaction of quadricyclane with  
 $\text{HOO/O}_2^-$ .....68

### Chapter 5.     **Comparison of Production Rates of $\text{HOO/O}_2^-$ in four water samples using quadricyclane as a probe**

Table 5.1 Attenuation coefficients ( $\alpha_\lambda$ ) and fraction of light absorbed ( $F_{s\lambda}$ ) in  
a 10 cm cell for different water samples.....114



## Abstract

The aquatic photochemistry of two high-energy compounds was investigated as a part of a larger study of their environmental fate. Ammonium dinitramide (ADN) absorbs light  $< 400\text{nm}$  and degrades rapidly upon exposure to sunlight. Half-lives for the photolysis of ADN at the surface of a body of water were calculated as ~ six minutes for a location in Syracuse, NY. However, much of the light that degrades ADN directly is absorbed in the top layer of water; the half-life at a depth of 2m was calculated as 15 years. A model of the absorption of light passing through the water column in combination with quantum yields was used in order to compare predicted and observed rates in Onondaga Lake, with good agreement. Dark solutions of ADN were stable indefinitely and indirect photolysis did not provide a significant decay mechanism.

Although quadricyclane did not photolyze in distilled water, it degraded if natural dissolved organic matter (DOM) was also present. This phenomenon was ascribed to the reaction of quadricyclane with hydroperoxy ( $\text{HOO}$ ) and its conjugate base, superoxide ( $\text{O}_2^-$ ). The kinetics of this reaction were tested through the use of an alternative  $\text{HOO}/\text{O}_2^-$  generator, xanthine-xanthine oxidase and a probe, ferricytochrome C.

Using quadricyclane as a probe, the pH dependence of the production rate of  $\text{HOO}/\text{O}_2^-$  was determined for a commercial humic solution. Results indicated that the predominant mechanism of formation of  $\text{HOO}/\text{O}_2^-$  was electron transfer from an excited DOM moiety to oxygen and not the reaction of oxygen with hydrated electrons, photoejected by excited DOM.

Additionally, the apparent quantum yields for the production of  $\text{HOO}/\text{O}_2^-$  at four different wavelengths for four water samples was determined. Values for Cayuga Lake and Lake Ontario were very similar; those for Onondaga Lake were observably different. In contrast, the values for the Aldrich humic acid solution were significantly higher, confirming that commercial humic solutions may not serve as an appropriate model of fresh water humic solutions. Indirect photolysis of quadricyclane provided a significant pathway for breakdown. Furthermore, quadricyclane was deployed effectively as a probe of  $\text{HOO}/\text{O}_2^-$  production rates in natural waters at a wide range of pHs.

## Chapter 1

### Introduction

This document is the final technical report for the research grants F49620-94-0296 and F49620-97-1-0355. It is adapted from the PhD dissertation of Michelle K. Beretvas, "Aquatic Photochemistry of Ammonium Dinitramide and Quadricyclane" (1999).

Many chemicals that are present in natural waters undergo some type of photochemical reaction. There is evidence that direct photolysis provides a substantial reaction pathway for toxic chemicals such as polycyclic aromatic hydrocarbons and various chlorinated hydrocarbons (1,2,3). In addition, a chemical may undergo an indirect or sensitized reaction where some other substance absorbs light and propagates a chemical reaction.

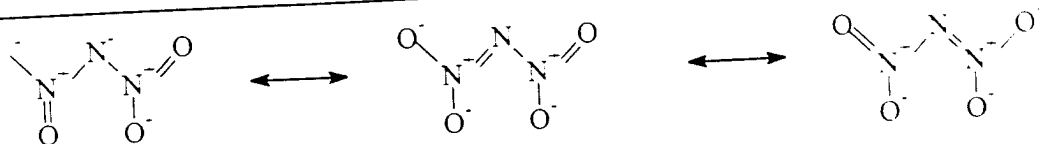
In order to understand these photochemical reactions, several parameters must be known over the range of wavelengths of interest: the intensity of light, the amount of light absorbed and the efficiency of the reaction under consideration. The intensity of incident light may be determined either through chemical actinometry or by some physical device (e.g. spectroradiometer). The behavior of light in passing through the water column may be measured or modeled through application of scattering and absorption parameters. The quantum yield for the chemical of interest should be well characterized for a range of incident intensities, temperatures and concentrations. For indirect photolysis, the appropriate parameter will actually be an apparent quantum yield that comprises the initial, light-induced steps in the reaction.

This report will deal with an example of both direct and indirect photolysis. ADN (ammonium dinitramide) undergoes rapid photolysis in distilled water solutions and this reaction is not accelerated by the presence of dissolved organic matter. An analysis of this direct photolysis is provided along with field data that compares the predicted vs. observed degradation of ADN at various depths in local lakes.

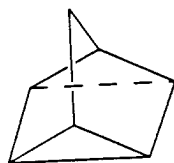
Quadricyclane is a strained hydrocarbon that had previously been suggested as a chemical energy storage species and more recently was proposed as a jet fuel. Although direct photolysis in light  $>290\text{nm}$  (the minimum wavelength reaching the earth's surface) is impossible, quadricyclane does degrade when a solution of quadricyclane and humic acid is irradiated. Experiments have shown that the hydroperoxy/superoxide radical pair produced by the photolysis of humic acids is the chemical agent responsible for this reaction. The second order rate constant for the reaction of quadricyclane with these radicals was determined at a variety of pHs, and these values were then applied to natural water studies. In this manner, the rate of production of hydroperoxy and superoxide radicals in a given body of water was calculated.

The background chapter will present some fundamental photochemical concepts that are necessary to the comprehension of the reported results. Initially, a description of the passage of light through the atmosphere and into the water column is given. Details about the kinetics of various photochemical reactions are provided in addition to the identification of some of the important photosensitizers present in

natural waters. Finally, specific information about superoxide radicals is given due to its involvement in the degradation of quadricyclane.



Representative resonance structures of the dinitramide ion:



Quadricyclane (tetracyclo[3.2.0.0.<sup>2,7</sup>0<sup>4,6</sup>]heptane:

Figure 1.1. Structures of (a) ADN, (b) Quadricyclane.

## Background

### *Sunlight:*

Before initiating discussion of the mechanism through which photochemical reactions take place at the earth's surface, it is essential to describe the characteristics of the light that is available. The intensity distribution as a function of wavelength depends on the presence of molecules that both absorb and scatter light in the atmosphere. As light enters a water body, reflection and refraction must be considered as well as the absorption and scattering within the water body itself.

The sun may be treated as a black body radiator at 6000K (4). Planck was able to describe the energy distribution of a black body radiator by considering the electromagnetic radiation of wavelength  $\lambda$  emitted by the black body to be due to the excitation of electromagnetic oscillators of wavelength  $\lambda$ . He proposed that the energy of each oscillator was limited to discrete values (i.e. quantized) (5) and that the energy density in the range of  $\lambda$  to  $\lambda + d\lambda$  is given by the Planck distribution:

$$d\xi = \rho d\lambda, \text{ where } \rho = \frac{8\pi hc}{\lambda^5} \left( \frac{1}{e^{hc/\lambda kT} - 1} \right) \quad (1)$$

where  $\xi$  is the total energy divided by the total volume (energy density),

$\rho$  is the energy density distribution,

$h$  is Planck's constant ( $6.62 \times 10^{-34}$  Js),

$c$  is speed of light *in vacuo* ( $3 \times 10^8$  ms<sup>-1</sup>), and

$k$  is Boltzmann's constant ( $1.38 \times 10^{-23}$  J K<sup>-1</sup>),

Planck's distribution of the emission of a black body radiator matched experimental curves closely and is the basis for describing the quality of light reaching the earth's surface. Superimposed on this curve are the absorption spectra of gases in the solar atmosphere - the Fraunhofer lines (4).

Solar radiation that reaches the earth's surface must pass through the earth's atmosphere. Thus, the incident irradiation is a function of time of day and year, latitude, elevation, thickness of the ozone layer and concentration of particles in the atmosphere. Ozone is particularly important in dictating the characteristics of the light in the UV-B region (280-320 nm); values for the average ozone thickness can be obtained from sources such as London (6). This light is of critical importance to humans not only in terms of causing biological damage but also in terms of causing the direct photolysis of many chemicals.

The attenuation of light in the atmosphere is due both to absorption and scattering. Computer models exist that allow prediction of solar intensities depending on time and latitude (4). The latest versions of these programs (GCSOLAR) include accurate descriptions of sky radiation in addition to seasonal and latitudinal variation in intensities (7). These models are certainly useful in predicting half-lives of chemicals, but for short-term field studies, a concurrent physical measurement of light flux is more appropriate. Neither cloud cover nor daily variation in ozone thickness is considered in most light models and yet this may be very important for a particular study.

Sunlight may also be scattered by aerosols, gaseous molecules and dust in the atmosphere. Scattering of light changes its direction but does not cause any conversion of energy. The extent of scattering is a function of wavelength. The intensity of Rayleigh scattered light, defined as scattering by particles with diameters much smaller than the wavelength of the incident light, is proportional to  $1/\lambda^4$  (5). Thus, it is most pronounced in the blue and ultraviolet regions of the spectrum. Sikorski and Zika reported that the fraction of light from the sky (that is scattered, diffuse light) is greater than 50% in the UV-B region (8).

The distinction between direct and diffuse light is important in consideration of the path length of light both in the atmosphere and also in the body of water. When solar radiation reaches the water surface, a fraction of it will be reflected. Applying Fresnel's Law, the fraction of direct light that is reflected by a flat water surface is  $< 0.1$  at all values of solar zenith angle ( $z$ ) until  $z$  approaches  $90^\circ$ . An average value for the fraction of diffuse light that is reflected is 0.07 (4); this figure was reached by treating the sky as uniformly bright. Both of these reflection parameters were determined using a refractive index ( $\eta$ ) value of 1.34 for the air to water interface. This value actually only corresponds to light of wavelength 436nm. Ideally, the variation of  $\eta$  with  $\lambda$  would be included in a model of the behavior of light, but over the wavelength range 290-400nm,  $\eta$  varies from 1.36 to 1.34 and so not much accuracy is forfeited (9).

The refraction of light as it enters a body of water determines its path length and hence the extent to which absorption takes place as a function of depth. The path length of direct light is:

$$l_d = D \sec \theta \quad (2)$$

where  $l_d$  is the path length,  $D$  is the depth and  $\theta$  is the angle of refraction, such that:

$$\eta = \frac{\sin z}{\sin \theta} \quad (3)$$

It is apparent that the path length of direct light will vary with solar zenith angle and hence latitude, local hour and the declination angle.

For diffuse light, an average path length in water may be determined by considering the sky as a luminous hemisphere of uniform brightness. Leifer describes this problem in detail (4); the result for diffuse light is that the average path length is equal to  $1.2D$ .

The absorption of light in the ocean is mostly due to the water itself and hence solar radiation in the blue region penetrates furthest (10). In bodies of fresh water, the absorption coefficient is greater due to the presence of dissolved organic matter. An exponential relationship between the absorption coefficient and wavelength has been observed in many samples of water; the absorption decreases with increasing wavelength (11,12).

Scattering is not considered to be as important of a mechanism in water for UV radiation unless the sample is exceptionally turbid. Because the size of the particles is large in comparison to the wavelength of light, the process is fairly



independent of wavelength. For most purposes, scattering in the UV region is deemed insignificant in comparison to absorption (7,10,13).

#### *Direct Photolysis:*

Direct photolysis involves the direct absorption of light and subsequent reaction by a chemical. The first law of photochemistry, the Grotthus-Draper law, states that only light that is absorbed by the reacting system can induce chemical change (14); Raman scattering is an exception to this law (5). In effect, there must be overlap in wavelength of the absorption spectrum of the chemical and the spectrum of the incident radiation. The second law, the Stark-Einstein law, dictates that each molecule that reacts must absorb one photon of light (14). Biphotonic processes, where the chromophore absorbs two photons consecutively are possible under conditions of very intense light such as lasers (15) but will not be considered any further in this paper.

The quantum yield,  $\phi_\lambda$ , designates the efficiency of a photochemical reaction:

$$\phi_\lambda = \frac{\text{moles that photoreact}}{\text{einsteins absorbed}} \quad (4)$$

where 1 einstein = 1 mole of photons, or equivalently:

$$\phi_\lambda = \frac{\text{molecules that photoreact}}{\text{photons absorbed}} \quad (5)$$

In order to define a quantum yield, the intensity of the incident light must be known, and furthermore, the exact process under consideration should be defined. A

quantum yield for the production of some end-product may be defined, as can a quantum yield for the disappearance of an initial reactant. These two values will not necessarily match, as in the case of a chain reaction.

For the photoreaction of some chemical, C irradiated by a monochromatic source:



where  $I_{a\lambda}$  is the average number of einsteins absorbed by the reactant per unit volume and per unit time. Then,

$$\text{rate of reaction} = \left( \frac{-d[C]}{dt} \right)_{\lambda} = \phi_{\lambda} I_{a\lambda} \quad (7)$$

$$I_{a\lambda} = I_{0\lambda} \left( \frac{A}{V} \right) F_{s\lambda} F_{c\lambda} \quad (8)$$

where A is the surface area of the irradiated vessel and V is the volume of that vessel, and at wavelength  $\lambda$ ,  $I_{0\lambda}$  is the intensity of the incident light (einsteins per unit area per unit time),  $F_{s\lambda}$  is the fraction of incident light absorbed by the entire system and  $F_{c\lambda}$  is the fraction of the absorbed light that is specifically absorbed by the chemical:

$$F_{s\lambda} = \left\{ 1 - 10^{-(\alpha_{\lambda} + \epsilon_{\lambda}[C])l} \right\} \quad (9)$$

$$F_{c\lambda} = \frac{\epsilon_{\lambda}[C]}{\alpha_{\lambda} + \epsilon_{\lambda}[C]} \quad (10)$$

where  $\epsilon_{\lambda}$  is the molar absorptivity of the reactant at wavelength  $\lambda$  ( $M^{-1} \text{ cm}^{-1}$ ),  $\alpha_{\lambda}$  is the attenuation coefficient of the solution in the absence of the reactant ( $\text{cm}^{-1}$ ) and  $l$  is the path length of light in the reaction vessel.

Using these basic equations, the kinetics of many photochemical reactions may be described. There are also simplifications that facilitate this process. For

instance, in a distilled water solution of chemical C,  $F_{c\lambda} = 1$  as all of the light that is absorbed by the system is in fact absorbed by C for low  $\lambda$ .

In the case of an optically thin solution, that is one where less than 2 % of the incident light is absorbed, a further simplification may be made.

$$\text{Rewriting } F_{s\lambda} = [1 - \exp\{-2.303\epsilon_{\lambda}[C]l\}] = [1 - \exp(-2.303 \text{ Ab})] \quad (11)$$

$$\text{where } \text{Ab} = \epsilon_{\lambda}[C]l \quad (\text{absorption}) \quad (12)$$

$$\text{Then for small Ab, } 1 - \exp(-2.303 \text{ Ab}) = 1 - (2.303 \text{ Ab}) + \frac{(2.303 \text{ Ab})^2}{2!} - \frac{(2.303 \text{ Ab})^3}{3!} + \dots$$

Ignoring any but the first two terms leads to:

$$F_{s\lambda} = \{1 - [2.303 \text{ Ab}]\} = 2.303 \text{ Ab} \quad (13)$$

$$\text{Hence, } \left(\frac{d[C]}{dt}\right)_{\lambda} = -2.303\epsilon_{\lambda}[C]\phi_{\lambda}I_{0\lambda}\left(\frac{A}{V}\right) \quad (14)$$

Since  $\epsilon_{\lambda}$ ,  $\phi_{\lambda}$ ,  $l$ ,  $(A/V)$ ,  $I_{0\lambda}$  are constants, this equation simplifies to a 1<sup>st</sup> order rate equation with the form:

$$\frac{-d[C]}{dt} = k[C] \quad (15)$$

and hence a plot of  $\ln[C]$  vs.  $t$  will yield a straight line with a slope equal to the first order rate constant,  $k$ :

$$k = 2.303 I_{0\lambda} \epsilon_{\lambda} \Phi_{\lambda} l (A/V) \quad (16)$$

If the incident intensity,  $I_{0\lambda}$  is known, then the quantum yield may be determined.

Another limiting case is that of an optically thick solution of one chemical; one where the fraction of light absorbed,  $F_{s\lambda}$ , may be approximated to 1. For this to occur, the absorption,  $\text{Ab}$ , should be  $>2$ . For this situation,  $F_{c\lambda} = 1$  and so the rate equation becomes:

$$-\left(\frac{d[C]}{dt}\right)_z = \phi_z I_{0z} \left(\frac{A}{V}\right) \quad (17)$$

and hence the disappearance of C is described by zero-order kinetics as long as the solution remains optically thick.

#### *Experimental Considerations:*

From the equations above, it can be seen that the quantum yield of a chemical reaction can be determined once the incident light intensity, molar absorptivity and path length of the irradiation cell are known. The molar absorptivity is easily measured using a spectrophotometer. The intensity of the incident light may be determined most conveniently through the use of chemical actinometers.

Actinometry relies on the well-described photoreaction of a reference compound under the same light conditions that are to be used in subsequent reactions. In most cases, potassium ferrioxalate as developed by Hatchard and Parker (16) is employed due to ease of use and its convenient wavelength range of 250-500nm. In this reaction, Fe(III) is reduced to Fe(II) under exposure to light; the concentration of Fe(II) is determined by monitoring the absorption at 510nm of Fe(II) phenanthroline. The determination of incident light is possible through knowledge of the quantum yield for the reduction of iron(III) and due to the optical thickness of the actinometer solution.

The final parameter that must be known is the path length of the irradiated cell. Zepp determined an experimental procedure for the measurement of the path length of a cell (17).

The photolytic rate equation for chemical C in distilled water is (*vide supra*):

$$\left( \frac{-d[C]}{dt} \right) = \phi_{\lambda} I_{0\lambda} \left( \frac{A}{V} \right) \{ 1 - 10^{-\epsilon_{\lambda}[C]l} \} \quad (18)$$

For the optically thick case, i.e. when  $\epsilon_{\lambda}[C]l > 2$ , the equation is simplified to:

$$\left( \frac{-d[C]}{dt} \right)_{\max} = \phi_{\lambda} I_{0\lambda} \left( \frac{A}{V} \right) \quad (19)$$

The ratio, X, of the rate at any concentration [C] to the maximum rate is given by:

$$\left( \frac{\text{Rate}_{[C]}}{\text{Rate}_{\max}} \right) = X = 1 - 10^{-\epsilon_{\lambda}[C]l} \quad (20)$$

Manipulation of this equation yields:

$$-\log(1-X) = \epsilon_{\lambda}[C]l \quad (21)$$

and so a plot of  $-\log(1-X)$  vs.  $\epsilon_{\lambda}[C]$  yields a straight line with a gradient equal to the path length. This procedure may not be necessary in the use of quartz cells that are commonly used in lab experiments, as the path length is well defined. However, in the case of environmental deployment, where culture tubes are sometimes used, the situation is less exact as sunlight will not be traveling along the major axis of the tube. For a 13 x 100 mm (Corning) glass culture tube, Zepp found that the effective path length was 11.2 mm (4).

Another consideration in the experimental set-up of photochemical reactions is the geometry of the irradiation cell. Whereas a chemical that is dissolved in a natural body of water will primarily receive light from above, a chemical that is

deployed in a tube will effectively receive light from all directions because of the scattering of light from the walls of the irradiation cell. A simple test of this effect is to expose a chemical both in an open dish and in an enclosed tube and compare their photolysis rates. It had been observed that the concentration of light in a culture tube is such that the photochemical reaction proceeds at a rate of 2.2 - 3 times that in an open dish (18). However, this was due to artifacts in the experimental setup and later experiments using carefully controlled conditions, minimizing reflection, have showed that there is no significant effect (19).

The rate at which a chemical undergoes direct photolysis in natural waters will depend on the amount of light reaching the chemical; therefore, shielding of light due to absorption by dissolved organic matter must be considered. A screening factor may be calculated which simply relates the ratio of the 1<sup>st</sup> order rate constant in natural water to that in distilled water.

For a chemical C in distilled water, the rate of photolysis for an optically thin solution of C has been derived above:

$$-\left(\frac{d[C]}{dt}\right)_{\lambda} = 2.303\varepsilon_{\lambda}[C]\phi_{\lambda}I_{0\lambda}I\left(\frac{A}{V}\right) \quad (22)$$

This can be rewritten:

$$-\left(\frac{d[C]}{dt}\right)_{\lambda} = k_{dw,\lambda}[C] \quad (23)$$

$$\text{where } k_{dw,\lambda} \text{ (distilled water rate constant)} = 2.303\varepsilon_{\lambda}\phi_{\lambda}I_{0\lambda}I\left(\frac{A}{V}\right) \quad (24)$$

For the same chemical C in a humic solution with attenuation coefficient  $\alpha_{\lambda}$ , the rate equation has the same form as equation (8), but  $F_{s\lambda}$  and  $F_{c\lambda}$  are different:

$$F_{s\lambda} = 1 - 10^{-(\alpha_{\lambda} + \epsilon_{\lambda}[C])l} \quad (25)$$

$$F_{c\lambda} = \frac{\epsilon_{\lambda}[C]}{\alpha_{\lambda} + \epsilon_{\lambda}[C]} \quad (26)$$

Assuming that  $\alpha_{\lambda} \gg \epsilon_{\lambda}[C]$ , this can be rewritten:

$$-\left(\frac{d[C]}{dt}\right)_{\lambda} = k_{ha,\lambda}[C] \quad (27)$$

$$\text{where } k_{ha,\lambda} \text{ (rate constant in humic acid solution)} = \frac{I_{0\lambda} \left(\frac{A}{V}\right) \phi_{\lambda} \epsilon_{\lambda} (1 - 10^{-\alpha_{\lambda}l})}{\alpha_{\lambda}} \quad (28)$$

$$\text{Hence, the screening factor, } S_{\lambda} = \frac{k_{ha,\lambda}}{k_{dw,\lambda}} = \frac{1 - 10^{-\alpha_{\lambda}l}}{2.303\alpha_{\lambda}l} \quad (29)$$

This screening factor allows prediction of the decrease of direct photolysis rates due to light shielding for an optically thin system.

#### *Indirect Photolysis:*

In indirect photolysis, one molecule absorbs light and initiates the chemical reaction of another substrate. In natural waters, there is a large pool of dissolved organic matter that absorbs light well into the visible region of the solar spectrum – it adds a brownish color to the water when present at high concentrations. The chromophore that absorbs light may either be regenerated as occurs in energy transfer reactions or it may undergo an irreversible change. In effect, the photosensitizer may

act as a photocatalyst or may itself undergo direct photolysis in inducing the indirect photolysis of another compound (20).

It has long been established that dissolved organic matter (DOM) present in natural waters is an important photosensitizer (21). The exact composition of this material is not known although there have been extensive efforts to elucidate the structure (22,23). Due to the variability of the material among different samples, it is somewhat futile to describe a generic structure, but some progress has been made in identifying important functional groups within the structure. Phenolic and carboxylic functionalities have been identified by a variety of methods (23) and may certainly play an important role in the photochemistry of natural waters.

There is not even a clear convention on the nomenclature of dissolved organic material. The term 'unknown photoreactive chromophore' (UPC) (20) may be the most suitable in light of the uncertainty involved in the structure, but other terms encountered in the literature are: gelbstoffe, dissolved organic carbon, humic acid, fulvic acid and heteropolycondensate (20). In this paper, the terms DOM and humic acid will be used. The distinction between humic and fulvic acids is an operational one; humic acids are soluble in dilute base but are precipitated at a pH=2 while fulvic acids are soluble in both dilute base and dilute acid (22).

Humic acids are the detritus of the biodegradation of plant and animal matter, which explains the variability of their composition. The concentration of dissolved organic carbon, [DOC], is a useful measure for comparison of different water samples. For a photochemist, the most important characteristic of humic materials is



their broad absorbance band extending up to ~ 600nm. Zepp has described an exponential model for this band (11):

$$k_h = \frac{2.303A_\lambda}{[\text{DOC}]l} \quad (30)$$

where  $k_h$  is the specific absorption coefficient for the humic substance

$A_\lambda$  is the absorption in  $\text{m}^{-1}$  at wavelength  $\lambda$

$[\text{DOC}]$  is the concentration of dissolved organic carbon ( $\text{mg L}^{-1}$ )

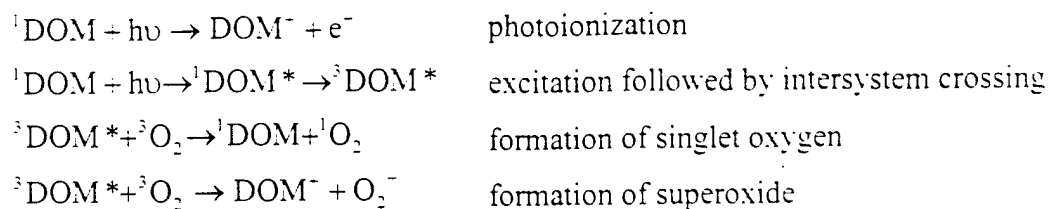
$l$  is the cell path length in m.

$$k_h = Ae^{B(450-\lambda)} \quad (31)$$

where  $A$  and  $B$  are constants and  $\lambda$  is the wavelength in nm. Zepp obtained excellent fits of real absorption spectra to this data with regression coefficients ( $> 0.95$ ) and noted a consistency in the value of  $B$  throughout different water samples. A similar comparison of inland waters was carried out by Davies-Colley with the same results (12).

Dissolved organic matter that is capable of photosensitization facilitates the photodegradation of chemicals that would otherwise be photochemically refractory. The irradiation of DOM produces a number of oxidative species that can initiate reactions - singlet oxygen ( $^1\text{O}_2$ ), superoxide radical ( $\text{O}_2^-$ ), hydrogen peroxide ( $\text{H}_2\text{O}_2$ ), and hydroxyl radical ( $\text{OH}$ ) (24).

Initially, the DOM is excited by the absorption of light; this is followed by transfer of energy or by the transfer of an electron to some other compound (25):



Some possible reactions are shown above. In fact, approximately 90% of the light absorbed by DOM is converted to heat on a very short time scale (24). Furthermore, much of the somewhat stable  $^3\text{DOM}$  is quenched by reacting to form  $^1\text{O}_2$ ; most of which decays by heating the water (20). The half-life of  $^1\text{O}_2$  is  $\sim 3\mu\text{s}$ ; a chemical would have to be present at millimolar levels to compete with the quenching by water. However, reaction with singlet oxygen may be a significant sink for some compounds (26).

Superoxide has been shown to be an intermediate in the natural production of hydrogen peroxide in surface waters (27). Although relatively stable (marine half-life on the order of minutes) and present in nanomolar concentrations, superoxide is not considered an important source of reactivity for organic chemicals in natural waters. However, it does have an important role in the redox cycle of transition metals such as copper and iron (28,29,30,31).

Although there is a relatively high quantum yield (0.005-0.008) (15) for the primary production of a hydrated electron, the lifetime is sufficiently short that most of the electrons do not escape the humic matrix in order to react with a chemical in bulk solution (15,32).

Finally, there is one other important reactive species that is produced through the irradiation of natural waters. The hydroxyl radical is the end product of the

photolysis of nitrate ( $\text{NO}_3^-$ ) (33) although it is produced in smaller quantities from humic acids too. The hydroxyl radical may be an important species because it reacts readily with many chemicals but it is present at very low concentrations in natural waters.

Photosensitized reactions of xenobiotics in natural waters frequently follow first order kinetics (34,35). In order to normalize the rate constant for a particular photosensitized reaction within different water samples, it is necessary to account for differences in the available light, both in terms of the irradiance as well as the amount of light that is absorbed. Zepp developed a response function,  $X_{s,\lambda}$ , as an appropriate parameter:

$$X_{s,\lambda} = \frac{k'_p}{E_{0,\lambda}^{av}} \quad (32)$$

where  $k'_p$  is the apparent first order constant for the reaction with some probe, P and  $E_{0,\lambda}^{av}$  is a function of the intensity of light available to the system.

$$\frac{d[P]}{dt} = -k'_p [P] \quad (33)$$

For a sensitizer, S, that produces a reactive intermediate, I, that reacts both with the probe, P, and natural scavengers, L, the response function ( $X_{s,\lambda}$ ) of the sensitizers can be plotted as a function of wavelength. In order to develop this idea more fully, it is sensible to consider the chromophoric DOM as two distinct parts: the sensitizing part (S) and the remainder. As such, the attenuation coefficient of the whole system can be broken up in the same way:

$$\alpha_\lambda = \alpha_\lambda' + \epsilon_\lambda[S] \quad (34)$$

where  $\alpha_\lambda'$  is the non-sensitizing part of the humic acid and  $\epsilon_\lambda[S]$  is the product of the

molar absorptivity of the sensitizer and its concentration.

Then:  $F_{s\lambda} = 1 - 10^{-\alpha_{\lambda} l}$  (35)

$$F_{c\lambda} = \frac{\epsilon_{\lambda} [S]}{\epsilon_{\lambda} [S] + \alpha_{\lambda}'} = \frac{\epsilon_{\lambda} [S]}{\alpha_{\lambda}} \quad (36)$$

The average rate of light absorption by the sensitizer:  $I_{a\lambda} = I_{0\lambda} F_{s\lambda} F_{c\lambda}$

$$I_{a\lambda} = \frac{I_{0\lambda} \left( \frac{A}{V} \right) (1 - 10^{-\alpha_{\lambda} l}) \epsilon_{\lambda} [S]}{\alpha_{\lambda}} \quad (37)$$

and rate of reaction of P:  $\frac{d[P]}{dt} = -k_p [P][I]$  (38)

and rate of reaction of I:  $\frac{d[I]}{dt} = P_1 - L_1$  (39)

where  $P_1$  and  $L_1$  are the production and loss reactions respectively of I.

Now,  $P_1 = I_{a\lambda} \phi_{\lambda}$  (40)

where  $\phi_{\lambda}$  is the quantum efficiency of the production of I from S.

$$L_1 = k_p [P][I] + k_l [I][L] \quad (41)$$

where L represents natural scavengers of I and  $k_l$  is the rate constant for the reaction of I with L. For low concentrations of P such that the presence of P does not affect the lifetime of the sensitizer, then the reaction of I with P is insignificant compared to the reaction of I with L.

Assuming steady state conditions for I such that  $P_1 = L_1$  and substituting equations (37), (39), (40) into (41) gives:

$$[I] = \frac{I_{0\lambda} \left( \frac{A}{V} \right) (1 - 10^{-\alpha_{\lambda} l}) \epsilon_{\lambda} \phi_{\lambda} [S]}{\alpha_{\lambda} k_l [L]} \quad (42)$$

Now substituting this into equation (38) yields:

$$\frac{d[P]}{dt} = - \frac{I_{0,\lambda} \left( \frac{A}{V} \right) (1 - 10^{-\alpha_\lambda l}) \epsilon_\lambda \phi_\lambda k_p [S][P]}{\alpha_\lambda k_i [L]} \quad (43)$$

For a system where  $[L]$  is constant, some of the above equation can be grouped together as constant  $Q_\lambda$ :

$$Q_\lambda = \frac{\phi_\lambda k_p}{k_i [L]} \quad (44)$$

Defining  $E_{0,\lambda}^{av}$ , a function of the available light intensity, particular to each water sample,

$$E_{0,\lambda}^{av} = \frac{I_{0,\lambda} \left( \frac{A}{V} \right) (1 - 10^{-\alpha_\lambda l})}{\alpha_\lambda} \quad (45)$$

Then,

$$\frac{d[P]}{dt} = -E_{0,\lambda}^{av} Q_\lambda \epsilon_\lambda [S][P] = -k'_p [P] \quad (46)$$

and thus, the response function,

$$X_{s,\lambda} = \frac{k'_p}{E_{0,\lambda}^{av}} = Q_\lambda \epsilon_\lambda [S] \quad (47)$$

The importance of this derivation lies in the observed relationship between the response function and wavelength. If there is a single substance within the humic matrix that is responsible for the photosensitization, then a plot of the response function vs. wavelength (action spectrum) should parallel its absorption spectrum (34). This phenomenon has been observed in the wavelength dependence of hydrogen peroxide production (36) as well as the reaction of singlet oxygen with a

probe compound (34) in various natural waters. The same equation also explains the linear relationship between  $X_{s.s.}$  and  $[S]$ . This relationship is frequently expressed through a linear plot of rate constant vs.  $[DOC]$ .

#### *Probes:*

The analysis of photochemically produced reactive species is complicated due to both their low concentrations ( $10^{-8} - 10^{-17}$  M) and short lifetimes ( $\mu s - s$ ). Chemical probes 'trap' transient species by forming a stable product, which can then be measured. There are two possible methods of deployment. The probe can be added at sufficiently low levels so that the steady state concentration of the radical is not perturbed. Pseudo-first order kinetics are assumed and hence ambient concentrations of the radical are deduced (29,33,37). Alternatively, the probe can be added at such high concentrations that it outcompetes all other scavengers of the radical. In this case, the rate of reaction of the probe will be equal to the formation rate of the reactive transient (24,37). The former method is somewhat more attractive due to the reduced chance of probe related artifacts associated with minimum variation of the system under study (37).

There are several requirements that a chemical probe must meet in order to be effective; the most important of which is a well-characterized rate constant with the specific reactive species. Ideally, that rate constant is high so that minimal amounts of probe are required. In terms of analysis, a wide range of concentrations of the probe should be able to be detected easily. If this is possible, the kinetics of the

system can be interpreted more thoroughly as the competition between the added probe and existent natural scavengers can be altered.

For use in photochemical experiments, it is advantageous if the probe does not absorb light in the region of interest, and if not completely transparent, the probe itself should be photochemically inert.

There is one significant disadvantage in using chemical probes to measure reactive species produced within the humic matrix. As humic acid solutions are not homogeneous, the concentration of the transient in the bulk solution may be orders of magnitude different from that inside the humic acid. Burns *et al.* developed a kinetic model that described the effects of degree of partitioning of a chemical to the humics (32). In particular, the humic mediated dechlorination of the hydrophobic pesticide mirex was discussed. For such a compound, use of a hydrophilic chemical probe such as chloroethanol would be inappropriate. In effect, the chemical probe is detecting levels of transient in one phase while the chemical is reacting with the transient in another phase.

Various probes have been deployed to assess the steady state concentrations and production rates of reactive transients in natural waters. Some kinetic and concentration data for transients in surface water are shown below; the results are taken from a review of the subject by Haag and Mill (24).

Transient	Sources	Sinks	$k_{\text{sink}}$	Loss Rate $\text{s}^{-1}$	Midday surface conc. M
$^3\text{DOM}$	DOM	$k[\text{O}_2]$	$2 \times 10^9 \text{ M}^{-1} \text{ s}^{-1}$	$5 \times 10^{-5}$	$(1-5) \times 10^{-15}$
$^1\text{O}_2$	DOM	$k[\text{H}_2\text{O}]$	$2.5 \times 10^5 \text{ s}^{-1}$	$2.5 \times 10^{-5}$	$10^{-14} - 10^{-12}$
OH	DOM, $\text{NO}_3^-$	$k[\text{DOM}]$	$2.5 \times 10^4 \text{ Lmg}^{-1} \text{ s}^{-1}$	$(0.2 - 2) \times 10^{-5}$	$(2-6) \times 10^{-16}$
$\text{e}^-$	DOM	$k[\text{O}_2]$ $k[\text{NO}_3^-]$	$2 \times 10^{10} \text{ M}^{-1} \text{ s}^{-1}$ $1 \times 10^{10} \text{ M}^{-1} \text{ s}^{-1}$	$(0.5 - 1.5) \times 10^{-5}$	$(1-2) \times 10^{-14}$
$\text{O}_2^-$	DOM	$k[\text{O}_2^-]$ $k[\text{DOM}]$	$6 \times 10^{12} [\text{H}^+] \text{ M}^{-1} \text{ s}^{-1}$ ?	$10^{-5} - 1$	$10^{-9} - 10^{-8}$



### *Superoxide:*

In as much as it is hypothesized that quadricyclane reacts with superoxide radicals produced by the photosensitization of DOM, some background is provided on superoxide. The exact mechanism through which superoxide is formed in irradiated natural waters is not known. It is possible that as dissolved organic matter (DOM) undergoes photoionization, oxygen is reduced, forming superoxide. However, the measured production rates of the hydrated electron are not sufficiently high to explain the observed steady state concentration of superoxide (13,36). Furthermore, the addition of electron scavengers to an irradiated humic acid solution does not reduce the production of hydrogen peroxide, a stable end product of superoxide reactions (13). An alternative explanation is that a direct electron transfer from an excited triplet state to  $O_2$  takes place (24).

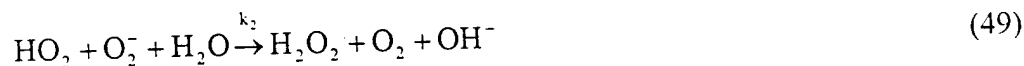
Measured steady state concentrations of superoxide in natural waters are in the range:  $10^{-9}$  -  $10^{-8}$  M (24). The reactions of superoxide are themselves not well understood. Superoxide will undergo dismutation but this is a relatively insignificant sink in the presence of transition metals (28,29). The reactions of superoxide with transition metals will depend on the speciation of the metals and hence the pH. Zafiriou *et al.* showed that in ocean waters, the reaction of superoxide with copper will be far more important than self-dismutation even if the poorly characterized organic complexes of Cu are inert (28). In fact, there is evidence that there are also non-metallic complexes that react with superoxide in natural waters (38). A metal-complexing reagent (EDTA or DTPA) was added to samples of natural waters to

quench the metal catalyzed reactions and samples were also boiled to reduce enzyme activity. In this way, it was suggested that the additional sink of superoxide was the dissolved organic material itself. Thus, superoxide has a role in the redox cycling of both transition metals and dissolved organic matter in natural waters.

#### *Superoxide Chemistry (pH):*

In this paper, reference is predominantly made to superoxide radicals rather than to both superoxide and its conjugate acid, perhydroxyl (hydroperoxyl) radicals. This is because HOO has a  $pK_A$  of 4.8 (39,40) and hence at common pHs of environmental importance (7-8.5), only 0.02% of the species is HOO.

The disproportionation of the pair may be expressed as:



$$\text{Rate of disproportionation, } R_{\text{obs}} = k_1 [HO_2][HO_2] + k_2 [HO_2][O_2^-] \quad (50)$$

$$\text{Defining, } c_T = [HO_2] + [O_2^-], \text{ then} \quad (51)$$

$$R_{\text{obs}} = [HO_2]^2 \left\{ k_1 + \frac{k_2 K_{HO_2}}{[H^+]} \right\} = \left\{ \frac{k_1 + \frac{k_2 K_{HO_2}}{[H^+]}}{\left( 1 + \frac{K_{HO_2}}{[H^+]} \right)^2} \right\} c_T^2 = k_{\text{obs}} c_T^2 \quad (52)$$

$$K_{HO_2} = \frac{[H^+][O_2^-]}{[HO_2]} \quad (53)$$

Bielski calculated the constants (40):

$$k_1 = (8.3 \pm 0.7) \times 10^5 \text{ M}^{-1} \text{ s}^{-1} \quad k_2 = (9.7 \pm 0.6) \times 10^7 \text{ M}^{-1} \text{ s}^{-1} \quad \text{and } K_{HO_2} = 1.6 \times 10^{-5} \text{ M}$$

Hence, above pH = 6, the rate constant for disproportionation simplifies to:

$$k_{\text{obs}} = 6 \times 10^{12} [\text{H}^-] \text{ M}^{-1} \text{ s}^{-1} \quad (54)$$

#### *Probes for Superoxide:*

For many years, biologists have made use of tetranitromethane, ferricytochrome c and nitro blue tetrazolium as probes for superoxide (40). Their main advantage is simplicity of use (colorimetric analytical techniques) but this is also the cause of their inappropriateness for use in natural waters. Superoxide is only produced in natural waters that have been irradiated and the above compounds are sensitive to light.

The metalloenzyme superoxide dismutase (SOD), which catalyzes the dismutation of superoxide has also been utilized as a probe for superoxide, but artifacts in photochemical experiments have been reported (29,41). The analytical technique is to measure the increased production of hydrogen peroxide in the presence of SOD, with the result that the measured superoxide is that fraction which does not generate  $\text{H}_2\text{O}_2$  in the absence of SOD. However, there is still some uncertainty as to whether superoxide disproportionation is the only source of hydrogen peroxide.

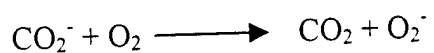
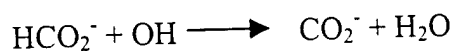
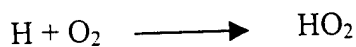
Recently, nitric oxide has also been applied as a specific probe for superoxide as well as general classes of radicals:  $\text{H}^\cdot$ ,  $\text{R}^\cdot$ ,  $\text{OH}^\cdot$ ,  $\text{ROO}^\cdot$ ,  $\text{O}_2^\cdot$  (37,41). Isotope mass spectrometry is used to measure the reaction of  $^{15}\text{N}$ -labeled NO with superoxide. The reaction of NO with  $\text{O}_2^\cdot$  has a rate constant of  $\sim 2 \times 10^9 \text{ Ms}^{-1}$ , forming peroxynitrite,

which then rearranges into nitrate. Nitrate is converted into  $N_2O$  for isotopic analysis by reduction with Cu/Cd to form nitrite and further reaction with azide. One possible shortcoming of this method is the possibility of peroxynitrite's cleaving into OH and  $NO_2$  within a solvent cage. It is possible for these species to escape the solvent cage and hence a fraction of the reaction (estimated at 30-40%) may not be measured (29).

#### *Experimental Methods for Production of Superoxide:*

Various methods have been used to produce superoxide radicals for the purpose of rate experiments. Certainly, radiolysis provides the most effective method in that very high concentrations of superoxide, up to 0.4mM, can be produced (42,43), but this method is not a universal option due to limited availability and so the enzymatic approach (xanthine-xanthine oxidase) provides a simple alternative.

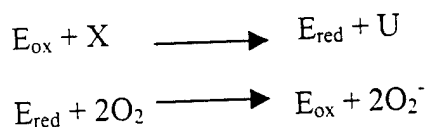
Radiolysis of water produces the primary radicals: H,  $e^-$  and OH (44). These can be converted into the superoxide and hydroperoxy radicals by including oxygen and either formate or ethanol:



The irradiated solution contains simply water, formate and some ethylenediamine – tetraacetic acid (EDTA) to chelate any trace metals. As a result, the risk of side reactions due to the presence of contaminants is very low. Metal impurities may react

with the superoxide formed (42); this would necessarily complicate the reaction under consideration.

Particularly in the biomedical fields, the enzymatic mode of production of superoxide is preferred due to the system's close approximation to *in vivo* situations. Xanthine is preferentially used as a substrate in the reaction with the xanthine oxidase enzyme. In this reaction, xanthine (X) is oxidized to uric acid (U) while the enzyme is reduced (40,45):



The pH range over which this technique can be applied is limited to that in which the xanthine oxidase is active.

#### *Chemicals of Interest:*

##### **Ammonium Dinitramide (ADN):**

Dinitramide salts ( $K^+$ ,  $Na^+$ ,  $NH_4^+$ ) were first developed in the U.S. by SRI International in 1988 (46), although it appears that the Soviet Union had been secretly using ADN ( $NH_4^+ NO_3^-$ ) in their weapons program since the 1970's (47). Dinitramides were primarily developed for use as an oxidizer in solid-fuel rocket propellants.

Presently, ammonium perchlorate (AP) is the most widely used oxidizer for propellants and explosives. ADN has several advantages over AP, most notably the absence of chlorine in the former. Chlorinated oxidants such as AP release chloride

from rocket motors: this is a concern both environmentally as well as militarily (48). The smoky white 'contrail', characteristic of AP allows ready tracking of rocket launches. Another advantage for ADN is its higher lift capacity, relative to AP, allowing launches of heavier payloads (48). ADN will probably not replace AP for ten years; ADN is both less thermally stable and more shock sensitive than AP (46).

### **Quadricyclane:**

Quadricyclane has recently been suggested as an additive to jet fuel (49) and rocket propellant (50). Quadricyclane is a highly strained hydrocarbon; its high heat of formation and relatively high density ( $0.982 \text{ gml}^{-1}$ ) suggest that it would have a high energy density.

Another practical application for which it was considered was as a solar energy storage species (51,52). Quadricyclane and its valence isomer, norbornadiene, have also been of interest to theoretical chemists due to their interconversion through a delocalized radical cation (53,54,55).

The environmental fate of quadricyclane has only recently been investigated due to its possible deployment by the U.S. Air Force. Half-lives of quadricyclane due to acid hydrolysis range from 25 minutes at  $\text{pH} = 3$  to  $\sim 2$  days at  $\text{pH} = 5$  (56). An extrapolated half-life at neutral  $\text{pH}$ 's is on the order of years.

In soil samples, after quadricyclane has undergone abiotic transformation to tricyclo[2.2.1.0<sup>2,6</sup>]heptan-3-ol and bicyclo[2.2.1]hept-5-en-ol, a further transformation

of the former cyclic alcohol takes place. Tricyclo[2.2.1.0<sup>2,6</sup>]heptan-3-one is formed biotically and is further mineralized to CO<sub>2</sub> (57).

### References

1. Dung, M.H.; O'Keefe, P.W. *Environ. Sci. Technol.* **1994**, 28, 549.
2. Boule, P.; Guyon, C.; Tissot, A.; Lemaire, J. In *Photochemistry of Environmental Aquatic Systems*; Zika, R.G.; Cooper, W.J., Eds.; ACS Symposium Series: American Chemical Society: Washington, DC, 1987, chapter 2.
3. Schwarzenbach, R.P.; Gschwend, P.M.; Imboden, D.M. *Environmental Organic Chemistry*; Wiley Interscience: New York, 1993.
4. Leifer, A. *The Kinetics of Environmental Aquatic Photochemistry*; ACS Professional Reference Book: Washington, DC, 1988.
5. Atkins, P.W. *Physical Chemistry*; Oxford University Press: Oxford, 1995.
6. London, J.; Beithr. *Phys. Atmos.* **1963**, 34, 254.
7. Zepp, R.G.; Cline, D.M. *Environ. Sci. Technol.* **1977**, 11, 359.
8. Sikorski, R.J.; Zika, R.G. *J. Geophys. Res.* **1993**, 98, 2315.
9. International Critical Tables, Vol VII, p. 13, McGraw-Hill, NY, 1930.
10. Duntley, S.Q. *Opt. Soc. Am.* **1941**, 31, 714.
11. Zepp, R.G.; Schlotzhauer, P.F. *Chemosphere*, **1981**, 10, 479.
12. Davies-Colley, R.J.; Vant, W.N. *Limnol. Oceanogr.* **1987**, 32, 416.
13. Moore, C.A.; Farmer, C.T.; Zika, R.G. *J. Geophys. Res.* **1993**, 98, 2289.

14. Brezonik, P.L. *Chemical Kinetics and Process Dynamics in Aquatic Systems*.  
Lewis Publishers: Boca Raton, 1994.
15. Zepp, R.G.; Braun, A.M.; Hoigné, J.; Leenheer, J.A. *Environ. Sci. Technol.* **1987**,  
21, 485.
16. Hatchard, C.G.; Parker, C.A. *Proc. R. Soc. (London)* **1956**, A235, 518.
17. Zepp, R.G. *Environ. Sci. Technol.* **1978**, 12, 327.
18. Dulin, D.; Mill, T. *Environ. Sci. Technol.* **1982**, 11, 815
19. Jankowski, J.J.; Kieber, D.K.; Mopper, K.; Submitted to *Photochemistry and  
Photobiology*, June, 1999.
20. Zafiriou, O.C.; Jousset-Dubien, J.; Zepp, R.G.; Zika, R.G. *Environ. Sci. Technol.*  
**1984**, 18, 12.358A-371A.
21. Zika, R.G. *Rev. Geophys.* **1987**, 25, 1390.
22. Preston, C.M. *Soil Science*, **1996**, 161, 144.
23. MacCarthy, P.; Rice, J.A. In *Humic Substances in Soil, Sediment, and Water:  
Geochemistry, Isolation and Characterization*; Aiken, G.R.; McKnight, D.M.;  
Wershaw, R.L.; MacCarthy, P., Eds.; Wiley-Interscience: New York, 1985, pp  
527-559.
24. Haag, W.R.; Mill, T., In *Effects of Solar Ultraviolet Radiation on Biogeochemical  
Dynamics in Aquatic Environments*; Blough, N.V.; Zepp, R.G., Eds.; Woods  
Hole Oceanographic Institution Technical Report, WHOI-90-09, 1990, pp 82-88.
25. Scully, N.M.; McQueen, D.J.; Lean, D.S.R.; Cooper, W.J. *Limnol. Oceanogr.*  
**1996**, 41, 540.



26. Scully, F.E.; Hoigné, J. *Chemosphere*. **1987**, 16, 681.
27. Moffett, J.W.; Zafirou, O.C. *Limnol. Oceanogr.* **1990**, 35, 1221.
28. Zafirou, O.C.; Voelker, B.M.; Sedlak, D.L. *J. Phys. Chem.* **1998**, 102 A, 5693.
29. Blough, N.V.; Zepp, R.G. In *Active Oxygen in Chemistry*; Foote, C.S.; Valentine, J.S.; Greenberg, A.; Liebman, J.F., Eds.; Blackie Academic and Professional: New York; 1995, pp 280-333.
30. Voelker, B.M.; Sulzberger, B. *Environ. Sci. Technol.* **1996**, 30, 1106.
31. Voelker, B.M.; Morel, F.M.M.; Sulzberger, B. *Environ. Sci. Technol.* **1997**, 31, 1004.
32. Burns, S.E.; Hassett, J.P.; Rossi, M.V. *Environ. Sci. Technol.* **1996**, 30, 2934.
33. Zhou, X.; Mopper, K. *Mar. Chem.* **1990**, 30, 71.
34. Zepp, R.G.; Baugham, G.L.; Schlotzhauer, P.F. *Chemosphere*, **1981**, 10, 119.
35. Zepp, R.G.; Schlotzhauer, P.F.; Merritt Sink, R. *Environ. Sci. Technol.* **1985**, 19, 74.
36. Cooper, W.J.; Zika, R.G.; Petasne, R.G.; Plane, J.M. *Environ. Sci. Technol.* **1988**, 22, 1156.
37. Zafirou, O.C.; Blough, N.V.; Micinski, E.; Dister, B.; Kieber, D.; Moffett, J. *Mar. Chem.*, **1990**, 30: 45.
38. Voelker, B.M. Preprints of Extended Abstracts, ACS, 1998.
39. Zafirou, O.C. *Mar. Chem.*, **1990**, 30, 31.
40. Bielski, B.H.J.; Cabelli, D.E.; Arudi, R.L. *J. Phys. Chem. Ref. Data*, **1985**, 14, 1041.

41. Micinski, E.; Ball, L.A.; Zafiriou, O.C. *J. Geophys. Res.* **1993**, 98: 2299.
42. Bielski, B.H.J.; Arudi, R.L. *Anal. Biochem.* **1983**, 133, 170.
43. Bielski, B.H.J.; Richter, H.W. *J. Am. Chem. Soc.* 1977, 99, 3019.
44. Schwarz, H.A. *J. Chem. Educ.* **1981**, 58:101.
45. Olson, J.S.; Ballou, D.P.; Palmer, G.; Massey, V. *J. Biol. Chem.* **1974**, 249, 4350.
46. Gilardi, R.; Flippen-Anderson, J.; George, C.; Butcher, R.J. *J. Am. Chem. Soc.* **1997**, 119, XXXX, 9411-9416.
47. Bottaro, J.C.; Penwell, P.E.; Schmitt, R.J. *J. Am. Chem. Soc.* **1997**, 119, 9405.
48. Borman, S. *C&E News*, **1994**, 18-22.
49. Alberici, F.; Cassar, L.; Monti, F.; Neri, C.; Nodari, N. 1991. High-Energy-Content Fuel Composition containing quadricyclane. US patent no. US5076813
50. Nichols, R.; McKelvey, T.A.; Rodgers, S.L. 1997. High Energy Rocket Propellant. US patent no. US561882.
51. Laird, T. *Chem. Ind.* **1976**, 186-193.
52. Sasse, W.H.F. Solar power and fuels : proceedings of the First International Conference New York : Academic Press, 1977, 227 - 245.
53. Roth, H.D.; Manion Schilling, M.L. *J. Am. Chem. Soc.* **1981**, 103, 7210.
54. Inadomi, Y.; Morihashi, K.; Kikuchi, O. *Theochem*, **1998**, 434, 59.
55. Kirkor, E.S.; Maloney, V.M.; Michl, J. *J. Am. Chem. Soc.* **1990**, 112, 148.
56. Hill, W.E.; Szechi, J.; Hofstee, C.; Dane, J.H. *Environ. Sci. Technol.* **1997**, 31, 651.
57. Jin, S.; Swoboda-Colberg, N.G.; Colberg, P.J.S. *Can. J. Microbiol.* **1997**, 43, 300.

## Chapter 2

### Modeling the Photolysis of Ammonium Dinitramide in Natural Waters

#### Abstract

Photolytic rate constants for the novel energetic compound, ammonium dinitramide (ADN) were determined in order to understand the fate of ADN in natural bodies of water. Quantum yields were measured between 290 and 400nm using a lamp system, and these values were combined with absorption of light in a water column to model photolysis rates as a function of depth. The validity of this model was tested in field trials in Onondaga Lake, Syracuse, N.Y. For a summertime irradiation, half-lives ranged from ~ 6 minutes at the surface to ~ 15 years at a depth of 2m. The predicted and observed degradation rates of ADN were sufficiently similar to justify use of this simple model. It was also found that the degradation of ADN is not enhanced to any measurable degree by sensitized photoreactions in humic solutions. Thus, the photodegradation of ADN can be predicted throughout the water column of a body of water.

#### Introduction

Ammonium dinitramide (ADN:  $\text{NH}_4^+\text{N}_3\text{O}_4^-$ ) is a novel compound under consideration as a rocket propellant (1,2,3). Prior to its deployment, its aquatic photodegradation should be studied as part of an overall comprehension of its fate. The major products of the photolysis of ADN are nitrate ( $\text{NO}_3^-$ ), nitrite ( $\text{NO}_2^-$ ) and nitrous oxide ( $\text{N}_2\text{O}$ ) (4).

The increased concentration of  $\text{NO}_3^-$  and  $\text{NO}_2^-$  as a result of ADN photolysis might affect the level of algal activity for a system where nitrogen is limiting. In addition, there are toxicological concerns due to the known oxidizing power of nitro groups, which can convert the ferrous iron in hemoglobin to ferric iron (5). Severe oxygen depletion, known as methemoglobinemia, can result (6). Consequently, there are recommended maximum concentrations in drinking water for similar nitro-containing propellants and explosives such as TNT, RDX, and HMX (7). TNT, in particular, has been studied extensively because it is a primary ingredient of most military explosives. An obvious manifestation that spurred interest in TNT photolysis is sunlight-induced color changes (pink water) in polynitroaromatic wastewater from munitions manufacturing and loading plants (8). As for ADN itself, at present, only acute toxicity in rats has been tested at levels of 1g/kg (9) while nothing is known about its impact as a result of prolonged exposure at lower levels.

ADN should photolyze in sunlight as it absorbs strongly in the UV-A region of the spectrum. To study this reaction, the photolytic rate constants were calculated over the range of wavelengths in which ADN absorbs light (290-400nm), using a lamp system. The objectives were not only to determine the active region of the sunlight spectrum in terms of ADN photolysis but also to model the degradation of this compound throughout the water column. To this end, ADN was deployed at various depths in a lake so that the predicted rate of degradation could be compared to the observed rate. A simple model of the absorption of light through the water column was applied and found to be accurate.

Interaction with dissolved organic material can affect the fate of a xenobiotic compound. For instance, TNT undergoes both direct and indirect photolysis with the result that the photodegradation of TNT is more rapid in a sample of natural water than in a sample of distilled water (8). Due to the complex mixture of products reported for TNT photolysis, there may be more than one sensitized pathway for the photodegradation of this compound (10,11). However, in the case of ADN, humic acid mediated reactions were found to be inconsequential compared to direct photolysis.

An understanding of the aquatic photochemistry of ammonium dinitramide (ADN) involves both direct and indirect photolysis at the surface and at depth. Although at present it has only been tested in one lake, the model that has been developed should be able to predict the direct photolysis of ADN spilled into any natural body of water, assuming that the attenuation coefficient of that water is known.

#### Experimental Section

**Materials:** ACS grade acetonitrile was obtained from J.T.Baker Inc. (Philipsburg, NJ). Puriss grade tetrabutylammonium hydroxide concentrate was obtained from Fluka Chemical Company (Buchs, Switzerland). Potassium oxalate monohydrate ( $\geq 99\%$ ) and commercial humic acid, as the sodium salt, were obtained from Aldrich Chemical Company (Milwaukee, WI). ACS reagent grade phenanthroline was obtained from Fisher Scientific (Pittsburgh, PA). Ferric chloride was obtained from Mallinckrodt Chemical Inc., (Paris, KY). ADN was kindly donated by Dr. T. Mill of SRI International, Menlo Park, CA.

All solutions were made using water purified with a Millipore 4-bowl standard system (Millipore Corp., Chicago, IL); the water had a resistivity of greater than  $18\text{M}\Omega\text{cm}$  and will henceforth be referred to as MilliQ water.

Humic acid solutions were prepared using a variation of the method of Zepp et al. (12). Humic material (2g) was extracted with 2L of 0.1N sodium hydroxide solutions and pressure-filtered through a  $0.2\mu\text{m}$  capsule filter (Gelman Sciences #12117) at 4-6 psi. The filtrate was filtered again after adjustment to pH 6 with HCl. Humic acid working solutions were prepared as necessary by diluting the stock solution and using buffers to adjust the pH (13). Dissolved organic carbon (DOC) measurements were made on working humic solutions using external digestion with potassium persulfate and a Beckman Model 215A infrared analyzer.

Potassium ferrioxalate solutions for actinometry were prepared by combining 5 ml each of ferric chloride (0.4M) and potassium oxalate (1.2M) and diluting to 100ml (14).

### Methods:

*Analysis by Ion-Pair Reverse Phase High Performance Liquid Chromatography (HPLC).* The HPLC system consisted of an Eldex Model B-100-S single piston pump (Eldex Laboratories, Menlo Park, CA) in series with a coil pulse dampener, a 0-6000 psi flow-through pressure gauge and a 6-port Rheodyne sample injection valve (Chromtech, Apple Valley, MN) with a  $100\mu\text{l}$  sample loop. A 4.6-mm x 100-mm Prodigy (Phenomenex, Torrance, CA)  $\text{C}_{18}$  column was used for all analyses. A 3:1:2 tetrabutylammonium hydroxide (0.005M): MilliQ water: acetonitrile mobile phase was pumped at a flow rate of 1.5 ml/min. Absorption was measured using an

ISCO V<sup>+</sup> variable wavelength absorption detector (ISCO Inc. Lincoln, NE), set at 284nm ( $\lambda_{\text{max}}$  of ADN).

Values for the [ADN] were determined from HPLC standard curves. The Beer-Lambert law was applied to relate absorption to concentration. Absorbances of solutions in 1 and 10 cm quartz cells were measured using a Hewlett-Packard UV-visible spectrophotometer (model 8453, Hewlett-Packard Company, Wilmington, DE).

Three experiments were performed with humic solutions ( $\text{DOC} = 8.5 \text{ mgL}^{-1}$ ) of ADN. First, long bandpass filters (Rolyn Optics) were used that would absorb the incident light below 400nm. Secondly, at 284nm, the quantum yield was determined at various temperatures. For these irradiations, the sample temperature was controlled with a Fisher Scientific water bath (model 9005). Finally, the quantum yield of ADN in a humic solution was determined at three wavelengths (285, 345, 380nm) and compared to that of ADN in MilliQ water.

#### *Laboratory Photolyses*

Two irradiation systems were used. The first was an Osram XBO 150W/1 Xenon lamp housed in an Oriel Uniform Beam Illuminator lamp housing (model 6148) and powered by a Spectral Energy (Westwood, NJ) universal power supply (model LPS 251 HR). In addition, a Bausch and Lomb high intensity monochromator was used with a bandwidth set to 4nm. The second was a 1 kW xenon lamp, a GM 252 high intensity quarter meter grating monochromator, with the same bandwidth, and an enclosed sample chamber (Spectral Energy Corp.). Light intensities were

measured using potassium ferrioxalate actinometry (15) and an IL1400A photometer. (International Light, Inc. Newburyport, MA)

### *Sunlight Photolyses*

Outdoor photolysis experiments were carried out in Onondaga Lake, Syracuse, NY on four days during the summer of 1997 and 1998 on both clear and cloudy days. Samples were deployed at depths ranging from 0.5 – 2.0 m using a rack (Figure 2.1) holding 13 x 100 mm Pyrex culture tubes (Corning Inc., Corning, NY). Since the tubes were not made of quartz, the incident light was corrected to take into account absorption by the glass by using transmission spectra provided by the manufacturer (minimum transmittance – 70% at 290nm). Surface irradiance was measured every twenty minutes over the six-hour irradiation period with an Optronics OL-754 spectroradiometer (Optronics Lab., Orlando, FL) over the range 290 – 700 nm.



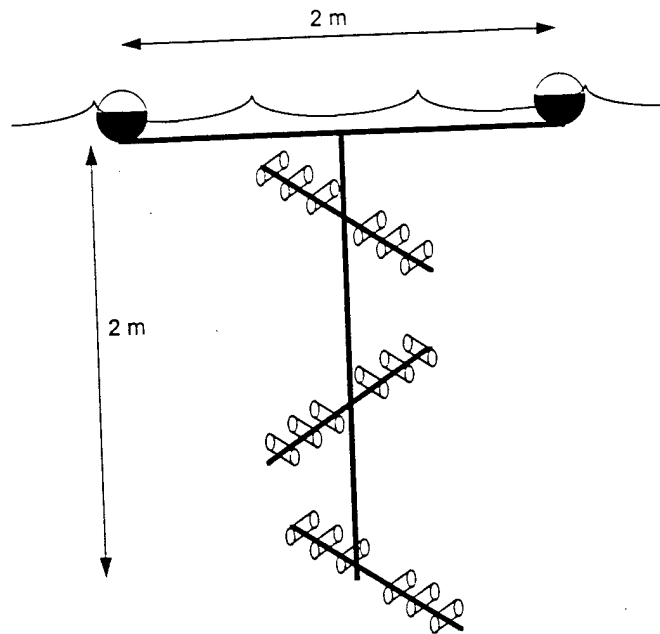


Figure 2.1. System for exposing samples to sunlight at depth in a lake. The supports are aluminum rods with clips to hold the screw-cap culture tubes.

## Results and Discussion

### *Determination of Photolysis Rates:*

In order to obtain the photolysis rate of ADN at the surface of a body of water, three parameters must be known. First, the molar absorptivity coefficient  $\epsilon_\lambda$ , was calculated by measuring the absorbance spectrum of aqueous solutions of ADN. Secondly, the quantum yield,  $\phi_\lambda$ , for the degradation of ADN was determined in the laboratory using a lamp system. Thirdly, the solar irradiance,  $I_\lambda$ , was measured with a spectroradiometer. These parameters were obtained across a wavelength range of 290-400nm. The minimum corresponds to the lowest wavelength to reach the surface of the earth and the maximum corresponds to the highest wavelength where ADN absorbs solar radiation.

Molar absorptivity coefficients were calculated from the absorption spectrum (Figure 2.2a). In the region of environmental significance, there is a peak at 284nm. and a shoulder that corresponds to a smaller peak centered at approximately 325nm.

In order to determine quantum yields, the irradiance of the incident light must be known. Thus, these experiments were performed with a lamp whose output was quite stable. The irradiance was measured on a daily basis with a photometer, and this instrument was calibrated weekly by performing simultaneous ferrioxalate actinometry. The quantum yields for ADN,  $\phi_\lambda$ , were determined by plotting  $\ln[\text{ADN}]$  vs. time. For an optically thin solution undergoing direct photolysis, the rate equation is (16):

$$\left\{ \frac{d[\text{ADN}]}{dt} \right\}_\lambda = -2.303 I_\lambda \phi_\lambda \epsilon_\lambda I [\text{ADN}] \quad (1)$$

where at a given wavelength  $\lambda$ ,  $I$  is the incident irradiance per unit volume of sample in Einstein  $\text{cm}^{-3} \text{min}^{-1}$ ,  $\phi$  is the quantum yield for the degradation of ADN,  $\epsilon$  is

the molar absorptivity coefficient of ADN ( $\text{cm}^2 \text{mol}^{-1}$ ) and  $l$  is the path length of the irradiated cell (cm). Note that  $I_\lambda = I_{0\lambda} (A/V)$  where  $I_{0\lambda}$  is the incident irradiance in Einstein  $\text{cm}^{-2} \text{min}^{-1}$ ,  $A$  is the surface area and  $V$  is the volume of the sample cell. Thus, equation (1) may also be written:

$$\left\{ \frac{d[\text{ADN}]}{dt} \right\}_\lambda = -2.303 I_{0\lambda} \phi_\lambda \epsilon_\lambda [\text{ADN}] \quad (2)$$

The quantum yield of ADN is about 0.1 over the first two absorption bands described above (Figure 2.2b) with a small increase near the high wavelength end of the absorption spectrum (Figure 2.2a).

The final parameter needed in order to predict photolysis rates is the solar irradiance. Solar irradiance was measured as a function of wavelength and time in Syracuse, N.Y. during the summer and early fall of 1998, and photolysis rates were predicted with that data. One such sample spectrum is included (Figure 2.2c).

For all wavelengths between 290 and 400nm, the irradiance as measured by the spectroradiometer in watts  $\text{cm}^{-2} \text{nm}^{-1}$  was converted into einstein  $\text{s}^{-1} \text{cm}^{-2} \text{nm}^{-1}$  using the following conversion:

$$1 \text{ einstein} = \frac{1.2 \times 10^8 \text{ J}}{\lambda (\text{nm})} \quad (3)$$

Thus, the photolysis rate constant,  $k_\lambda$ , in  $\text{min}^{-1} \text{nm}^{-1}$ , of ADN was calculated (Figure 2.2d). Referring to equation (2),

$$k_\lambda = -2.303 \epsilon_\lambda \phi_\lambda I_{0\lambda} \quad (4)$$

where  $\epsilon_\lambda$  ( $\text{cm}^2 \text{mol}^{-1}$ ),  $\phi_\lambda$  are measured values,  $I_{0\lambda}$  is the solar irradiance.

Integrating the curve in Figure 2.2d over the specified wavelength yields a net rate constant,  $k$ , of  $0.11 \text{ min}^{-1}$ , corresponding to a half-life for ADN of six minutes under these conditions.

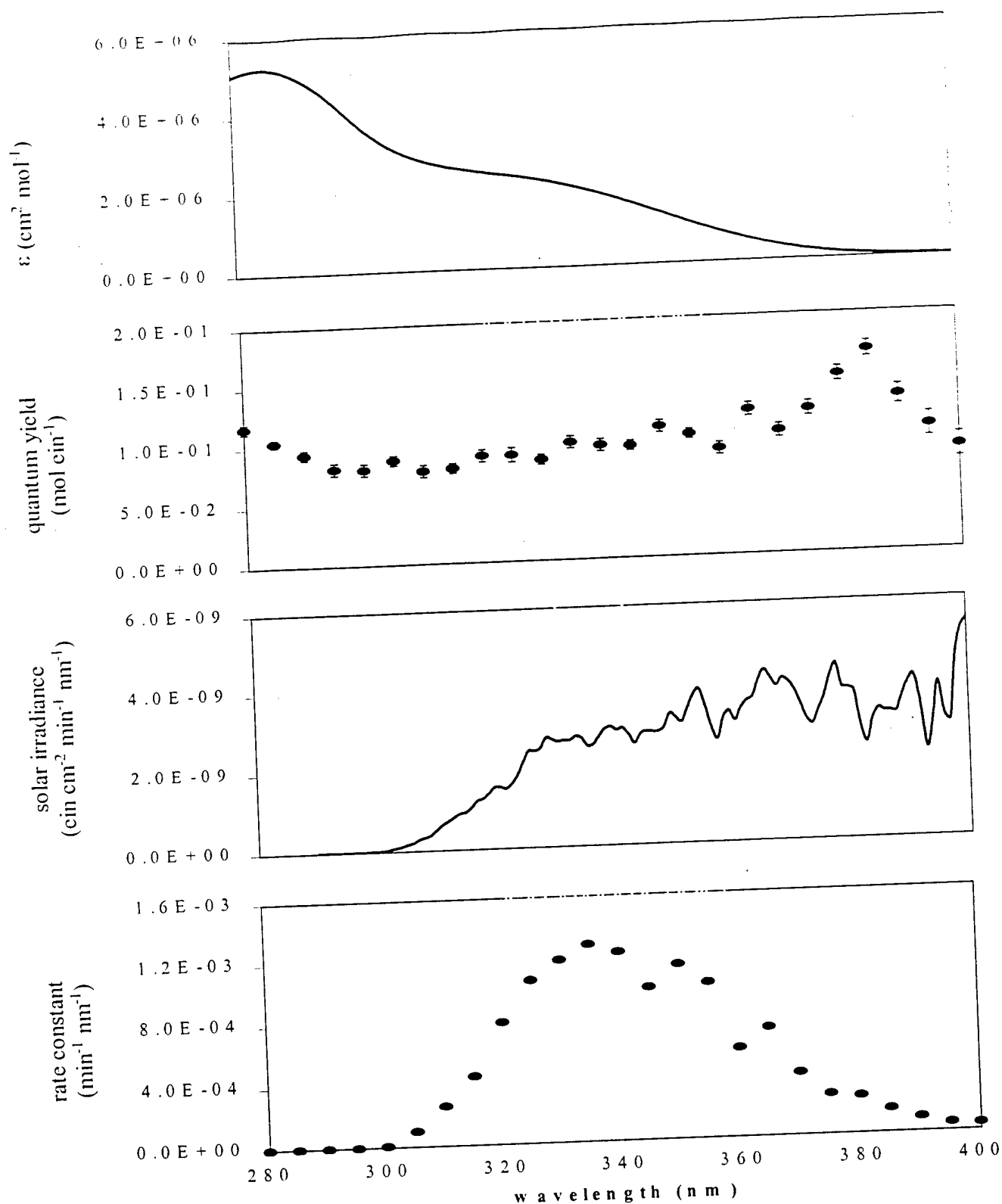


Figure 2.2. (a) Absorption spectrum of ADN. (b) Quantum yield for ADN photolysis, mean with 95% confidence interval is given. (c) Solar irradiance measured at noon on September 25<sup>th</sup>, 1998 in Syracuse, NY. (d) Predicted photolysis rate constants for ADN at surface, using irradiance data from (c).

### *Modeling photolysis rates at depths*

In order to predict the degradation rates at different depths, the quantum yields determined above were applied to a model that incorporated the absorption of light as it travels through the water column. The irradiance of sunlight in the water column was estimated using the following equation, derived from Lambert's Law (17):

$$E_{z,\lambda} = E_{0,\lambda} (10^{-\alpha_{\lambda} l_s}) \quad (5)$$

where  $E_{0,\lambda}$  and  $E_{z,\lambda}$  are the light intensities at depths of 0 and  $z$  meters respectively,  $\alpha_{\lambda}$  is the attenuation coefficient of the lake water and  $l_s$  is the path length the light must travel to reach depth  $z$ .

This path length is greater than the actual depth of deployment ( $z$ ) due to the refraction of light and is dependent on the nature of light as it hits the surface of the water – direct or diffuse (17). For analysis of the photodegradation of ADN, only UV radiation need be considered, as ADN does not absorb visible light. Due to scattering in the atmosphere, UV radiation is predominantly diffuse (18) – the irradiance of scattering is proportional to  $\lambda^{-4}$ . For diffuse light, Zepp *et. al.* derived a mean path length of  $1.2 z$  (19). For direct light,  $l_s$  varies from  $z$  to  $1.5z$  for solar zenith angles  $0 - 85^\circ$ . Although, UV radiation does have a direct component, a set value of 1.2 was used for the path length in the light absorption model.

Values for  $\alpha_{\lambda}$  were determined from the absorption spectra of the lake water. This coefficient accounts for absorption and not scattering. The latter is generally less significant in most natural waters for short wavelengths (20) and has been ignored in this work. Solar irradiance at four different depths, calculated by equation (4) is shown in Figure 2.3.

The validity of the above model was tested through deployment of ADN at different depths. The predicted concentration of ADN was derived using measured

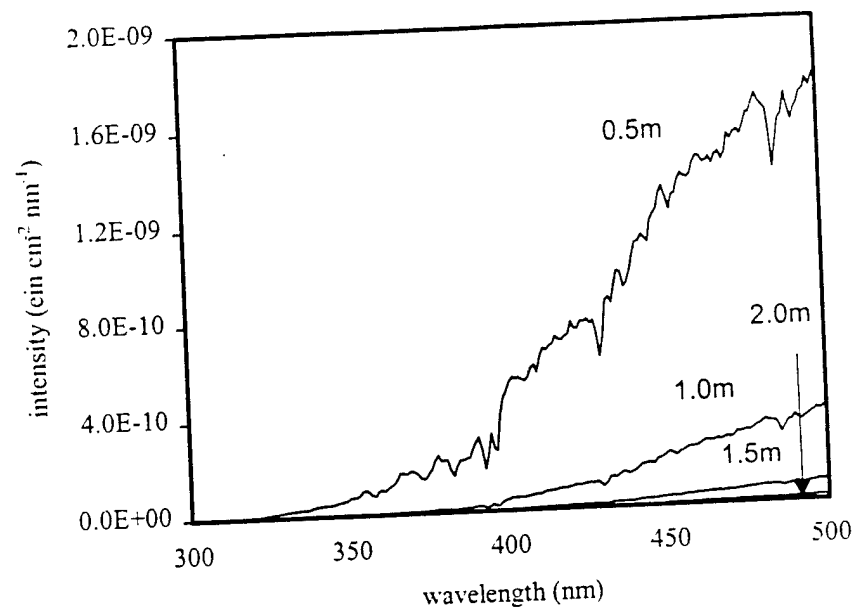


Figure 2.3. Modeled intensity at different depths in Onondaga Lake for solar irradiance of Figure 2 (c).

surface irradiances taken every twenty minutes in combination with the light attenuation model and this was compared to that actually measured, following six hours of exposure to sunlight. This is displayed for September 25<sup>th</sup>, 1998 in Figure 2.4. The predicted and measured values show the same decline in photolysis rate from the surface to 2m. In this case, actual degradation of ADN was greater than predicted at all depths. However, as seen in Figure 2.5, on average, over all the deployment dates, no systematic error is detected.

#### *Indirect Photolysis:*

The rate of direct photolysis of ADN decreases rapidly with increasing depth, due to the absorption of light that degrades ADN directly. However, indirect photolysis, photosensitized reaction of ADN by other chemicals in the water, may still be important. Humic acids, which have been shown to photosensitize various chemicals, can absorb visible light and therefore may cause photolysis at greater depths. Three experiments were performed in order to determine the importance of indirect photolysis on the overall photolysis rate of ADN.

First, ADN samples in humic solutions were irradiated with a  $< 400\text{nm}$  longpass cutoff filter. ADN, itself, does not absorb in this region and hence any degradation could be attributed to indirect photolysis. No degradation was observed.

Secondly, quantum yields at  $284\text{nm}$  were determined at a range of temperatures from  $5$  to  $30^{\circ}\text{C}$ . The rate of direct photolysis is not affected by temperature whereas any indirect reaction might be. Again, there was no evidence of indirect photolysis, as the quantum yield did not vary over this temperature range (Table 2.1).

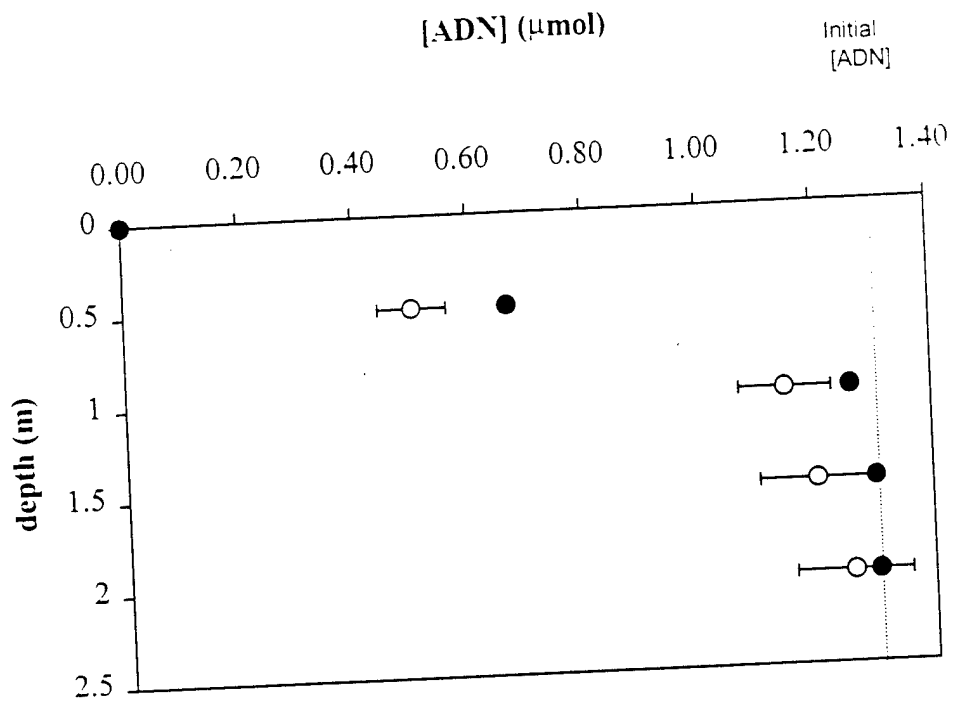


Figure 2.4. Predicted (●) and observed (○) concentrations of ADN remaining after six hour irradiation in Onondaga Lake on September 25<sup>th</sup>, 1998. Error bars are the 95 confidence interval on the observed values.



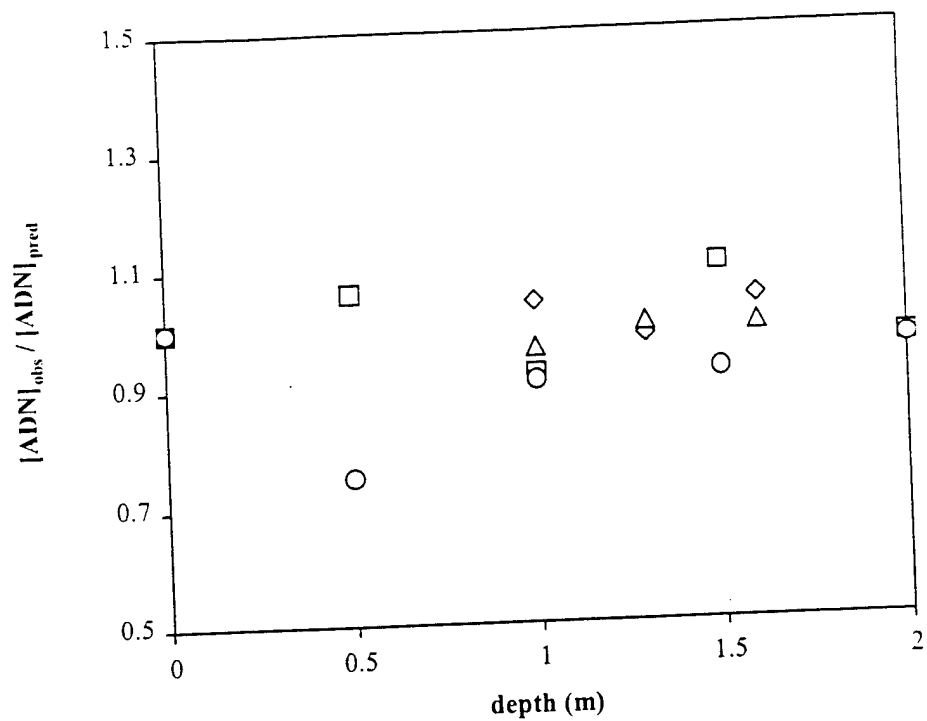


Figure 2.5. Ratio of  $[ADN]_{obs}$  to  $[ADN]_{pred}$  for different depths in Onondaga Lake on four sampling days: ( $\diamond$ ) 8/15/97, ( $\square$ ) 9/26/97, ( $\triangle$ ) 10/17/97, ( $\circ$ ) 9/25/98.

Table 2.1. Quantum yields ( $\phi_L$ ) for degradation of ADN at 284nm at four different temperatures in MilliQ and humic solutions.

Temperature ( $^{\circ}\text{C}$ )	$\phi_L$ (MilliQ) 95% C.I.	$\phi_L$ (Humics) 95% C.I.
5	$0.102 \pm 0.005$	$0.098 \pm 0.006$
15	$0.105 \pm 0.005$	$0.100 \pm 0.006$
25	$0.104 \pm 0.003$	$0.102 \pm 0.004$
35	$0.103 \pm 0.004$	$0.099 \pm 0.005$

Finally, the quantum yield of ADN in MilliQ water was compared to that in a humic solution. For this experiment, the shielding effect of the humic acids had to be taken into account as shown in the following equations:

$$\left\{ \frac{d[\text{ADN}]}{dt} \right\}_{\lambda} = -I_{\lambda} \phi_{\lambda} F_{s\lambda} F_{c\lambda} \quad (6)$$

where  $F_{s\lambda}$  is the fraction of incident light absorbed by the system (ADN and humics) and  $F_{c\lambda}$  is the fraction of that light that is absorbed by ADN itself (16).

$$F_{s\lambda} = 1 - 10^{-(A_{\lambda} + H_{\lambda})} \text{ and } F_{c\lambda} = \left\{ \frac{A_{\lambda}}{A_{\lambda} + H_{\lambda}} \right\} \quad (7)$$

where  $A_{\lambda}$  and  $H_{\lambda}$  are the absorption of ADN and the humic solution respectively at  $\lambda$  nm. The absorption of the humic acid solution was measured prior to irradiation and was assumed to remain constant throughout the six-hour irradiation. ADN absorbs very little of the light absorbed by the system and for the purpose of simplification,  $F_{s\lambda}$  is assumed to remain constant over the irradiation period.

Substituting into equation (6):

$$\text{rate} = -I_{\lambda} \phi_{\lambda} (1 - 10^{-H_{\lambda}}) \left\{ \frac{A_{\lambda}}{A_{\lambda} + H_{\lambda}} \right\} \quad (8)$$

This equation can be integrated using the Beer-Lambert Law to substitute for the absorption of ADN. The resulting equation is:

$$[\text{ADN}]_t - [\text{ADN}]_0 + \left( \frac{H_{\lambda}}{\epsilon_{\lambda} I} \right) \ln \left\{ \frac{[\text{ADN}]_t}{[\text{ADN}]_0} \right\} = -I_{\lambda} \phi_{\lambda} (1 - 10^{-H_{\lambda}}) t \quad (9)$$

Values for the quantum yield of ADN in humic solution were calculated by non-linear regression of the integrated rate equation (Table 2.2). Even at this high [DOC] (8.5 mgL<sup>-1</sup>), there is no statistically significant change in the quantum yield

Table 2.2. Absorbances of ADN ( $A_\lambda$ ) and Aldrich humic acid ( $H_\lambda$ ) solutions with measured quantum yields of ADN. For the quantum yields, values are 95% confidence intervals.

$\lambda$ (nm)	$A_\lambda$	$H_\lambda$	$\phi_\lambda$ (MilliQ) 95% C.I.	$\phi_\lambda$ (Humics) 95% C.I.
284	0.0067	0.2300	$0.104 \pm 0.003$	$0.102 \pm 0.004$
345	0.0021	0.1273	$0.110 \pm 0.004$	$0.107 \pm 0.006$
380	0.0002	0.0888	$0.176 \pm 0.006$	$0.184 \pm 0.012$

for ADN photolysis in the presence of dissolved organic matter at three representative wavelengths. Thus, the indirect photolysis of ADN is insignificant in comparison to its direct photolysis.

### *Significance of Results*

The predicted half-life of ADN in sunlit surface waters (depth < 0.1m) is approximately six minutes in the summer. ADN photodegrades slowly at greater depths ( $t_{1/2}$  for summer-time irradiation at 2m in Onondaga Lake is 15 years). This is purely a function of shielding by the dissolved organic matter present in the lake.

The light model used to predict the photodegradation of ADN is simple in that it ignores light scattering and assumes a constant value for the degree of refraction of incident light. However, a more elaborate model is not justified in this case as the extent of photolysis is predicted sufficiently accurately. This model might not work as effectively in a water body with less DOM where scattering would be a significant portion of the attenuation coefficient.

### References

1. Gilardi, R.; Flippen-Anderson, J.; George, C.; Butcher, R.J. *J. Am. Chem. Soc.* **1997**, 119, 9411.
2. Bottaro, J.C.; Penwell, P.E.; Schmitt, R.J. *J. Am. Chem. Soc.* **1997**, 119, 9405.
3. Borman, S. *C&E News*, **1994**, 18.
4. Mill, T.; Spanggord, R. GRA&I 6. Government Reports Announcements & Index, **1998**, Springfield, VA.

5. Gordon, L.; Hartley, W.R. In *Drinking Water Health Advisory: Munitions*; Lewis Publishers, Boca Raton, FL, 1992.
6. Sittig, M. In *Handbook of Toxic and Hazardous Chemicals and Carcinogens*; Noyes Publications, NJ, 1981.
7. Walsh, M.E.; Jenkins, T.F.; Schnitker, P.S.; Elwell, J.W.; Stutz, M.H. In Evaluation of SW846 Method 8330 For Characterization of Sites Contaminated with Residues of High Explosives. CRREL Report, 93. US Army Cold Regions Research and Engineering Laboratory, Hanover, NH, 1993.
8. Mabey, W.R.; Tse, D.; Baraze, A.; Mill, T. *Chemosphere*. **1983**, 12, 3.
9. Kinkead, E.R.; Salins, S.A.; Wolfe, R.E.; Marit, G.B. 1996. Acute and Subacute Toxicity Evaluation of Ammonium Dinitramide. GRA&I 6. Government Reports Announcement and Index, Springfield, VA.
10. Schmelling, D.C; Gray, K.A.; Kamat, P.V. *Environ Sci Technol* **1998**, 32, 971.
11. Spangord, R.J.; Gibson, B.W.; Keck, R.G.; Thomas, D.W. *Environ Sci Technol*. **1982**, 16, 229.
12. Zepp, R.G.; Braun, A.M.; Hoigné, J.; Leenheer, J.A. *Environ Sci Technol*. **1987**, 21, 485.
13. Burns, S.E.; Hassett, J.P.; Rossi, M.V. *Environ Sci Technol*. **1996**, 30, 2934.
14. Murov, S.L. In *Handbook of Photochemistry*; M. Dekker, New York, NY, 1973.
15. Hatchard, C.G.; Parker, C.A. *Proc Roy Soc (London)*. **1956**, A235, 518.
16. Zepp, R.G. *Environ Sci Technol*. **1978**, 12, 327.

17. Leifer, A.. In *The Kinetics of Environmental Aquatic Photochemistry*: ACS Professional Reference Book, American Chemical Society, Washington DC, 1988.
18. Sikorski, R.J.; Zika, R.G. *J Geophys Res.* **1993**, 98, 2315.
19. Zepp, R.G.; Cline, D.M. *Environ Sci Technol.* **1977**, 11, 359.
20. Duntley, S.Q. *Opt Soc Am.* **1963**, 53, 214.

### Chapter 3

#### Determining the Rate constant for the Reaction of Quadricyclane with $\text{HOO}/\text{O}_2^-$

##### Abstract

The indirect photolysis of quadricyclane, a high-energy compound, has been investigated. It has been proposed that quadricyclane is oxidized both by hydroperoxy and its conjugate base, superoxide. These radicals are produced by the photosensitization of dissolved organic matter. The kinetics of this reaction have been interpreted through the use of an enzymatic production technique (xanthine-xanthine oxidase) in concert with a specific probe (ferricytochrome C). A pH study was carried out in order to isolate the reactions of quadricyclane with hydroperoxy and superoxide; the two rate constants for the reactions of quadricyclane with these radicals are  $5.2 \times 10^6$  and  $2.7 \times 10^5 \text{ M}^{-1} \text{ min}^{-1}$  respectively. These rate constants are sufficiently high to provide a significant decay pathway for quadricyclane. For many bodies of water, the  $\text{pH} \gg \text{pK}_a$  of hydroperoxy and so the predominant species will be superoxide which has typical concentrations in natural waters in the nanomolar range. Therefore, the half-life of quadricyclane for indirect photolysis in shallow water (depth  $< 1 \text{ cm}$ ) is on the order of days. In addition, quadricyclane can be added to natural water samples at sufficiently high levels that it will outcompete other scavengers for superoxide. As such, the possibility of using quadricyclane as a probe for superoxide production in natural waters is investigated.



## Introduction

Quadricyclane, (tetracyclo[3.2.0.0.<sup>2,7</sup>0<sup>4,6</sup>]heptane), a strained cyclic hydrocarbon, has recently been suggested as an additive both to jet fuel and rocket propellant (1,2). It is ideally suited to these purposes due to its stability and high energy density – a factor of its high heat of formation and density. Prior to its wide-scale deployment, the environmental fate of quadricyclane should be considered as losses to the atmosphere, soil and watershed are inevitable. Specifically, photolysis of quadricyclane is presented in this paper and its relative importance as a possible degradative mechanism is considered.

Quadricyclane is considered a light nonaqueous phase liquid (LNAPL) for the purposes of modeling its movement in soil. As such, the liquid will migrate towards the capillary fringe; its further movement will depend on the degree of its solubility in groundwater. Quadricyclane undergoes acid hydrolysis to form two alcohols: nortricycyl alcohol and *exo*-5-norbornen-2-ol (3), both of which are more soluble than their parent compound. In addition, only nortricycyl alcohol undergoes biotic transformation, forming tricyclo[2.2.1.0<sup>2,6</sup>]heptan-3-one (4). Hence, to a large degree, the amount and identity of compounds found in the ground water following a spill will depend on the pH.

Prior to its present suggested function, quadricyclane was of interest to chemists because of the properties and reactions of it and its valence isomer, norbornadiene. For instance, the isomerization of this pair has long been considered as a possible means of storing solar energy (5). Norbornadiene is converted to

quadricyclane through the absorption of light. Then the reverse process can take place, releasing heat. Unfortunately, norbornadiene does not absorb light at wavelengths  $> 290$  nm (the minimum wavelength of light to reach the earth's surface), and so a sensitizer such as cuprous chloride or o-benzoylbenzoic acid must be added to the system (6).

The energy-releasing reaction ( $\Delta H = 92-110 \text{ kJmol}^{-1}$ ) (5,7) of quadricyclane is thought to proceed via a free radical-cation chain reaction where the quadricyclane radical cation rearranges to a norbornadiene radical cation. A ground-state quadricyclane molecule reacts with the norbornadiene radical cation, producing norbornadiene and another quadricyclane radical cation. This process is initiated by a photosensitized one-electron oxidation (8,9). The photocycloaddition of quinones with quadricyclane was also noted as side reaction (10).

Consideration of the photochemistry of quadricyclane must focus on its indirect photolysis as quadricyclane does not absorb light of wavelength  $> 290\text{nm}$ , the shortest wavelength to reach the earth's surface. Quadricyclane degrades in irradiated humic solutions. Tests were performed in order to identify the specific reactive transient responsible for this reaction (11). It was noted that no reaction took place in the absence of oxygen, suggesting one of the oxidants produced by the irradiation of humic acids:  $\text{OH}^\cdot$ ,  $^1\text{O}_2$ ,  $\text{HOO}^\cdot$ ,  $\text{O}_2^\cdot$ ,  $\text{H}_2\text{O}_2$  as the initiator. Quadricyclane underwent photolysis at the same rate in humic solutions in the presence of DMF (a singlet oxygen scavenger) and at approximately the same rate in the presence of methanol (a hydroxyl radical scavenger). The reaction of quadricyclane and hydrogen peroxide

was tested directly; no degradation was observed. Therefore, the hydroperoxy radical (HOO) and its conjugate base, the superoxide radical anion ( $O_2^-$ ) ( $pK_a = 4.8$ ) (12), are in all likelihood responsible for the humic sensitized photoreaction of quadricyclane.

In order to determine the rate constant for the reaction of quadricyclane with  $HOO/O_2^-$ , reactions were carried out using  $HOO/O_2^-$  generators and probes. This relatively stable radical can be produced enzymatically with the xanthine-xanthine oxidase system (13,14) and radiolytically by irradiating oxygenated water containing either methanol or formate (15,16). Ferricytochrome C is reduced by  $HOO/O_2^-$  and this reaction is well characterized at a large range of pH's (12). Nonetheless, there is some variation in reported rate constants,  $k_{cyt}$ . For example at pH 7, literature values range from  $2.7 \times 10^7$  to  $1.4 \times 10^8 \text{ M}^{-1}\text{min}^{-1}$  (17). Variability in the measured rate constants can partly be assigned to ionic strength differences as well as to the presence of trace contaminants such as copper.

There is even some uncertainty as to the  $pK_a$  of ferricytochrome C. Two studies reported  $pK_a$ s in the region of 7.4 and 9.2 in order to explain the observed pH dependence of  $k_{cyt}$  (18,19) but this could be an artifact of the experimental conditions. Butler *et al.* proposed in a later paper (20) that the apparent  $pK_a$  at 7.4 was due to Cu impurities which could react at near-diffusion controlled rates with  $HOO/O_2^-$  (12). The interference from Cu ions also depends on the pH; at pHs > 9, the predominant copper species will be hydrolysis complexes which might be less redox active (20). Due to the presence of low levels of Cu impurities in commercial ferricytochrome C preparations, chelating agents such as EDTA or DTPA are included in reaction

solutions. Butler reported that millimolar levels of EDTA were sufficient to counteract the interference from Cu impurities (20).

Koppenol *et al.* studied the effect of ionic strength on  $k_{\text{cyt}}$  in order to further explain discrepancies in reported values (21). Ionic strength will certainly have an impact on the observed rate constant of  $\text{O}_2^-$  and ferricytochrome C as they are both charged species.

$$\log k_{\text{cyt}}^{\text{obs}} = \log k_{\text{cyt}}^{I=0} + \frac{1.02 Z_A Z_B I^{1/2}}{1 + \alpha I^{1/2}} \quad (1)$$

The Brønsted equation, above, relates the variation in the observed rate constant,  $k_{\text{cyt}}^{\text{obs}}$  to the ionic strength,  $I$ , in terms of the charges,  $Z_A$ ,  $Z_B$  of the two species and a constant,  $\alpha$ , dependent on the minimum distance between them. As  $I$  increases, the charges on the reacting species are shielded from each other. In the case of  $\text{O}_2^-$  and ferricytochrome C, it was found that the apparent charge on ferricytochrome C at pH 7.9 was + 6.3 and the rate constant at  $I=0$  was determined to be  $1.9 \times 10^8 \text{ M}^{-1}\text{min}^{-1}$ . Consideration of these two artifacts: copper impurities and ionic strength differences account for observed differences in values of  $k_{\text{cyt}}$  at neutral pHs. Whereas Koppenol *et al.* reported  $k_{\text{cyt}} = 5.3 \times 10^7 \text{ M}^{-1}\text{min}^{-1}$  using 1 mM phosphate and 2 mM formate preparations, Butler *et al.* reported  $k_{\text{cyt}} = 2.4 \times 10^7 \text{ M}^{-1}\text{min}^{-1}$  using 10mM phosphate and 100mM formate solutions.

Clearly, in using ferricytochrome C as a probe of  $\text{HOO}/\text{O}_2^-$ , care must be taken in adjusting for both pH and ionic strength as well as chelating trace Cu. At present, there is confidence in the prediction of the pH dependence of  $k_{\text{cyt}}$ , based on a

single relevant  $pK_a$  of 9 (16, 22). Thus, a value of  $k_{cyt} = 6.6 \times 10^{-7} \text{ M}^{-1} \text{ min}^{-1}$  at  $pH = 9$  was applied in this paper (20,21).

The alkaline form of ferricytochrome C above  $pH = 9$  is not reduced by superoxide. This characteristic is unfortunate, as higher  $pH$  experiments are appealing due to the reduced rate of dismutation of  $\text{HOO}/\text{O}_2^-$ . Bielski *et al.* circumvented this problem by preserving ferricytochrome C at  $pH = 5.8$  before mixing it with a superoxide solution at  $pH = 9$ . The reduction of ferricytochrome took place more quickly than its configurational change; in effect,  $k_{cyt}$  at  $pH = 5.8$  was being measured but the superoxide solutions were maintained at a stable  $pH$  (16).

One last weakness in the ferricytochrome C probe system is directly related to its greatest strength. The reduction of ferricytochrome C is observed by monitoring the change in absorbance at 550nm; a simple and widely available method (23). However, increasingly, there is interest in probing the production of reactive transients by irradiated solutions of dissolved organic matter. Since ferricytochrome C absorbs strongly itself in the visible region, its photochemical applications are limited (24).

The reduction of ferricytochrome C by a given  $\text{HOO}/\text{O}_2^-$  generating system was monitored in order to determine the production rate of  $\text{HOO}/\text{O}_2^-$ . Then, quadricyclane was added to the same system and the reduction of ferricytochrome C was again monitored. Knowing the production rate of  $\text{HOO}/\text{O}_2^-$ , a rate constant for the competing reaction of  $\text{HOO}/\text{O}_2^-$  with quadricyclane could be calculated.

This reaction was performed at several pHs so that the rate constant of quadricyclane with both superoxide and hydroperoxy could be determined. Methanol was included in the reaction mixture in order to quench any reaction of quadricyclane with hydroxyl radicals. In addition, control experiments were performed in order to account for the disappearance of quadricyclane through hydrolysis.

Rate constants for the reaction of quadricyclane with  $\text{HOO}/\text{O}_2^-$  were determined, allowing prediction of the importance of indirect photolysis as a fate for quadricyclane in natural waters. In addition, the feasibility of using quadricyclane as a probe of  $\text{HOO}/\text{O}_2^-$  was considered.

### Experimental

**Materials:** Sodium hydroxide (99.99%), quadricyclane (~99%) and commercial humic acid, as the sodium salt, were obtained from Aldrich Chemical Company (Milwaukee, WI). Ferricytochrome C (>95%, from horse heart), xanthine oxidase (from buttermilk) suspension in a 60% saturated ammonium sulfate solution – 1.3U/mg protein, puriss. grade xanthine (99%) and superoxide dismutase (from bovine erythrocytes) – 3900 units/mg, were obtained from Fluka Chemical Company (Springfield, NJ). ACS grade EDTA and potassium hydrogen phthalate (KHP) were obtained from Fisher Scientific (Springfield, NJ). HPLC grade methanol was obtained from Allied Signal Inc. (Muskegon, MI). Ultrapure  $\text{KH}_2\text{PO}_4$  was obtained from J.T. Baker (Phillipsburg, NJ) and ACS grade sodium tetraborate decahydrate

and ACS grade hydrochloric acid were obtained from EM Science (Cherry Hill, NJ). All chemicals were used as received.

All solutions were made using water purified with a Millipore 4-bowl standard system (Millipore Corp., Chicago, IL); the water had a resistivity of greater than  $18\text{M}\Omega\text{cm}$  and will henceforth be referred to as MilliQ water.

Humic acid solutions were prepared using a variation of the method of Zepp *et al.* (25). Humic material (2g) was extracted with 2L of 0.1N sodium hydroxide solutions and pressure-filtered through a  $0.2\mu\text{m}$  capsule filter (Gelman Sciences #12117) at 4-6 psi. The filtrate was filtered again after adjustment to pH 6 with HCl. Humic acid working solutions were prepared as necessary by diluting the stock solution and using buffers to adjust the pH (26). Dissolved organic carbon (DOC) measurements were made on working humic solutions using external digestion with potassium persulfate and a Beckman Model 215A infrared analyzer.

**Methods:** HPLC: A Waters (Milford, MA) HPLC system was used to analyze the quadricyclane concentration with the following components: 515 pump, 717 plus autosampler, 996 photodiode array detector, Millennium chromatography manager, a  $3.9 \times 150\text{ mm}$  Novapak  $\text{C}_{18}$  column and a  $10\mu\text{l}$  sample loop. An isocratic mobile phase of 90% methanol and 10% MilliQ water was pumped at a flow rate of  $1\text{ml/min}$  and quadricyclane was monitored at  $210\text{nm}$ .

Stock quadricyclane solutions were prepared by adding  $20\mu\text{l}$  of quadricyclane to  $100\text{ml}$  of mM buffered solution, shaking the resulting mixture on a wrist-action

shaker and storing the solutions at 4°C. In addition, solutions with added methanol (OH scavenger) were used in order that the superoxide reaction could be isolated.

The reduction of ferricytochrome C was followed using a Spectronic® 20 Genesys™ spectrophotometer (Spectronic Instruments, Rochester, NY) and the molar absorption coefficients provided by Massey (23).

Buffer solutions of 0.001M were prepared with KHP,  $\text{KH}_2\text{PO}_4$ , sodium tetraborate decahydrate, HCl and NaOH. The pH was measured with an Acumet pH meter 915 (Fisher Scientific, Springfield, NJ). At this concentration of buffers, the general acid catalysis of quadricyclane is insignificant. In addition, at pHs < 7, quadricyclane undergoes hydrolysis observably. For experiments performed under these conditions, it is possible to account for this reaction (27).

In the experiments involving the enzymatic production of superoxide, 0.1 ml of EDTA (0.5 mM), 0.5ml ferricytochrome C ( $1.5 \times 10^{-4}\text{M}$ ) and 0.5 ml xanthine (8 mM) were added to 2.4 ml of a buffered quadricyclane solution (2mM) containing 50 mM methanol. Timing of the reaction began with the addition of 0.5 ml of xanthine oxidase (30nM). These experiments were repeated with added superoxide dismutase in order to test the extent of the reduction of ferricytochrome C by  $\text{HOO}/\text{O}_2^-$  as opposed to OH radicals. This enzyme catalyzes the dismutation of  $\text{HOO}/\text{O}_2^-$ ; thus, any reduction of ferricytochrome C observed in its presence will be due to alternative reactions (21).

Irradiations were performed with a Hanovia 450 W medium pressure Hg lamp housed in a reflector (Ace Glass #7883-02) and powered by an Ace Glass cased



power supply (#7830-60). The solutions were prepared in 13 x 100 mm Pyrex disposable culture tubes (Corning Inc., Corning, NY) with screw-cap vials with PTFE liners. Eight culture tubes were simultaneously irradiated using a merry-go-round apparatus.

### Results and Discussion

The degradation of quadricyclane in an irradiated humic solution was observed over four hours. This process could be modeled effectively by assuming either zero ( $r^2 = 0.99$ ) or first order kinetics ( $r^2 = 0.99$ ) (Figure 3.1). In order to interpret these results more fully, it was necessary to determine the rate constant of the reaction of quadricyclane with  $\text{HOO/O}_2^-$ .

The reduction of ferricytochrome C by  $\text{HOO/O}_2^-$  radicals in the xanthine-xanthine oxidase system was monitored by following the change in absorbance at 550nm. It has been determined that the molar absorption coefficients of both the reduced and oxidized form of this hemoprotein are relatively constant over the pH range 7-10 (13). Furthermore, the rate constant for this reaction is well characterized over this same pH range. Thus, the enzymatic production rate,  $P$ , of  $\text{HOO/O}_2^-$  at a range of pHs was determined by using published values for  $k_{\text{cyt}}$  (20), the second order rate constant for the reduction of ferricytochrome C,  $[\text{cyt}]_{\text{ox}}$ , with  $\text{HOO/O}_2^-$  and  $k_{\text{dis}}$ , (12) the second-order rate constant for the dismutation of  $\text{HOO/O}_2^-$ .

$$\frac{d[\text{cyt}]_{\text{ox}}}{dt} = -k_{\text{cyt}}[c_T][\text{cyt}]_{\text{ox}} \quad (2)$$

$$\frac{d[c_T]}{dt} = P - k_{\text{cyt}}[c_T][\text{cyt}]_{\text{ox}} - k_{\text{dis}}c_T^2 \quad (3)$$

$$c_T = [\text{O}_2^-] + [\text{HOO}] \quad (4)$$

An approximation can be made that the rate of dismutation of  $\text{HOO O}_2^-$  is insignificant in comparison to reaction with cytochrome, particularly as EDTA is added as a chelator for transition metals. In this case, the rate of reduction of ferricytochrome C is equal to the production rate of  $\text{HOO/O}_2^-$  radicals. This assumption is valid in that  $k_{\text{cyt}} \sim k_{\text{dis}}$  (Table 3.1) whereas  $[\text{cyt}] \gg [\text{c}_T]$  ( $\mu\text{M}$  vs.  $\text{nM}$ ). Thus, the gradient of a plot of ferricytochrome C concentration vs. time will be equal to the rate of production of  $\text{HOO/O}_2^-$  radicals (Table 3.1).

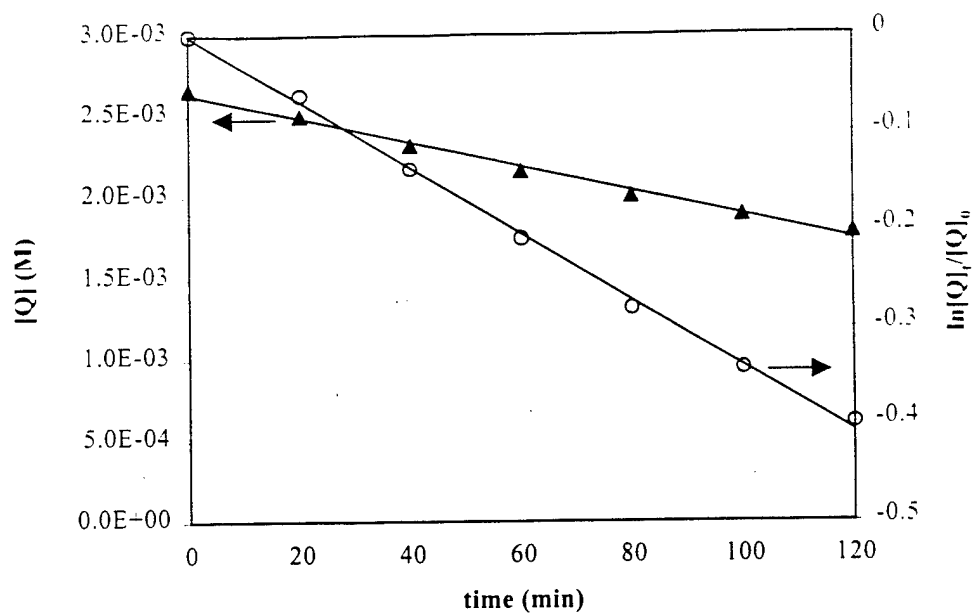


Figure 3.1. The degradation of quadricyclane in an irradiated humic solution,  
pH = 5.6.

(▲) 0<sup>th</sup> – order kinetics: [quadricyclane] vs. time, ( $r^2 = 0.996$ ),

(○) 1<sup>st</sup> – order kinetics:  $\ln \frac{[\text{quadricyclane}]_t}{[\text{quadricyclane}]_0}$  vs. time, ( $r^2 = 0.999$ )

In subsequent reactions, the test solution also contained 1.3mM quadricyclane. Since quadricyclane also reacts with  $\text{HOO}^-\text{O}_2^-$ , the observed decrease in rate of reduction of ferricytochrome C can be related to the competition for  $\text{HOO}^-\text{O}_2^-$  as shown for pH 7.02 in Figure 3.2. In this case, the relevant rate equations are as follows:

$$\frac{d[c_T]}{dt} = P - k_{\text{cyt}}[c_T][\text{cyt}]_{\text{ox}} - k_{\text{dis}}[c_T]^2 - k_Q[Q][c_T] \quad (5)$$

$$\frac{d[Q]}{dt} = -k_Q[Q][c_T] \quad (6)$$

$$\frac{d[\text{cyt}]_{\text{ox}}}{dt} = -k_{\text{cyt}}[c_T][\text{cyt}]_{\text{ox}} \quad (7)$$

$[Q]$  is the concentration of quadricyclane and  $k_Q$  is the observed second-order rate constant for the reaction of quadricyclane with  $\text{HOO}^-\text{O}_2^-$ . Since the production rate was already known, a value for  $k_Q$  was deduced using a non-linear regression in Figure 3.2, and the values for  $P$ ,  $k_{\text{cyt}}$ ,  $k_{\text{dis}}$  in Table 3.1. Curve fitting was performed on equations (5), (6), and (7) using Scientist Version 2.0, a MicroMath Scientific Software data fitting program. The curve was fit to the data for  $[\text{cyt}]_{\text{ox}}$ ; it was not possible to monitor  $[Q]$  and  $[c_T]$  during the reaction. Once a value for  $k_Q$  was

Table 3.1. Production rates of  $\text{HOO O}_2^-$  using xanthine-xanthine oxidase at different pHs and relevant rate constants:  $k_{\text{dis}}$ , the rate constant for the dismutation of  $\text{HOO O}_2^-$  (12),  $k_{\text{cyt}}$ , the rate constant for the reduction of ferricytochrome C with  $\text{HOO O}_2^-$  (20,21), and  $k_Q$ , the calculated rate constant for the reaction of quadricyclane with  $\text{HOO/O}_2^-$ .

pH	Production rate $\times 10^6 \text{ (Mmin}^{-1}\text{)}$	$k_{\text{dis}} \times 10^{-7}$ $\text{(M}^{-1}\text{min}^{-1}\text{)}$	$k_{\text{cyt}} \times 10^{-7}$ $\text{(M}^{-1}\text{min}^{-1}\text{)}$	$k_Q \times 10^{-5}$ $\text{(M}^{-1}\text{min}^{-1}\text{)}$
7.02	2.55	3.44	6.60	2.95
7.15	2.58	2.55	6.58	2.87
7.23	2.60	2.12	6.56	2.83
7.31	2.57	1.76	6.54	2.80
7.40	2.60	1.43	6.51	2.77
7.48	2.57	1.19	6.47	2.76
9.00	1.50	0.036	1.20	2.67

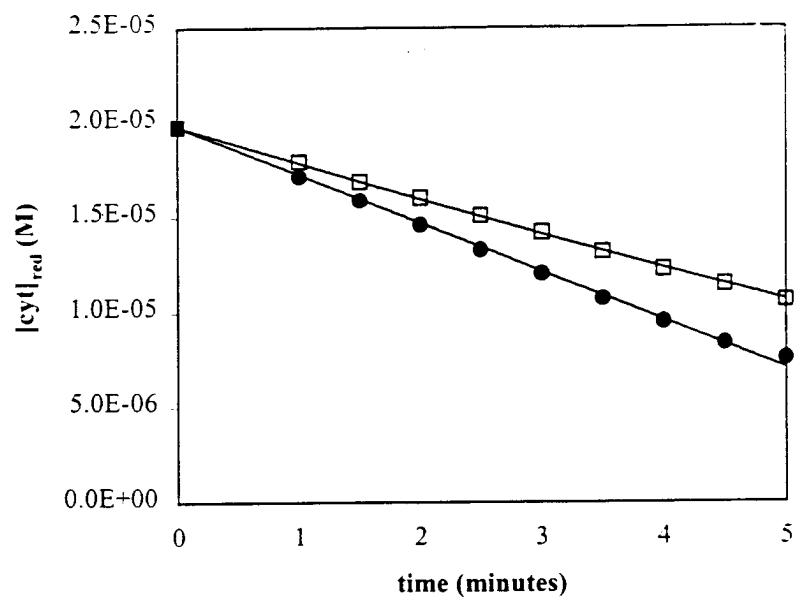


Figure 3.2. Reduction of ferricytochrome C by  $\text{HOO}/\text{O}_2^-$  at pH 7.02 in xanthine-xanthine oxidase system with (□) and (●) without quadricyclane present; the curves represent the fitted lines to the rate equations by non-linear regression.

determined at a particular pH, it was possible to predict the extent of reaction of quadricyclane and  $\text{HOO/O}_2^-$  by substituting for  $k_Q$  in equation (5). Quadricyclane concentration is predicted to be essentially constant as can be seen by the simulation at pH 7.02 in Figure 3.3;  $[Q]$  should decrease from 1.3mM to 1.296mM over the course of 5 minutes. In addition, the concentration of  $c_T$ , according to the model, was in the nanomolar range.

The rate constant,  $k_Q$ , varied from  $2.67 - 2.95 \times 10^5 \text{ M}^{-1}\text{min}^{-1}$  over the pH range 7.02 – 9.00. The variation of the determined value is due to relative concentrations of hydroperoxy and its conjugate base, superoxide ( $\text{pK}_a = 4.80$ ) (12). The specific values for the rate constant with superoxide and hydroperoxy were determined by calculating the ionization fractions,  $\alpha_i$ , and the specific rate constants,  $k_i$ .

$$\frac{[\text{HOO}]}{c_T} = \alpha_0 = \frac{[\text{H}^+]}{[\text{H}^+] + K_a} \quad (8)$$

$$\frac{[\text{O}_2^-]}{c_T} = \alpha_1 = \frac{K_a}{[\text{H}^+] + K_a} \quad (9)$$

$$k_Q = \alpha_0 k_0 + \alpha_1 k_1 \quad (10)$$

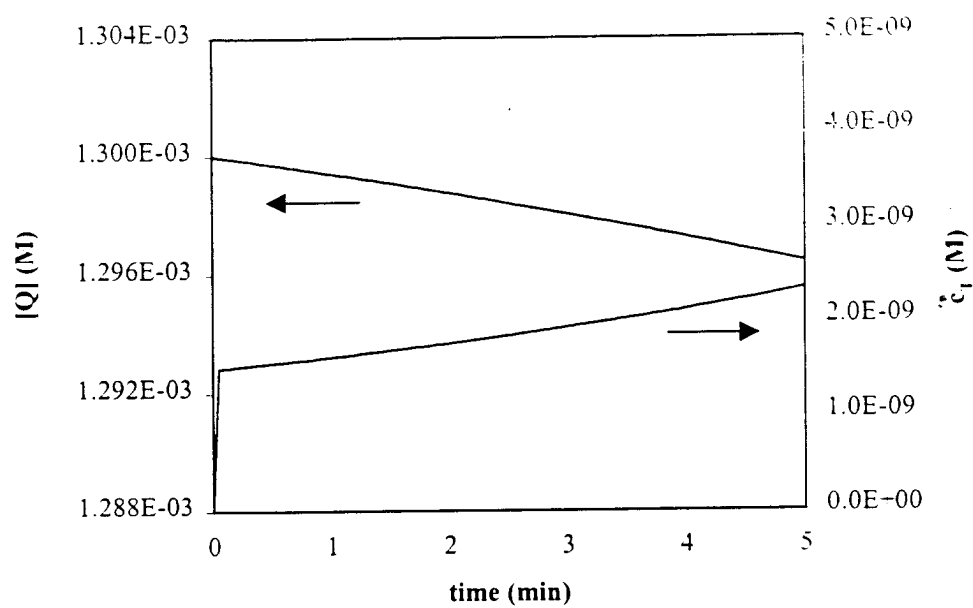


Figure 3.3. Simulation of [quadricyclane] and  $[\text{HOO}/\text{O}_2^-]$  during enzymatic production at pH 7.02 using model with best-fit value for  $k_Q$ , the rate constant for the reaction of quadricyclane with  $\text{HOO}/\text{O}_2^-$ .



Values for  $k_0$  and  $k_1$  were determined as  $(5.2 \pm 0.3) \times 10^6$  and  $(2.7 \pm 0.1) \times 10^5$   $\text{M min}^{-1}$  using non-linear regression of equations (8),(9),(10) with the literature value for  $K_a$  (12). The values for  $k_Q$  at different pHs as well as the fitted curve are shown in Figure 3.4. The excellent fit of the pH dependency of  $k_Q$  is consistent with the hypothesis that quadricyclane is reacting with  $\text{HOO}/\text{O}_2^-$ .

There is a degree of uncertainty in estimation for  $k_0$  and  $k_1$  due to the restricted range of pHs over which experiments were performed. Near-neutral pHs were chosen in part due to the constancy of ferricytochrome C's extinction coefficients in that region and also because ferricytochrome C has been of particular interest to biochemists and so there have been numerous studies of ferricytochrome C's reactivity in that pH range. The absolute value of  $k_Q$  is linked to that of ferricytochrome C with its inherent uncertainties.

The reported error in  $k_0$  and  $k_1$  is experimental and does not account for the error in literature value of  $k_{\text{cyt}}$ . Other workers have reported an error of 10% for similar experiments (21) and so it is reasonable to do the same for  $k_{\text{cyt}}$ ; this will confer an additional 10% uncertainty to the calculated value of  $k_Q$ . This error will be propagated to  $k_0$  and  $k_1$  depending on their relative contribution to  $k_Q$ ; see equation (10). In the pH range of our experiments, this will necessarily confer a large uncertainty onto  $k_0$  as the concentration of HOO is so low;  $\alpha_0 = 6.3 \times 10^{-4}$  at pH = 8. However, the fit of the observed values of  $k_Q$  to equation (10) at pH 7 – 9 is sufficient for use of interpolating values of  $k_Q$  anywhere in that range; that error is simply due to error in  $k_{\text{cyt}}$ .

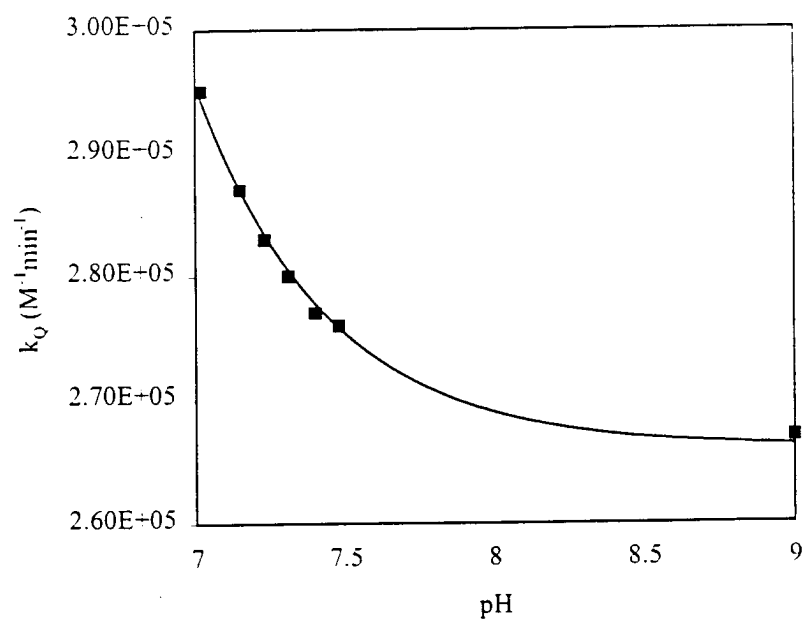


Figure 3.4. Variation of observed  $k_Q$ , rate constant for the reaction of quadricyclane with  $HOO/O_2^-$ , with pH in enzymatic experiments. The curve represents the fit to a model that describes the variation in  $k_Q$  due to the ionization fractions of  $HOO$  and  $O_2^-$  radicals.

The higher rate constant for HOO vs.  $O_2^-$  is not unusual. Gebicki and Bielski have noted this phenomenon for linoleic acid, alanine and cysteine (28). For these compounds, values for  $k_0$  and  $k_1$  were  $1.8 \times 10^4$  and  $0.26 \times 10^4$  and  $3.6$ ,  $3.6 \times 10^4$  and  $9 \times 10^2 \text{ M}^{-1} \text{ min}^{-1}$  respectively.

Once  $k_Q$  had been determined, it was possible to deploy both ferricytochrome C and quadricyclane as probes of HOO/ $O_2^-$  production using conditions that would ensure that all other reactions were insignificant. Separate Aldrich humic solutions,  $[\text{DOC}] = 8.5 \text{ mgL}^{-1}$ , buffered at  $\text{pH}=8.5$ , containing quadricyclane (2mM) and ferricytochrome C (20 $\mu\text{M}$ ) were irradiated in Pyrex tubes with a medium pressure Hg amp. EDTA (0.5mM) was included in both samples to minimize alternative reactions of HOO/ $O_2^-$ .

It was assumed that the rate of degradation of quadricyclane and the rate of reduction of ferricytochrome C would be equal to the rate of production of HOO/ $O_2^-$ . The quadricyclane samples were irradiated for up to 90 minutes to allow observable reaction while the ferricytochrome solutions were irradiated for no more than 5 minutes to avoid complete reaction.

Solutions of ferricytochrome C without added humic acids were irradiated in order to test for photoreduction of ferricytochrome C (Figure 3.5). Since the concentration of the product first increases and then decreases, it appears that both ferri- and ferro-cytochrome C are photoreactive. However, during the course of the experiment ( $< 30$  minutes), their reactivity is quite predictable. This alternative reduction of ferricytochrome was factored out of the observed reaction that took place

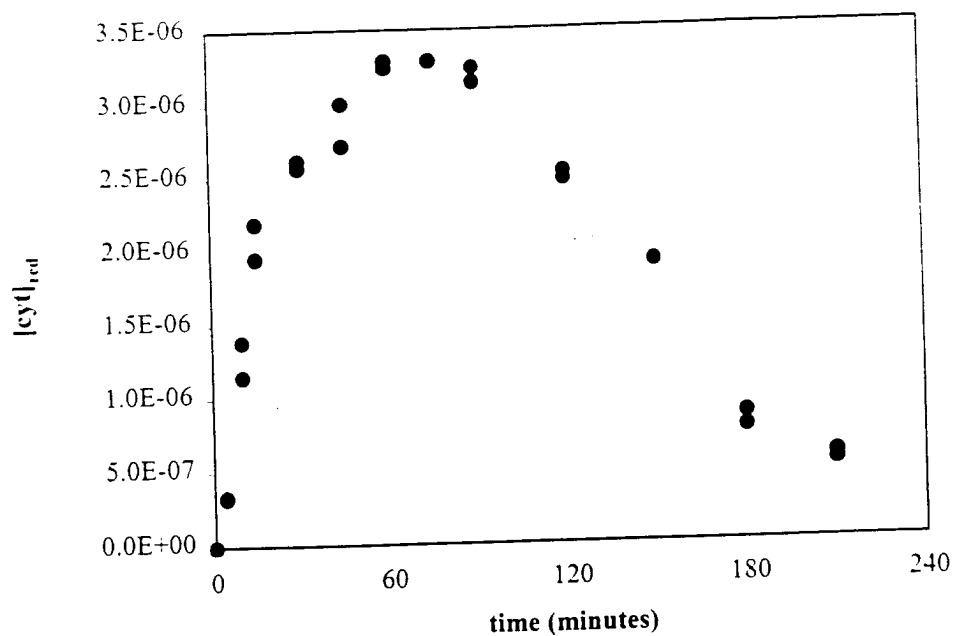


Figure 3.5. Reduction of ferricytochrome C ( $cyt_{ox}$ ) to ferrocyanochrome C ( $cyt_{red}$ ) in irradiated MilliQ water.

in the presence of humic acids. The calculated production rates were  $(2.98 \pm 0.25) \times 10^{-6}$  and  $(2.79 \pm 0.02) \times 10^{-6} \text{ M min}^{-1}$  (95% confidence interval) from the quadricyclane and ferricytochrome C solutions, respectively. The two production rates are not significantly different; however, ferricytochrome C is not ideal for photochemical experiments due to the uncertainties in its own photoreactivity. Quadricyclane does not absorb light of wavelength  $> 290 \text{ nm}$  and so is more suited for reactions involving light.

#### *Environmental fate of quadricyclane:*

The kinetics exhibited during the degradation of quadricyclane in irradiated humic solutions (Figure 3.1) become clearer after rate constant,  $k_Q$  has been determined. Typical half-lives of quadricyclane in natural waters due to indirect photolysis may be determined by applying typical production rates of  $\text{HOO}/\text{O}_2^-$ .

$$\frac{d[c_T]}{dt} = P - k_Q[\text{quad}][c_T] - k_{\text{dis}}[c_T]^2 - k'_{\text{sink}}[c_T] \quad (11)$$

where  $k'_{\text{sink}}$  is the pseudo-first order rate constant for all other reactions – sinks such as reactions with transition metals as well as dissolved organic matter (29). It has been proposed that in fact the uncatalyzed dismutation of superoxide is insignificant in comparison to these other reactions in natural waters (30).

If quadricyclane were present in an aqueous system at high levels (2.5mM), its degradation rate would be equal to the production rate of  $\text{HOO}/\text{O}_2^-$  as all the other terms in equation (11) would be insignificant. This is based on the values:  $k_Q = 9.3 \times 10^5 \text{ M}^{-1} \text{ min}^{-1}$ ,  $k_{\text{dis}} = 6.9 \times 10^8 \text{ M}^{-1} \text{ min}^{-1}$ ,  $k'_{\text{sink}} \sim 50 \text{ min}^{-1}$  (29) and  $c_T \sim \text{nM}$  for pH 5.6.

As such, it would be appropriate to apply zero-order kinetics to the irradiation shown in Figure 3.1.

Marine production rates of  $\text{HOO}/\text{O}_2^-$  have been estimated at  $6 \times 10^{-9} \text{ M min}^{-1}$  (30). For an initial quadricyclane concentration of 2mM, such as might be encountered in the case of a spill, the half-life would be on the order of 100 days whereas the half-life due to hydrolysis is approximately 185 days at pH=7 and 1850 days at pH =8. In effect, indirect photolysis provides a significant sink for quadricyclane.

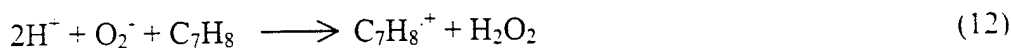
#### *Quadricyclane as a probe for $\text{HOO}/\text{O}_2^-$ :*

The indirect photolysis of quadricyclane provides an important sink for this hydrocarbon. In addition, a better understanding of the kinetics and mechanism of this process allows the use of quadricyclane as a probe for  $\text{HOO}/\text{O}_2^-$  formation in natural waters. The values for the rate constant of quadricyclane were determined indirectly; the decrease in rate of reduction of ferricytochrome was attributed to scavenging of  $\text{HOO}/\text{O}_2^-$  radicals by quadricyclane. Direct measurements of the disappearance of quadricyclane in the enzymatic experiments were not possible due to analytical limitations. Quadricyclane concentrations in the experiments were sufficiently high that its degradation was undetectable.

The competition kinetics of probe reactions have been described at length (24). Chemical probes are generally applied at one of two concentrations: high enough to outcompete all other reactions or sufficiently low so as not to affect the

steady state concentration of the radical under investigation. The former technique was applied in this work.

A further consideration of the reaction of quadricyclane with  $\text{HOO O}_2^-$  is the identification of products and the possibility of their subsequent reaction with the same radicals. No products have been observed through HPLC with photodiode array or GC with flame ionization detector (11). It is assumed that the first step of the reaction of quadricyclane is as follows:



This reaction is likely due to the extremely low oxidation potential of quadricyclane ( $E^0 = 0.9 \text{ v}$ ); itself a feature of the strained structure (31). Combining this half-reaction with the reduction of superoxide ( $E^0 = 0.89 \text{ v}$ ) (32), will result in a value of  $E^0 = 1.79 \text{ v}$  for reaction (12) at  $\text{pH} = 7$ , and using the Nernst equation to predict cell potential at non-equilibrium conditions:

$$E = E^0 - \frac{RT}{nF} \ln Q \quad (13)$$

where  $Q$  is the reaction quotient,  $T$  is the absolute temperature,  $R$  is the universal gas constant,  $F$  is Faraday's constant,  $n$  is the number of electrons involved in the reaction and  $E$  is the cell potential. The concentration of the quadricyclane radical cation is assumed to be very low in natural waters, a fact which will only increase the value of  $E$  for this reaction. Thus, this reaction will have a large positive  $E$  and hence large negative Gibbs free energy and so thermodynamically, this reaction should proceed.

Subsequently, the quadricyclane radical cation can be converted to a norbornadiene radical cation and hence to a norbornadiene molecule through the

oxidation of another quadricyclane molecule. This chain reaction has been observed for other photosensitized one-electron oxidations (7,8). However, it appears that this reaction is not an important one under the experimental conditions employed for this paper (enzymatic or irradiated humic production of radicals), as norbornadiene can readily be identified concurrently with quadricyclane in the HPLC method used and yet none was observed. Alternatively, the quadricyclane radical cation could add onto the humic matrix, thus preventing product identification. For the purpose of determining the kinetics of the reaction of quadricyclane, the end-products are unimportant as long as the initial step is indeed rate limiting as is assumed here.

In using quadricyclane as a probe of  $\text{HOO}/\text{O}_2^-$  production, it is important to determine the distribution of quadricyclane between the humic substances and the bulk solution. It has been determined that the kinetics of humic photoreactions cannot be accurately described assuming a homogeneous nature for the humic solution for compounds that bind to humic matter (26). Using the UNIFAC estimation technique, activity coefficients for quadricyclane in water,  $\gamma^w$ , and in octanol ( $\gamma^o$ ) were determined (33),  $K_{ow}$  can be calculated knowing these parameters ( $\gamma^o/\gamma^w$ ). Then a value for the organic carbon partition coefficient,  $K_{oc}$ , was predicted on the basis of a linear free-energy relationship between  $K_{oc}$  and  $K_{ow}$  (34). It appears that quadricyclane resides primarily in the bulk solution with the dissolved fraction  $\sim 0.998$ , a value so close to 1 that order-of-magnitude errors in  $K_{oc}$  estimation will not affect the conclusion. Apparent production rates within the humic matrix may be



very different due to the possibility of scavenging of  $\text{HOO O}_2^-$  by the DOM itself (29).

Provided that precautions are taken to account for its hydrolysis and reaction with OH radical, quadricyclane provides a simple means of probing the production rate of  $\text{HOO/O}_2^-$ . The relevant rate constants were determined using an enzymatic system and their variation with pH was predicted well on the basis of ionization fractions. Consequently, production rates of  $\text{HOO/O}_2^-$  in an irradiated humic solution, measured simultaneously by quadricyclane and ferricytochrome C, were compared with very good agreement.

#### References

1. Alberici, F.; Cassar, L.; Monti, F.; Neri, C.; Nodari, N. 1991. High-Energy-Content Fuel Composition containing quadricyclane. US patent no. US5076813
2. Nichols, R.; McKelvey, T.A.; Rodgers, S.L. 1997. High Energy Rocket Propellant. US patent no. US561882.
3. Hill, W.E.; Szechi, J.; Hofstee, C.; Dane, J.H. *Environ. Sci. Technol.* **1997**, 31, 651.
4. Jin, S.; Swoboda-Colberg, N.G.; Colberg, P.J.S. *Can. J. Microbiol.* **1997**, 43, 300.
5. Laird, T. *Chem. Ind.* **1976**, 186-193.
6. Sasse, W.H.F. Solar power and fuels : proceedings of the First International Conference New York : Academic Press, 1977, 227 – 245.
7. Inadomi, Y.; Morihashi, K.; Kikuchi, O. *Theochem*, **1998**, 434, 59.

8. Ishiguro, K.; Khudyakov, I.V.; McGarry, P.F.; Turro, N.J.; Roth, H.D. *J. Am. Chem. Soc.* **1994**, 116, 6933.
9. Kirkor, E.S.; Maloney, V.M.; Michl, J. *J. Am. Chem. Soc.* **1990**, 112, 148.
10. Goetz, M.; Frisch, I. *J. Am. Chem. Soc.* **1995**, 117, 10486.
11. Burns, S.E. Personal communication.
12. Bielski, B.H.J.; Cabelli, D.E.; Arudi, R.L. *J. Phys. Chem. Ref. Data.* **1985**, 14, 1041.
13. Fridovich, I. *J. Biol. Chem.* **1970**, 245, 4053.
14. McCord, J.M.; Fridovich, I. *J. Biol. Chem.* **1968**, 243, 5753.
15. Bielski, B.H.J.; Arudi, R.L. *Anal. Biochem.* **1983**, 133, 170.
16. Bielski, B.H.J.; Richter, H.W. *J. Am. Chem. Soc.* **1977**, 99, 3019.
17. Ross, A.B.; Mallard, W.G.; Helman, W.P.; Buxton, G.V.; Huie, R.E.; Neta, P. NIST Standard Reference Database 40, Solution Kinetics Database. 1994.
18. Butler, J.; Jayson, G.G.; Swallow, A.J. *Biochim. Biophys. Acta.* **1975**, 408, 215.
19. Seki, H.; Ilan, Y.A.; Ilan, Y.; Stein, G. *Biochim. Biophys. Acta.* **1976**, 440, 573.
20. Butler, J.; Koppenol, W.H.; Margoliash, E. *J. Biol. Chem.* **1982**, 257, 10747.
21. Koppenol, W.H.; Van Buren, K.J.H.; Butler, J.; Braams, R. *Biochim. Biophys. Acta.* **1976**, 449, 157.
22. Fridovich, I. In *CRC Handbook of Methods for Oxygen Radical Research*; Greenwald, R.A., Ed.; CRC Press: Boca Raton, FL; 1985, pp 121-122.
23. Massey, V. *Biochim. Biophys. Acta.* 1959, 34, 255.

24. Blough, N.V.; Zepp, R.G. In *Active Oxygen in Chemistry*; Foote, C.S.; Valentine, J.S.; Greenberg, A.; Liebman, J.F., Eds.; Blackie Academic and Professional: New York; 1995, pp 280-333.
25. Zepp, R.G.; Braun, A.M.; Hoigné, J.; Leenheer, J.A. *Environ. Sci. Technol.* **1987**, 21, 485.
26. Burns, S.E.; Hassett, J.P.; Rossi, M.V. *Environ. Sci. Technol.* **1996**, 30, 2934.
27. Beretvas, M.K.; Hassett, J.P.; Basford, T.M. In preparation.
28. Gebicki, J.M.; Bielski, B.H.J. *J. Am. Chem. Soc.* **1981**, 103, 7020.
29. Voelker, B.M. Preprints of Extended Abstracts, ACS, 1998.
30. Zafiriou, O.C.; Voelker, B.M.; Sedlak, D.L. *J. Phys. Chem.* **1998**, 102 A, 5693.
31. Stearns, R.A.; Ortiz de Montellano, P.R. *J. Am. Chem. Soc.* **1985**, 107, 4081.
32. Sawyer, D.T.; Valentine, J.S. *Acc. Chem. Res.* **1981**, 14, 393.
33. Gmehling, J.; Rasmussen, P.; Fredenslund, A. *Ind. Eng. Chem. Process Des. Dev.* **1981**.
34. Karickhoff, S.W. *Chemosphere*. **1981**, 10, 833.

## Chapter 4

### Production Rates of $\text{HOO}/\text{O}_2^-$ in Aldrich Humic Solutions

#### Abstract

The pH dependence of the production of hydroperoxy ( $\text{HOO}$ ) and superoxide radicals ( $\text{O}_2^-$ ) from irradiated humic solutions was monitored using a novel probe, quadricyclane. High concentrations of the probe were used in order that it effectively scavenged all the radicals and thus its decay rate was equal to the production rate of the radicals. The variation of production rate with pH was related to possible production mechanisms. Additionally, chloroethanol, a scavenger of hydrated electrons ( $e^-_{\text{(aq)}}$ ), was added to irradiated solutions to elucidate whether this reactive species, ( $e^-_{\text{(aq)}}$ ), is an intermediate in the production of  $\text{HOO}/\text{O}_2^-$ . The decrease in production rate of  $\text{HOO}/\text{O}_2^-$  with increasing pH in conjunction with the undetectable effect of the addition of chloroethanol indicates that the most significant formation pathway involves the transfer of an electron from an excited state of the dissolved organic matter to molecular oxygen.

#### Introduction

$\text{HOO}/\text{O}_2^-$  is formed during sunlight irradiation of natural waters. The two possible paths of production involve either the direct transfer of an electron from an excited state of dissolved organic matter, DOM, ( $^3\text{DOM}$ ) to molecular oxygen ( $\text{O}_2$ ) or the reaction of  $\text{O}_2$  with a hydrated electron that was produced from the photoionization of DOM (1,2). It has been suggested that semiquinone radical anions within the humic

matrix are specifically responsible for the former mechanism (3) whereas the latter mechanism seems unlikely in view of the low formation rates of hydrated electron (4).

Measured values for the production rate of superoxide in natural waters range from  $6 \times 10^{-11}$  to  $6 \times 10^{-9} \text{ M min}^{-1}$  (5,6) while steady state concentrations range from  $10^{-11}$  to  $10^{-8} \text{ M}$  (5,7). Most measurements thus far have been for marine systems but estimates of fresh water production rates are  $\sim 2 \times 10^{-9} - 2 \times 10^{-7} \text{ M min}^{-1}$  (8). Predicted fresh water rates are higher than those for marine waters because of the higher dissolved organic carbon concentration, [DOC], generally observed in fresh water samples. The dependence of production rates on [DOC] has been observed for photosensitized reactions such as the production rate of hydrogen peroxide (9) and since superoxide is considered to be the primary precursor of hydrogen peroxide (10), a similar relationship for superoxide is appropriate.

The chemistry, and in particular the fate, of  $\text{HOO}/\text{O}_2^-$  in natural waters is still somewhat uncertain. Originally, it was assumed that dismutation of  $\text{HOO}/\text{O}_2^-$  to form  $\text{O}_2$  and  $\text{H}_2\text{O}_2$  was the most important sink of  $\text{HOO}/\text{O}_2^-$ . However, at pHs of most natural water systems (pH 7–8.5), given that the  $\text{pK}_a$  of HOO is 4.8 (11),  $\text{O}_2^-$  is the predominant species.  $\text{O}_2^-$  reacts far more slowly with  $\text{O}_2^-$  ( $0.3 \text{ M}^{-1}\text{s}^{-1}$ ) than either it reacts with HOO ( $7.61 \times 10^5 \text{ M}^{-1}\text{s}^{-1}$ ) or than HOO reacts with itself ( $8.86 \times 10^7 \text{ M}^{-1}\text{s}^{-1}$ ) and so this loss mechanism is in fact of minimal importance (12). The possibility of other scavengers was proposed in explaining why the production rate of  $\text{H}_2\text{O}_2$  was increased as superoxide dismutase (SOD) was added to the system (5). In effect, there was an alternative sink of superoxide other than its dismutation. As SOD was

added in higher concentrations, it could compete effectively for  $\text{HOO/O}_2^-$ . The alternative sinks were grouped together by a pseudo-first order rate constant,  $k'_{\text{sink}}$ , assuming a constant concentration of the sink species. Initial values for  $k_{\text{sink}}$  were estimated as  $0.15 \text{ min}^{-1}$ , but this prediction is based on the assumption that all the  $\text{H}_2\text{O}_2$  formed in the absence of SOD was produced only by the disproportionation of  $\text{HOO/O}_2^-$ .

The identity of this sink for  $\text{HOO/O}_2^-$  was initially thought to be Fe (III) (13) or Cu(II) (7) as the reaction of these metals with  $\text{HOO/O}_2^-$  occurs at nearly diffusion controlled rates. These reactions were considered important even though both of these metals will to a large degree be complexed in natural waters. However, it was later observed that even when EDTA was added as a complexing agent of these metal species, there was still an ill-defined loss mechanism. The only treatment that seemed to reduce the activity of this sink was bleaching of the natural waters, suggesting reaction with the dissolved organic matter as a possible fate (6). Values for this rate constant were determined as  $12 - 84 \text{ min}^{-1}$  for coastal waters.

The variation of production rates of these radical species with pH gives some indication of their formation as well as their potential fates. The structure of the humic acids, themselves, will change with pH, particularly at the  $\text{pK}_a$ s of predominant functional groups such as carboxylic and phenolic moieties. The stability of the superoxide/hydroperoxy group is also a function of the pH in terms of dismutation rate (11). Certainly, steady state concentrations of  $\text{HOO/O}_2^-$  will depend on the

concentration and speciation of transition metals as well as the nature of the DOM. It is clear that pH will affect both the formation and destruction of  $\text{HOO/O}_2^-$ .

Further insight into the formation mechanism can be gained through inclusion of scavengers of the hydrated electron such as chloroethanol. Thus, a discussion of production rates will necessarily involve consideration of all these factors. In this paper, the focus is a comparison of production rates over the pH range: 4–12.

Quadricyclane, a strained cyclic hydrocarbon, appears to react with both the hydroperoxy radical and the superoxide anion (14). The rate of reaction of quadricyclane is such that the dismutation of  $\text{HOO/O}_2^-$  is insignificant in comparison to its reaction with millimolar concentrations of quadricyclane. Thus, if humic solutions of quadricyclane are irradiated, the production rate of this pair of radicals can be determined through measurement of the degradation of quadricyclane. Hence, the variation of production rates with pH can be interpreted, providing some insight into the mechanism of formation of  $\text{HOO/O}_2^-$ .

Quadricyclane is a useful probe for  $\text{HOO/O}_2^-$  as it can be used over a wide range of pHs, provided that its acid hydrolysis (15) is accounted for through the use of control experiments. In addition, the possible reaction of quadricyclane with the hydroxyl radical should be quenched through the addition of a scavenger such as methanol.

Values for  $k_Q$ , the rate constant of quadricyclane with  $\text{HOO/O}_2^-$  were determined using an enzymatic mode of production, the xanthine-xanthine oxidase system, and a well-characterized probe of  $\text{HOO/O}_2^-$ , ferricytochrome C (14). The pH

dependence of the reaction was quantified by performing the experiment at different pHs and accounting for the varying reaction rate of  $\text{HOO/O}_2^-$  with the different forms of ferricytochrome C (16). The experimental conditions were such that the possible reactions of  $\text{HOO/O}_2^-$  were with ferricytochrome C, quadricyclane or possibly bimolecular dismutation. The dismutation of  $\text{HOO/O}_2^-$  was deemed insignificant in comparison to the other reactions given the low concentration of  $\text{HOO/O}_2^-$  present. Values for the dismutation rate constant have been determined under many different conditions (11). EDTA was included in the reaction mixture as a chelating agent for trace metals present that might react with  $\text{HOO/O}_2^-$ . Values for  $k_Q$  are  $5.2 \times 10^6$  and  $2.7 \times 10^5 \text{ M min}^{-1}$  for the reaction of quadricyclane with  $\text{HOO}$  and  $\text{O}_2^-$  respectively. Using these values, it is possible to deploy quadricyclane as a probe for  $\text{HOO/O}_2^-$  production in irradiated humic solutions at a wide range of pHs.

The kinetics of probe systems has been described at length in the literature (17,18,19). Probes are added to reaction mixtures at a range of concentrations, allowing variation of the relative significance of the reaction with the probe as opposed to natural scavengers. In this manner, the production rate of the species of interest as well as its steady state concentration in the absence of the probe can be determined. Once the kinetics of the total reaction system is well understood, one of two methods is employed. Either the probe is used at such low concentrations that it does not alter the steady state concentration of the reactive species, or it is used at sufficiently high concentrations that the reaction of the species with the probe outcompetes all other reactions. In the former method, pseudo-1<sup>st</sup> order kinetics are



assumed for the reaction of the probe allowing determination of the unperturbed steady-state concentration of the species. In the latter case, the rate of reaction of the probe approaches the formation rate of the species. Both production rates and steady state concentrations are important to a fuller understanding of the chemistry of the species in natural waters.

At present  $\text{HOO/O}_2^-$  are not considered to be important to the degradation of many xenobiotics in natural waters. However, these radicals have a crucial role in the redox cycle of both DOM, through the cycling of quinones and semi-quinone radicals (20), and transition metals, holding transition metals in unstable oxidation states such as Cu(I) and Fe(II). As a result,  $\text{HOO/O}_2^-$  may indirectly play a role in the formation of other significant oxidants such as  $\text{OH}^\cdot$  and  $\text{H}_2\text{O}_2$ .

### Experimental

**Materials:** Sodium hydroxide (99.99%), quadricyclane (~99%) and commercial humic acid, as the sodium salt, were obtained from Aldrich Chemical Company (Milwaukee, WI). Puriss. grade 2-chloroethanol was obtained from Fluka Chemical Company (Springfield, NJ). ACS grade EDTA and potassium hydrogen phthalate were obtained from Fisher Scientific (Springfield, NJ). HPLC grade methanol was obtained from Allied Signal Inc. (Muskegon, MI). ACS grade hydrochloric acid and ACS grade sodium tetraborate decahydrate (borax) were obtained from E.M. Science (Gibbstown, NJ). Ultrapure  $\text{KH}_2\text{PO}_4$  and  $\text{K}_2\text{HPO}_4$  were obtained from J.T. Baker (Phillipsburg, NJ). All chemicals were used as received.

All solutions were made using water purified with a Millipore 4-bowl standard system (Millipore Corp., Chicago, IL); the water had a resistivity of greater than 18MΩcm and will henceforth be referred to as MilliQ water.

Humic acid solutions were prepared using a variation of the method of Zepp *et al.* (4). Humic material (2g) was extracted with 2L of 0.1N sodium hydroxide solutions and pressure-filtered through a 0.2μm capsule filter (Gelman Sciences #12117) at 4-6 psi. The filtrate was filtered again after adjustment to pH 6 with HCl. Humic acid working solutions were prepared as necessary by diluting the stock solution and using buffers to adjust the pH (21). Dissolved organic carbon (DOC) measurements were made on working humic solutions using external digestion with potassium persulfate and a Beckman Model 215A infrared analyzer.

#### **Methods:**

HPLC: A Waters (Milford, MA) HPLC system was used to analyze the quadricyclane concentration with the following components: 515 pump, 717 plus autosampler, 996 photodiode array detector, Millennium chromatography manager, a 3.9 x 150 mm Novapak C<sub>18</sub> column and a 10μl sample loop. An isocratic mobile phase of 90% methanol and 10% MilliQ water was pumped at a flow rate of 1ml/min and quadricyclane was monitored at 210nm.

Stock quadricyclane solutions were prepared by adding 25μl of quadricyclane to 100ml of buffered solution, shaking the resulting mixture on a wrist-action shaker and storing the solutions at 4°C. For all experiments, the concentration of

quadricyclane was related to a dark control to account for the hydrolysis of quadricyclane. In addition, solutions with added methanol (OH scavenger) were used in order that the superoxide reaction could be isolated.

Irradiations were performed with a Hanovia 450 W medium pressure Hg lamp housed in a reflector (Ace Glass #7883-02) and powered by an Ace Glass cased power supply (#7830-60). The solutions were prepared in Pyrex disposable culture tubes (Corning Inc., Corning, NY) with screw-cap vials with PTFE liners. Eight culture tubes were simultaneously irradiated using a merry-go-round apparatus.

Buffer solutions with concentrations of 0.001M were prepared with  $\text{KH}_2\text{PO}_4$ ,  $\text{K}_2\text{HPO}_4$ , KHP, borax, NaOH, HCl. The pH was measured with an Acumet pH meter 915 (Fisher Scientific, Springfield, NJ).

## Results and Discussion

### *Competition Kinetics:*

Humic solutions containing different concentrations of quadricyclane were irradiated in order to find the degree to which quadricyclane reacted with available  $\text{HOO}/\text{O}_2^-$ . The relevant rate equations are as follows:

$$\frac{d[c_T]}{dt} = P - k_Q[c_T][Q] - k'_{\sin k}[c_T] - k_{\text{dis}}[c_T]^2 \quad (1)$$

$$\frac{d[Q]}{dt} = -k_Q[c_T][Q] \quad (2)$$

Where  $c_T = [\text{O}_2^-] + [\text{HOO}]$

$k_Q$  is the apparent rate constant for the reaction of quadricyclane with  $\text{HOO}/\text{O}_2^-$ .

[Q] is the quadricyclane concentration.

$k_{dis}$  is the rate constant for the self-dismutation of  $\text{HOO/O}_2^-$ .

$k'_{sink}$  is the pseudo-first order rate constant for all other sinks of  $\text{HOO/O}_2^-$ .

The system can be greatly simplified if it is assumed that  $\text{HOO/O}_2^-$  reaches steady state and that the dismutation of  $\text{HOO/O}_2^-$  provides an insignificant sink of the radicals. Using published values for  $k_{dis}$  (11) and approximate values for  $c_T$  (nM), dismutation is negligible. In this case, the rate of reaction of quadricyclane with  $\text{HOO/O}_2^-$  can be derived:

$$R_Q = \frac{-d[Q]}{dt} = \frac{P[Q]}{\frac{k'_{sink}}{k_Q} + [Q]} \quad (3)$$

Figure 4.1 displays the variation of  $R_Q$  with [Q] at pHs of 5 and 8. Values for  $R_Q$  were determined by following the degradation of quadricyclane over a 10% drop

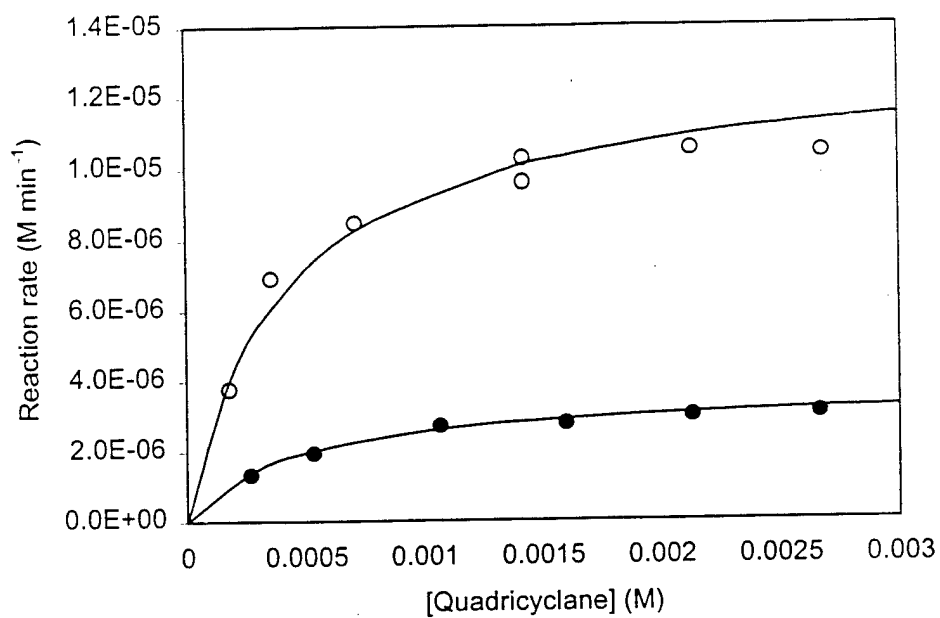


Figure 4.1. Effect of quadricyclane concentration on rate of reaction with  $\text{HOO/O}_2^-$  at pH 5 (○) and pH 8 (●). The curve shows the fitted line.

in concentration. At concentrations near the solubility limit of quadricyclane (2.8mM) (15),  $R_Q$  approaches  $P$ , the production rate, indicating that quadricyclane outcompetes natural scavengers in the solution for  $\text{HOO} \cdot / \text{O}_2^-$ . This hyperbolic relationship can be linearized by plotting  $1/R_Q$  vs.  $1/[Q]$ :

$$\frac{1}{R_Q} = \frac{1}{P} + \left( \frac{k'_{\text{sink}}}{k_Q P} \right) \frac{1}{[Q]} \quad (4)$$

In this manner, values for  $P$ , the production rate, and  $k_{\text{sink}}$  were calculated:  $P = 1.3 \times 10^{-5}$  and  $3.7 \times 10^{-6} \text{ Mmin}^{-1}$  and  $k'_{\text{sink}} = 900$  and  $122 \text{ min}^{-1}$  at pH 5 and 8 respectively.

Values from this work for  $k'_{\text{sink}}$  at pH 8 agree with literature values of  $12 - 84 \text{ min}^{-1}$  (6) while the value at pH 5 two orders of magnitude higher. Values for production rates in the irradiated humic solutions ( $3.6 \times 10^{-6} \text{ M min}^{-1}$ ) are considerably higher than those predicted for fresh waters ( $2 \times 10^{-9} - 2 \times 10^{-7} \text{ M min}^{-1}$ ) (8). However, the Aldrich solutions that were used did have a high  $[\text{DOC}] = 8.5 \text{ mgL}^{-1}$ , and there has also been some debate over the use of commercial humic solutions as a model for aquatic DOM (22). The source of commercial humic acids is often not documented and in fact, the IR spectra of such solutions resemble that of a natural peat sample. Furthermore, the Hg lamp that was used for the irradiations emits intensely at several wavelengths in the region of the spectrum where humic acids absorb light, as opposed to the more continual solar emission (23).

In Figure 4.1, the rate of reaction of quadricyclane with  $\text{HOO} \cdot / \text{O}_2^-$  appears to reach a plateau at quadricyclane concentrations of 2.1 mM. Thus, at concentrations

equal to or greater than this, the observed reaction rate of quadricyclane reflects the production rate of  $\text{HOO}/\text{O}_2^-$ . All further experiments were performed using at least this concentration of quadricyclane, allowing a comparison of production rates.

There is always some concern about possible artifacts in using such high concentrations of probe, but the shape of the curves in Figure 4.1 suggests that the kinetics for the reaction of  $\text{HOO}/\text{O}_2^-$  are being accurately described.

*Accounting for hydrolysis:*

As quadricyclane does undergo hydrolysis, control experiments were performed in order to account for possible loss of quadricyclane by this mechanism. Dark samples of quadricyclane buffered at  $\text{pHs} < 7$  exhibited observable loss and so all results were treated in order to take hydrolysis into account:



Where Q is quadricyclane, and  $k_1$ , is the second-order rate constant =  $26 \text{ M}^{-1}\text{min}^{-1}$  at  $25^\circ\text{C}$  (15). Assuming a steady  $[\text{H}^+]$  for a buffered solution, a pseudo-first order rate constant can be derived at a particular pH:

$$k' = k_1[\text{H}^+] \quad (6)$$

Since these experiments involved a Hg lamp and hence elevated solution temperatures of  $\sim 35^\circ\text{C}$ , values for  $k'$  were determined directly for each pH by measuring the extent of reaction of quadricyclane in a dark control humic solution at the same temperature, rather than using the literature values for  $25^\circ\text{C}$ . For such a sample,

$$\frac{d[Q]}{dt} = -k'[Q] \text{ and integrating over the reaction time, gives :} \quad (7)$$

$$\ln\left(\frac{[Q]_t}{[Q]_0}\right) = -k't \quad (8)$$

Once the value for  $k'$  had been determined from the dark control, the extent of reaction due to hydrolysis could be factored out of the irradiated samples.

The relevant rate equation for the reaction of quadricyclane with  $\text{HOO/O}_2^-$  including hydrolysis is:

$$\frac{d[Q]}{dt} = -k_Q[c_T][Q] - k'[Q] \quad (9)$$

At high concentrations of quadricyclane, it is assumed that all of the  $\text{HOO/O}_2^-$  radicals produced react with quadricyclane and so, for a rate of production of  $\text{HOO/O}_2^-$ ,  $P$ :

$$P = k_Q[c_T][Q] \quad (10)$$

A simplification of equation (9) is possible:

$$\frac{d[Q]}{dt} = -P - k'[Q] \quad (11)$$

Integrating this over the time period of the reaction:

$$\ln\left\{\frac{P + k'[Q]_t}{P + k'[Q]_0}\right\} = -k't \quad (12)$$

Since  $[Q]_t$  and  $[Q]_0$ , the concentrations of quadricyclane at time zero and time  $t$  are known, manipulation of this equation allows calculation of  $P$ , the production rate of  $\text{HOO/O}_2^-$ . One further note of caution is that quadricyclane does undergo general acid catalysis and so the weak acid form of the buffer could also catalyze hydrolysis.



Dark controls were tested at varying concentrations of buffers in order to test appropriate levels of buffer. Buffer concentrations of  $< 1\text{mM}$  were used as no observable contribution to hydrolysis occurred under these conditions.

#### *Variation of Production Rate with pH:*

Using high quadricyclane concentrations (2.5mM), irradiations of humic solutions were performed at pHs from 4 to 12. Figure 4.2 displays the variation in P over this pH range. The production rate of  $\text{HOO}/\text{O}_2^-$  increases noticeably at lower pHs. One explanation of this might be an effect of pH on the absorbance spectrum of humic acids.

Since the rate of a photochemical reaction follows the general form (23):

$$\text{Rate of reaction} = I_{a\lambda} \phi_{\lambda} \quad (13)$$

where  $I_{a\lambda}$  represents the amount of light absorbed and  $\phi_{\lambda}$  the quantum efficiency of the reaction.  $I_{a\lambda}$  depends on the incident light intensity and on the degree to which that light is absorbed.

If absorbance increased with decreasing pH,  $I_{a\lambda}$  and the reaction rate would also increase. However, the absorbance increases with increasing pH for this humic solution (Figure 4.3), consistent with observations of other workers (24,25). Therefore, the increase in production rate at low pH cannot be explained by net absorbance of the humic acids.

In Figure 4.2, it is apparent that there is a decrease in the apparent production rate of  $\text{HOO}/\text{O}_2^-$  over the pH range 4 - 10 with a small increase from 10 - 12. This

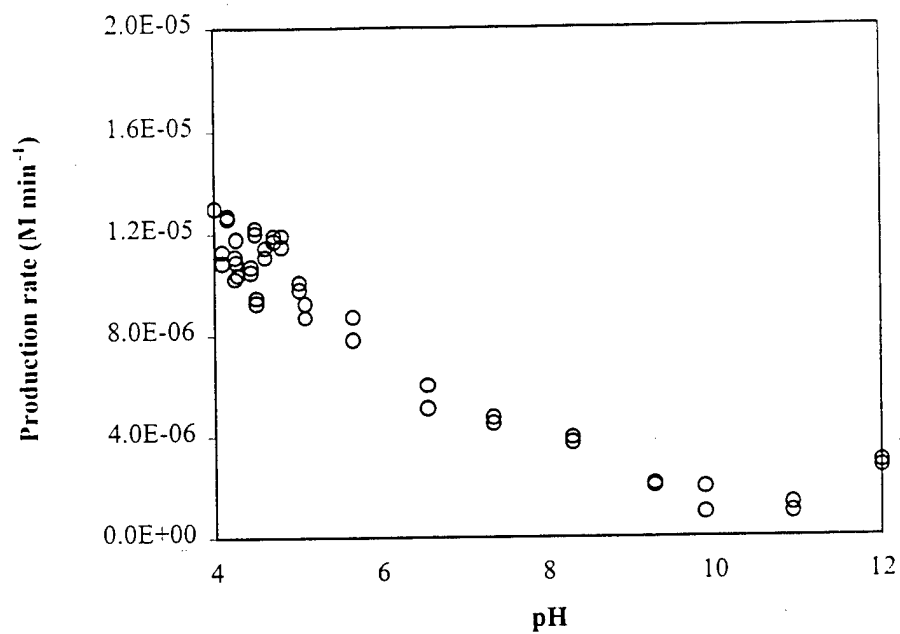


Figure 4.2. Variation of production rate of  $\text{HOO}/\text{O}_2^-$  by irradiated Aldrich humic solutions with pH.

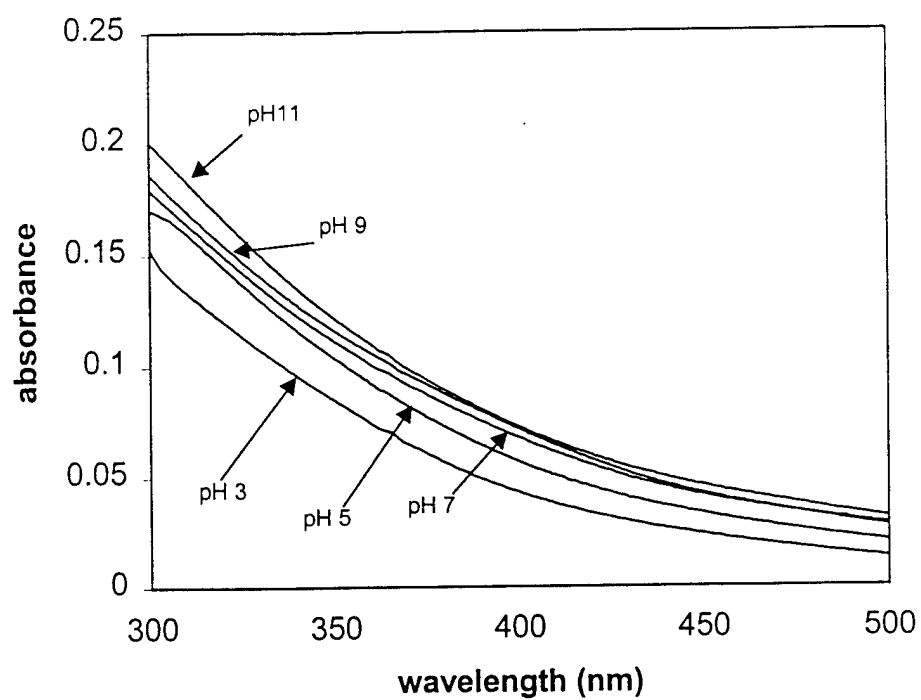
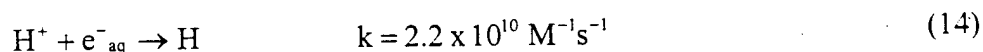


Figure 4.3. Absorbance spectra of Aldrich humic solutions ( $[\text{DOC}] = 8.5 \text{ mgL}^{-1}$ ) at pHs 3 – 11, taken in a 1cm quartz cell.

decrease is not due to the speciation of HOO and  $O_2^-$  and the significantly different rate constants for the reaction of quadricyclane with  $O_2^-$  and HOO. The experimental conditions are such that quadricyclane reacts with nearly all of the HOO  $O_2^-$  produced regardless of the pH; in effect  $k_Q[Q] \gg k'_{\text{sink}}$  in equation (1); see *competition kinetics* above. The variation of production rate is also not due to the pH dependent dismutation rate of HOO/ $O_2^-$ . Over the entire pH range studied, this reaction path does not provide a significant sink for HOO/ $O_2^-$ , given the published rate constants for this reaction (11).

The fact that the production rate increases dramatically at pHs < 6 suggests that the reaction of the hydrated electron,  $e^-_{\text{(aq)}}$ , with molecular oxygen is not an important source of HOO/ $O_2^-$ . Protons will react with  $e^-_{\text{(aq)}}$  (11):



The concentration of protons,  $[H^+]$  is high enough at pH=4 to compete with  $O_2$  (typical concentrations of 0.25 mM) for hydrated electrons produced by the photoionization of humic acids (26). This would lead to a decrease rather than the observed increase in the production rate of HOO/ $O_2^-$ .

Chloroethanol, a scavenger of hydrated electrons (4), was added at varying concentrations at pH 12 and 5.5. This high pH was chosen because the contribution of the hydrated electron reacting with molecular oxygen to produce superoxide is likely to be most significant at this pH. This is partly due to lack of competition for the hydrated electron from protons but also because at this pH, most phenolic groups within the DOM will have dissociated. Phenolic groups have been identified as a

likely source of photoejected electrons (27) and the quantum efficiency of this process increases with increased ionization. Therefore, the increase in the apparent production rate of  $\text{HOO/O}_2^-$  might be due to greater hydrated electron production. However, chloroethanol had no effect on the degradation rate of quadricyclane at either pH (Figure 4.4) suggesting that this pathway is insignificant to the overall production of  $\text{HOO/O}_2^-$ . The addition of chloroethanol has also been shown to have no effect on the amount of hydrogen peroxide produced from a humic solution (8). Since much of the  $\text{HOO/O}_2^-$  produced in an irradiated humic solution may be reduced to hydrogen peroxide, this is further evidence against hydrated electron's contribution to  $\text{HOO/O}_2^-$  formation.

As pH increases so does  $[\text{OH}^-]$  with two important effects on the photochemistry of humic acids. Inorganic anions such as  $\text{OH}^-$  can quench electron transfer reactions (24), suggesting a decreased production rate of  $\text{HOO/O}_2^-$  from electron transfer from a dissolved organic matter functionality to molecular oxygen as pH increases.



In effect, the hydroxide anion reacts with the excited singlet state of DOC before inter-system crossing (ISC) to the excited triplet state can take place, therefore reducing the possibility of reaction with  $\text{O}_2$ . However,  $[\text{OH}^-]$  increases by 6 orders of magnitude from pH 4 to 10, which should lead to a larger pH effect than that

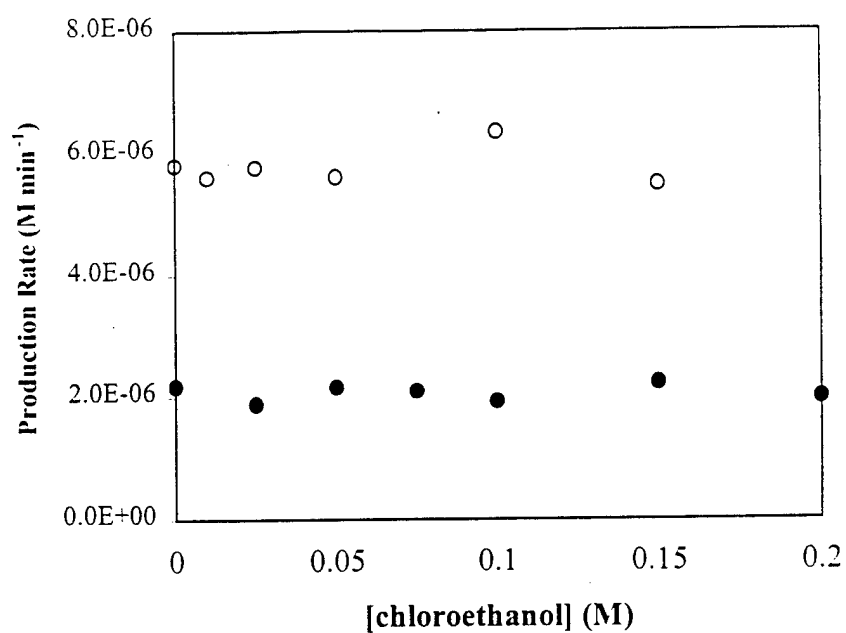


Figure 4.4. Production rate of  $\text{HOO/O}_2^-$  at pH 5.5 (○) and pH 12 (●) with varying concentration of chloroethanol. (Note that values for production rates do not match those in Figure 4.2 exactly due to slightly different experimental set-ups).

observed. Thus, it would appear that the quenching of singlet states is not the only explanation for the decrease in production rate.

Bruccoli *et al.* also observed a decrease in the energy stored in triplet states as pH increases (26). The underlying cause was assumed to be due to an increase in the internal conversion of singlets to the ground state as opposed to more rapid radiationless decay of triplet states. One explanation for the observed decrease is the changing character of the humic acids as more acidic groups deprotonate at higher pHs. This phenomenon might explain the shape of Figure 4.2 where a decrease in apparent production rates is observed at the average  $pK_a$  of carboxylic groups ( $pH=4.5$ ) and a slight increase near the phenolic  $pK_a$  ( $pH = 10$ ) (28). No justification was given as to why the deprotonated functionality might exhibit shorter lifetimes for the excited singlet state.

An alternative explanation is the changing conformation of humic acids with increasing pH. At a larger degree of deprotonation, the humic acid assumes a more extended conformation with reduced aggregation. Chromophore interactions will occur more readily in an aggregated molecule and will provide pathways for intersystem crossing and decrease radiationless decay of excited singlet states. Both of these processes will serve to increase the population of excited triplet states and thus the production of  $HOO/O_2^-$ . Variation in pH may alter not only the production rates of  $HOO/O_2^-$  but also their possible scavenging through reaction with trace metals or quinone functionalities.

Thus, it appears that the electron transfer from DOM to molecular oxygen produces the majority of  $\text{HOO}^{\cdot}/\text{O}_2^{\cdot-}$ . The pH dependence of this process is complicated not only by the complex structure of the humic acids but also by the varying speciation of scavengers of these radicals. It is clear that there are two distinct modes of transferring an electron from the DOM to a substrate. Burns *et al.* provided evidence that the reactive transient responsible for the dechlorination of the pesticide, mirex, was the hydrated electron (24). In those experiments, chloroethanol, trichloroacetate and  $\text{N}_2\text{O}$  were deployed as scavengers of the hydrated electron and a significant change in the reaction rate was noted. In this work, since 0.2 M chloroethanol did not quench the quadricyclane reaction, another mechanism must be involved.

#### References

- (1) Cooper, W.J.; Zika, R.G.; Petasne, R.G.; Plane, J.M.C. *Environ. Sci. Technol.* **1988**, 22, 1156.
- (2) Haag, W.R.; Mill, T., In Effects of Solar Ultraviolet Radiation on Biogeochemical Dynamics in Aquatic Environments; Blough, N.V.; Zepp, R.G., Eds.; Woods Hole Oceanographic Institution Technical Report, WHOI-90-09, 1990, pp.82-88.
- (3) Baxter, R.M.; Carey, J.H. *Nature*. **1983**, 306, 575.
- (4) Zepp, R.G.; Braun, A.M.; Hoigné, J.; Leenheer, J.A. *Environ. Sci. Technol.* **1987**, 21, 485.
- (5) Petasne, R.G.; Zika, R.G. *Nature*. **1987**, 325, 516.



- (6) Voelker, B.M. Preprints of Extended Abstracts. ACS. 1998.
- (7) Zafiriou, O.C.; Voelker, B.M.; Sedlak, D.L. *J. Phys. Chem.* **1998**, 102 A, 5693.
- (8) Cooper, W.J.; Zika, R.G.; Petasne, R.G.; Fischer, A.M. In *Aquatic Humic Substances: Influence on Fate and Treatment of Pollutants*; Suffett, I.H., MacCarthy, P., Eds.; Advances in Chemistry Series 219; American Chemical Society: Washington DC, 1989; pp 333-362.
- (9) Scully, N.M.; McQueen, D.J.; Lean, D.R.S.; Cooper, W.J. *Limnol. Oceanogr.* **1996**, 41, 540.
- (10) Moffett, J.W.; Zafiriou, O.C. *Limnol. Oceanogr.* **1990**, 35, 1221.
- (11) Bielski, B.H.J.; Cabelli, D.E.; Arudi, R.L. *J. Phys. Chem. Ref. Data*, **1985**, 14, 1041.
- (12) Bielski, B.H.J.; Allen, A.O. *J. Phys. Chem.* **1977**, 81, 1048.
- (13) Voelker, B.M.; Sedlak, D.L. *Mar. Chem.* **1995**, 50, 93.
- (14) Beretvas, M.K.; Hassett, J.P.; Burns, S.E. In preparation.
- (15) Hill, W.E.; Szechi, J.; Hofstee, C.; Dane, J.H. *Environ. Sci. Technol.* **1997**, 31, 651.
- (16) Butler, J.; Jayson, G.G.; Swallow, A.J. *Biochim. Biophys. Acta.* **1975**, 408, 215.
- (17) Zhou, X.; Mopper, K. *Mar. Chem.* **1990**, 30, 71.
- (18) Blough, N.V.; Zepp, R.G. In *Active Oxygen in Chemistry*; Foote, C.S.; Valentine, J.S.; Greenberg, A.; Liebman, J.F., Eds.; Blackie Academic and Professional: New York; 1995, pp 280-333.

- (19) Zafiriou, O.C.; Blough, N.V.; Micinski, E.; Dister, B.; Kieber, D.; Moffett, J. *Mar. Chem.* **1990**, *30*, 45.
- (20) Jacoby, M. *C&E News*. **1998**, 47.
- (21) Burns, S.E.; Hassett, J.P.; Rossi, M.V. *Environ. Sci. Technol.* **1996**, *30*, 2934.
- (22) MacCarthy, P.; Malcolm, R.L. In *Aquatic Humic Substances: Influence on Fate and Treatment of Pollutants*; Suffett, I.H., MacCarthy, P., Eds.; *Advances in Chemistry Series 219*; American Chemical Society: Washington DC, **1989**; pp 58-63.
- (23) Zepp, R.G. In *the Handbook of Environmental Photochemistry*; Hutzinger, O., Ed.; Springer-Verlag: New York, **1981**; Vol.2 Part B, pp 19.
- (24) Burns, S.E.; Hassett, J.P.; Rossi, M.V. *Environ. Sci. Technol.* **1997**, *31*, 1365.
- (25) Zepp, R.G.; Schlotzhauer, P.F. *Chemosphere*, **1981**, *10*, 479.
- (26) Brucoleri, A.; Pant, B.C.; Sharma, D.K.; Langford, C.H. *Environ. Sci. Technol.* **1993**, *27*, 889.
- (27) Grabner, G.; Köhler, G.; Zechner, J.; Getoff, N. *Photochem. Photobiol.* **1977**, *26*, 449.
- (28) Perdue, E.M.; Reuter, J.H.; Parrish, R.S. *Geochim. Cosmochim. Acta.* **1984**, *48*, 1257.

## Chapter 5

### Comparison of Production Rates of $\text{HOO}/\text{O}_2^-$

#### in Four Water Samples using Quadricyclane as a probe.

##### Abstract

The wavelength dependence of the production of hydroperoxy and superoxide radicals by the irradiation of four water samples was investigated. Quadricyclane was used to probe this production rate at 313, 365, 405 and 435 nm using a Hg lamp and narrow bandpass filters to isolate the emission lines. The results were compared after normalizing for differences in light attenuation and incident intensity that were specific to the sample. Since the radicals under consideration are precursors to hydrogen peroxide, the values for the apparent quantum yield were compared to literature values for  $\text{H}_2\text{O}_2$ , both in terms of consistency between samples and also variation with wavelength. The apparent quantum yields for the two species followed the same trend in variation in wavelength. The values for  $\text{HOO}/\text{O}_2^-$  were significantly higher than for  $\text{H}_2\text{O}_2$ , confirming that there are other sinks for  $\text{HOO}/\text{O}_2^-$ . For the natural water samples, there was good agreement among apparent quantum yields of  $\text{HOO}/\text{O}_2^-$ . Samples of all the waters, containing quadricyclane, were also exposed to sunlight on a rooftop over a two-week period. The production rate of  $\text{HOO}/\text{O}_2^-$  under these conditions was proportional to the attenuation coefficient of the water sample.

## Introduction

Superoxide ( $O_2^-$ ) and its conjugate acid hydroperoxy (HOO) are produced from the irradiation of DOM. This is thought to occur either through the reaction of a photoejected hydrated electron with dissolved molecular oxygen or through direct electron transfer from an excited DOM moiety (1). The apparent quantum yield for production of HOO/ $O_2^-$  decreases with increasing wavelength. This has been shown to be true for other photosensitized reactions induced by the photolysis of DOM such as production of singlet oxygen (2,3), energy transfer (3) and production of hydrogen peroxide (4).

Differences in production rates of reactive transients by assorted water samples affect the half-lives of xenobiotics contained therein. At present, neither superoxide nor hydroperoxy are considered to be important to the breakdown of any xenobiotics, but certainly, these radicals are involved in the redox cycle of transition metals such as copper and iron (5,6). A result of this is an indirect impact on steady state levels of other oxidants such as hydroxyl radical and hydrogen peroxide that are products of the redox reactions of HOO/ $O_2^-$ .

The reaction of quadricyclane, a strained cyclic hydrocarbon, with HOO/ $O_2^-$  has recently been presented (7,8). By monitoring the degradation of quadricyclane in an irradiated sample of natural water, the production rate of these radicals can be determined. If the radiant flux of the applied light and the attenuation coefficients of the water samples are known, then an apparent quantum efficiency, normalized for the absorbance of the water can be determined.

At the concentration of quadricyclane used in these experiments (2 mM), the rate of reaction with  $\text{HOO}/\text{O}_2^-$  outcompetes the other scavenging mechanisms for these radicals. This necessitates that quadricyclane be allowed to degrade only as far as this condition is still met. Another precaution that must be taken in the application of this probe for superoxide is that both the hydrolysis (9) and the possible reaction of quadricyclane with the hydroxyl radical (10) be taken into consideration. This is achieved through using dark controls and adding a hydroxyl scavenger such as methanol.

The apparent quantum yield of four water samples at four wavelengths is presented. Differences between the apparent quantum yields are related to differences between the different sources including the concentration of dissolved organic matter (DOM) as well as the pH.

Using the determined spectra (quantum yields vs.  $\lambda$ ) for different waters, it is possible to predict environmental degradation rates using published solar intensities (11). A long-term roof-top study was performed in order to compare qualitatively the degradation of quadricyclane under different pH and DOM conditions. Quadricyclane can act as an effective probe of  $\text{HOO}/\text{O}_2^-$  production in irradiated natural waters under both lab conditions and in the field.

### Experimental

**Materials:** Quadricyclane (~99%), potassium oxalate monohydrate ( $\geq 99\%$ ) and commercial humic acid, as the sodium salt, were obtained from Aldrich Chemical

Company (Milwaukee, WI). HPLC grade methanol was obtained from Allied Signal Inc. (Muskegon, MI). ACS reagent grade phenanthroline was obtained from Fisher Scientific (Pittsburgh, PA). Ferric chloride was obtained from Mallinckrodt Chemical Inc. (Paris, KY). All chemicals were used as received.

Water samples were collected during the summer of 1998 and the unfiltered samples were stored at 4°C until needed. Samples were taken from: Onondaga Lake (a eutrophic lake in Syracuse, NY), Cayuga Lake (oligotrophic Finger Lake in Central NY), and in the western portion of Lake Ontario (Laurentian Great Lake). In addition, an Aldrich humic solution was used.

All solutions were made using water purified with a Millipore 4-bowl standard system (Millipore Corp., Chicago, IL); the water had a resistivity of greater than 18M $\Omega$ cm and will henceforth be referred to as MilliQ water.

Humic acid solutions were prepared using a variation of the method of Zepp *et al.* (12). Humic material (2g) was extracted with 2L of 0.1N sodium hydroxide solutions and pressure-filtered through a 0.2 $\mu$ m capsule filter (Gelman Sciences #12117) at 4-6 psi. The filtrate was filtered again after adjustment to pH 6 with HCl. Humic acid working solutions were prepared as necessary by diluting the stock solution and using buffers to adjust the pH (13). Dissolved organic carbon (DOC) measurements were made on working humic solutions using external digestion with potassium persulfate and a Beckman Model 215A infrared analyzer.

Potassium ferrioxalate solutions for actinometry were prepared by combining 5ml each of ferric chloride (0.4M) and potassium oxalate (1.2M) and diluting to 100ml (14).

### Methods:

HPLC: A Waters (Milford, MA) HPLC system was used to analyze the quadricyclane concentration with the following components: 515 pump, 717 plus autosampler, 996 photodiode array detector, Millenium chromatography manager, a 3.9 x 150 mm Novapak C<sub>18</sub> column and a 10 $\mu$ l sample loop. An isocratic mobile phase of 90% methanol and 10% MilliQ water was pumped at a flow rate of 1ml/min and quadricyclane was monitored at 210nm.

Stock quadricyclane solutions were prepared by adding 25 $\mu$ l of quadricyclane to 100ml of the water sample, shaking the resulting mixture on a wrist-action shaker and storing the solutions at 4°C. For all experiments, the concentration of quadricyclane was related to a dark control to account for the hydrolysis of quadricyclane. In addition, solutions with added methanol (OH<sup>-</sup> scavenger) were used in order that the superoxide reaction could be isolated.

Irradiations were performed with a Hanovia 450 W medium pressure Hg lamp housed in a reflector (Ace Glass #7883-02) and powered by an Ace Glass cased power supply (#7830-60). Four 10-cm ES cylindrical quartz cells with Teflon stoppers (NSG Precision Cells, Farmingdale, NY) were irradiated simultaneously using a merry-go-round apparatus. In front of each cell was a 1-inch diameter narrow

band interference filter (CVI Laser Corp., Livermore, CA). These triple-cavity filters were centered at 313.0, 365.0, 405.0 and 435.8nm, had a FWHM of 10nm and an optical density of 4. The intensity of light was measured using ferrioxalate actinometry (15). A Spectronic® 20 Genesys™ spectrophotometer was used to monitor the absorption of the iron(II) phenanthroline complex formed at 550nm.

The pH of each of the water samples was measured with an Accumet pH meter 915 (Fisher Scientific, Springfield, NJ) and the absorption spectrum was measured with the UV-Vis spectrophotometer.

For the rooftop irradiations, the solutions were prepared in disposable 13 x 100 mm Pyrex culture tubes (Corning Inc., Corning, NY) with screw-cap vials with PTFE liners. The tubes were deployed on a rack in a circulating water bath with a mean temperature of 18°C, with the vials just below the surface. The samples were left on the roof of Baker Laboratory (State University of New York, College of Environmental Science and Forestry, Syracuse, NY) during August, 1998.

### Results and Discussion

The absorbance spectra of the water samples in 10 cm quartz cells were recorded and are shown in Figure 5.1. Values for  $\alpha_\lambda$ , the attenuation coefficients at wavelength  $\lambda$  were derived:

$$A_\lambda = \alpha_\lambda l \quad (1)$$

Where  $A_\lambda$  is the absorbance and  $l$  is the pathlength of the cell.



The fraction of light absorbed,  $F_{s\lambda}$ , at wavelength  $\lambda$ , in the 10 cm cell used during irradiations by the Hg lamp, was calculated:

$$F_{s\lambda} = 1 - 10^{-A_{\lambda}} \quad (2)$$

At the four wavelengths for which apparent quantum yields were calculated, the values of  $\alpha_{\lambda}$  and  $F_{s\lambda}$  are shown in Table 5.1.

It has been shown that quadricyclane reacts with  $\text{HOO}/\text{O}_2^-$  that is produced by the photosensitization of dissolved organic matter found in water samples. This reaction can be described:

$$\frac{dc_T}{dt} = P - k_Q[Q][c_T] - k'_{\text{sink}}[c_T] - k_{\text{dis}}[c_T]^2 \quad (3)$$

$$\frac{d[Q]}{dt} = -k_Q[Q][c_T] \quad (4)$$

$$c_T = [\text{O}_2^-] + [\text{HOO}] \quad (5)$$

where  $[Q]$  is the concentration of quadricyclane,  $k_Q$  is the rate constant for the reaction of quadricyclane with  $\text{HOO}/\text{O}_2^-$ ,  $k_{\text{dis}}$  is the rate constant for the dismutation of  $\text{HOO}/\text{O}_2^-$  and  $k'_{\text{sink}}$  is the pseudo-first order rate constant for all other reaction pathways of  $\text{HOO}/\text{O}_2^-$ . Values for  $k_{\text{dis}}$  (16) and  $k_Q$  (1) and estimates of  $k'_{\text{sink}}$  (17) are

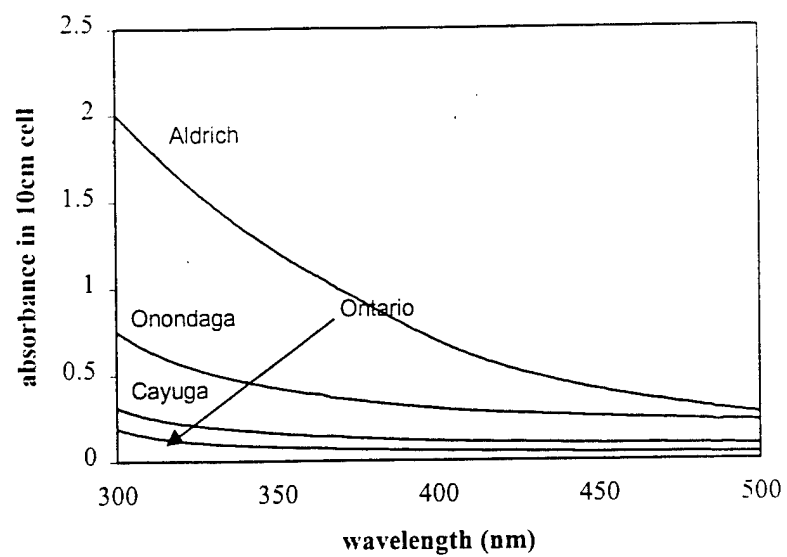


Figure 5.1. Absorbance spectra of Onondaga Lake, Cayuga Lake, Lake Ontario water and a  $8.5\text{mgL}^{-1}$  [DOC] Aldrich humic acid solution. The spectra are taken in 10cm quartz cells.

Table 5.1. Attenuation coefficients ( $\alpha_\lambda$ ) and fraction of light absorbed ( $F_{s\lambda}$ ) in a 10cm cell for different water samples.

$\lambda$ (nm)	Aldrich		Onondaga		Cayuga		Ontario	
	$\alpha_\lambda$	$F_{s\lambda}$	$\alpha_\lambda$	$F_{s\lambda}$	$\alpha_\lambda$	$F_{s\lambda}$	$\alpha_\lambda$	$F_{s\lambda}$
313	0.1767	0.983	0.0619	0.760	0.0243	0.428	0.0134	0.265
365	0.1045	0.910	0.0377	0.580	0.0143	0.281	0.0072	0.153
405	0.0652	0.777	0.0295	0.493	0.0112	0.227	0.0055	0.119
435	0.047	0.661	0.0264	0.455	0.0101	0.207	0.0048	0.105

known and all experiments were performed with quadricyclane concentrations > 2mM in order that the only significant reaction of  $\text{HOO/O}_2^-$  was with quadricyclane.

For instance, at pH = 7.48,

$k_Q = 2.76 \times 10^5 \text{ M}^{-1}\text{min}^{-1}$ ,  $k_{\text{dis}} = 1.19 \times 10^7 \text{ M}^{-1}\text{min}^{-1}$ ,  $k'_{\text{sink}} < 1 \times 10^2 \text{ min}^{-1}$  and  $c_T \sim \text{nM}$ .

As a result, the rate of reaction of quadricyclane is assumed to be equal to the rate of production of  $\text{HOO/O}_2^-$ :

$$\frac{-d[Q]}{dt} = P \quad (6)$$

The rate of production of  $\text{HOO/O}_2^-$  can also be defined in terms of the incident light.

The rate of light absorption,  $I_{a,\lambda}$ , by the sensitizer can be described in the typical manner:

$$I_{a,\lambda} = I_\lambda F_{s,\lambda} F_{c,\lambda} \quad (7)$$

$F_{s,\lambda}$  = fraction of light absorbed by the entire system =  $1 - 10^{-\alpha_\lambda l}$

$I_\lambda$  = incident light intensity in einstein per liter per minute.

$F_{c,\lambda}$  = fraction of light absorbed by the system that is absorbed by a particular sensitizer.

Finally, the rate of production of  $\text{HOO/O}_2^-$  is defined in terms of the apparent quantum yield,  $\phi'_\lambda$ , a function of the fraction of light absorbed by the sensitizer responsible for the production of  $\text{HOO/O}_2^-$  ( $F_{c,\lambda}$ ), and the quantum efficiency of this reaction, ( $\phi_\lambda$ ). Since neither of these terms could be measured, only  $\phi'_\lambda$  could be determined:

$$P_\lambda = \frac{-d[Q]}{dt} = I_{a,\lambda} \phi'_\lambda = I_\lambda (1 - 10^{-\alpha_\lambda l}) \phi'_\lambda \quad (8)$$

And so the apparent quantum yield,  $\phi'_{\lambda}$ :

$$\phi'_{\lambda} = \frac{d[Q]}{dt} \cdot \frac{1}{I_{\lambda}(1 - 10^{-a_{\lambda}})} \quad (9)$$

The variation of  $\phi'_{\lambda}$  with  $\lambda$  is shown in Figure 5.2. In all four water samples,  $\phi'_{\lambda}$  decreases as  $\lambda$  increases with the one exception of the value of  $\phi'_{405}$  for the Aldrich solution. The values of  $\phi'_{\lambda}$  are similar for Cayuga and Ontario, both oligotrophic lakes, with long hydraulic residence times - 12 and 6 years respectively (18,19). In contrast, Onondaga Lake which has higher values of  $\phi'_{\lambda}$ , has a hydraulic residence time of approximately three years (20).

In order to compare the values for different waters, it is necessary to consider why  $\phi'_{\lambda}$  may vary. The simplified treatment of the light-induced production of  $\text{HOO/O}_2^-$  treats the DOM as one entity. As such, the light absorbed by the chromophoric DOM is considered to be the crucial parameter in normalizing between different samples. However, in all likelihood, there are multiple functionalities within the DOM that are directly responsible for the production of  $\text{HOO/O}_2^-$ ; it has been suggested that quinone moieties might be involved (21). It would be more appropriate to factor out the fraction of light absorbed by the actual photosensitizing fraction ( $F_{c,\lambda}$ ) of the chromophoric DOM. Zepp *et al.* developed the necessary theory to describe this process in his description of response functions for singlet oxygen production (2) as well as energy transfer reactions (3), assuming a single sensitizing fraction. A true description of the kinetics may be written:

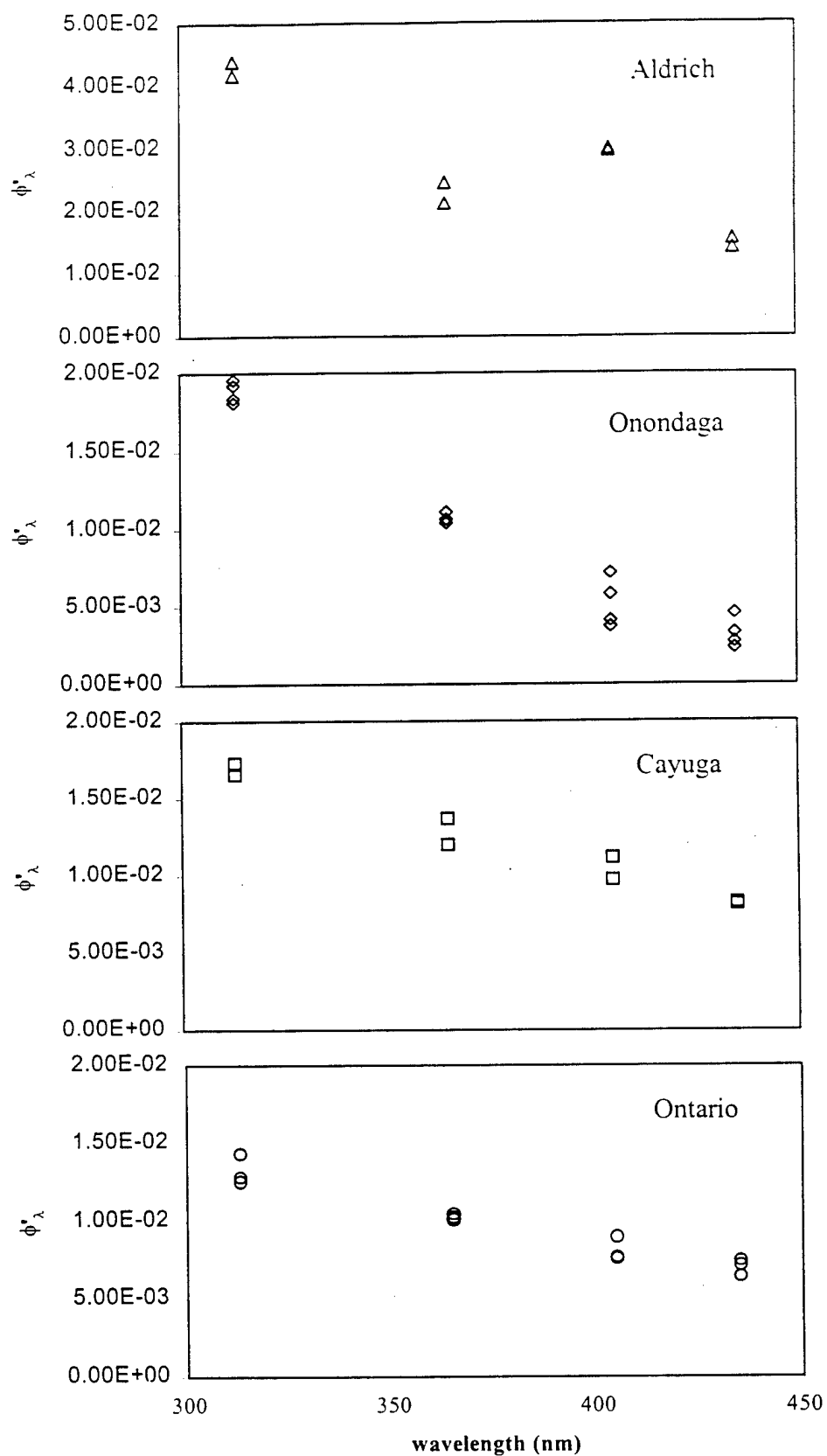


Figure 5.2. Plots of apparent quantum yield of  $\text{HOO}/\text{O}_2^-$  production from irradiated samples of (a) Aldrich, (b) Onondaga Lake, (c) Cayuga Lake and (d) Lake Ontario water.

$$P_{\lambda} = I_{\lambda} F_{s,\lambda} \sum_i F_{c,\lambda,i} \phi'_{\lambda,i} = I_{\lambda} F_{s,\lambda} \phi'_{\lambda} \quad (10)$$

where the contributions of each of the sensitizing fractions,  $i$ , are summed up to equal the apparent quantum yield. For this reason, discrepancies between  $\phi'_{\lambda}$  are expected for different waters because of the varied nature of DOM. The proportion of a certain photosensitizing fraction will vary although its individual quantum yield for production of  $\text{HOO}/\text{O}_2^-$  will not. This argument offers a reasonable explanation for why the values of  $\phi'_{\lambda}$  are similar for the two most similar lakes in this study; they have similar compositions. Furthermore, there has been some debate over the appropriateness of the use of commercial humic acids such as Aldrich humic salts because of the distinct chemical composition and source of the material; their IR spectrum most resemble a natural peat sample (22). It can be seen that the values of  $\phi'_{\lambda}$  are particularly high for the Aldrich samples. Another reason for this may be prior exposure to sunlight. Dissolved organic matter in lake water is altered in structure over the course of summer due to photobleaching (23). Lake water samples in this study were collected from the epilimnion in July, while the Aldrich humic acids had not been previously exposed to light.

There is one final cause for discrepancy in the apparent quantum yields derived above. The pH of the samples varies as 7.63, 8.16, 8.34, and 8.03 for Aldrich, Onondaga, Cayuga and Ontario respectively. A study of the pH dependence of the production of  $\text{HOO}/\text{O}_2^-$  shows a decrease of approximately 10% in the production rate over the pH range 7.63 to 8.34 (8). This suggests slightly higher

values for  $\phi'_{\lambda}$  for the Aldrich solution compared to the others, but not of the observed magnitude.

Similar studies have been performed for hydrogen peroxide ( $\text{H}_2\text{O}_2$ ) where a comparison was made between the effective quantum yields of  $\text{H}_2\text{O}_2$  production in different waters (4,24). These studies also suggested that a normalization of the production rates by accounting for attenuation effects did not account for the different reaction rates of the samples. There was variation by up to a factor of 4 in the value of  $\phi'_{\lambda}$  in the waters studied by Scully *et al.* and by Cooper *et al.*; our results show similar variation.

A direct comparison of  $\phi'_{\lambda}$  for  $\text{H}_2\text{O}_2$  and  $\text{HOO}/\text{O}_2^-$  is appropriate as  $\text{HOO}/\text{O}_2^-$  is a precursor to  $\text{H}_2\text{O}_2$  in natural water bodies (25):



In general, the values that were determined here for  $\phi'_{\lambda}$  ( $\text{HOO}/\text{O}_2^-$ ) were up to ten times as high as those for  $\phi'_{\lambda}$  ( $\text{H}_2\text{O}_2$ ). Some of this discrepancy is explained by the existence of other reaction pathways for  $\text{HOO}/\text{O}_2^-$ . Equation (11) describes the disproportionation of hydroperoxy and superoxide radicals. In addition,  $\text{HOO}/\text{O}_2^-$  can be reduced by transition metals such as Cu(I) (5) and Fe(II) (6) as well as by semiquinone radicals (26) to form  $\text{H}_2\text{O}_2$ . However,  $\text{HOO}/\text{O}_2^-$  can also undergo oxidation through reaction with transition metals in a higher oxidation state or with quinones to form oxygen. Therefore, not all of the  $\text{HOO}/\text{O}_2^-$  that is produced will produce  $\text{H}_2\text{O}_2$  and the relationship between the two formation rates is a complex function of the composition of the water. Petasne and Zika deduced differences of



approximately a factor of three between the production rates for  $\text{HOO O}_2^-$  and for  $\text{H}_2\text{O}_2$  for marine samples (27).

Solutions of quadricyclane (2.13 mM) in each of the different waters were exposed to natural sunlight for a long-term study. The degradation of quadricyclane in each solution is shown in Figure 5.3. The extent of reaction of quadricyclane followed the expected order, based on the derived values of  $F_{s,\lambda}$  and  $\phi'_\lambda$ : Aldrich > Onondaga > Cayuga > Ontario. The light to which the samples were exposed was the same; the difference in rate is attributed to the differing amounts of light absorbed as well as to the relative proportion of sensitizing fraction of DOM.

Previous workers have studied the variation of production rate of  $\text{H}_2\text{O}_2$  with attenuation coefficient at 313nm and found a linear relationship (4). With the limited number of lakes in this study, a ratio of production rate to  $\alpha_{313}$  was used as an alternative to a plot. The Cayuga and Ontario Lake waters agree well in this respect with values of  $8 \times 10^{-7}$  and  $9 \times 10^{-7}$  respectively. In these experiments, the lake water solutions were optically thin as the deployment cells had an effective pathlength of 1.12 cm. In this case, a simplification can be applied to the fraction of light absorbed:

$$F_{s,\lambda} = 1 - 10^{-\alpha_\lambda l} \sim 2.303\alpha_\lambda l \quad (12)$$

Therefore, the fraction of light absorbed is proportional to the attenuation coefficient.

Assuming a consistent value for  $\phi'_\lambda$  for these lake waters, the rate of production of  $\text{HOO/O}_2^-$  will be proportional to  $\alpha_\lambda$ . The fact that Cayuga and Ontario had similar values for this ratio implies similar  $\phi'_\lambda$  whereas the ratio for Onondaga Lake water

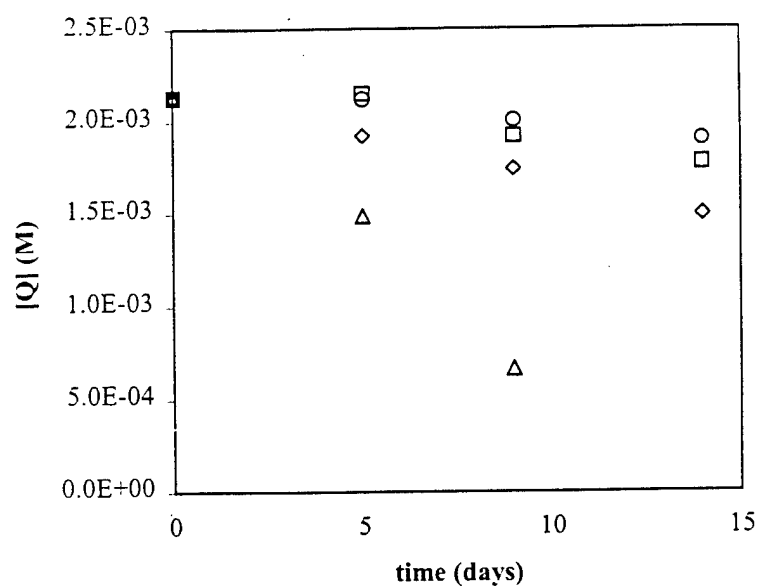


Figure 5.3. Degradation of quadricyclane in (Δ) Aldrich, (◇) Onondaga, (□) Cayuga, (●) Ontario water during a rooftop irradiation in the summer of 1998.

was  $5 \times 10^{-7}$ , suggesting a higher value for the apparent quantum yield of production of  $\text{HOO}/\text{O}_2^-$ .

Figure 5.4 shows the relative significance of different wavelengths to the overall production of  $\text{HOO}/\text{O}_2^-$  in the top 1cm of a lake. This was modeled using the experimentally determined values for  $\phi'_\lambda$  and  $F_{s\lambda}$  for each of the lakes in combination with solar spectral irradiation data recorded at noon in August 1998 in Syracuse, NY. Peak production occurs in the UV-A portion of the spectrum, but visible light is also important to the process. This is because even though the apparent quantum yield is lower in the visible region, sunlight intensity is higher.

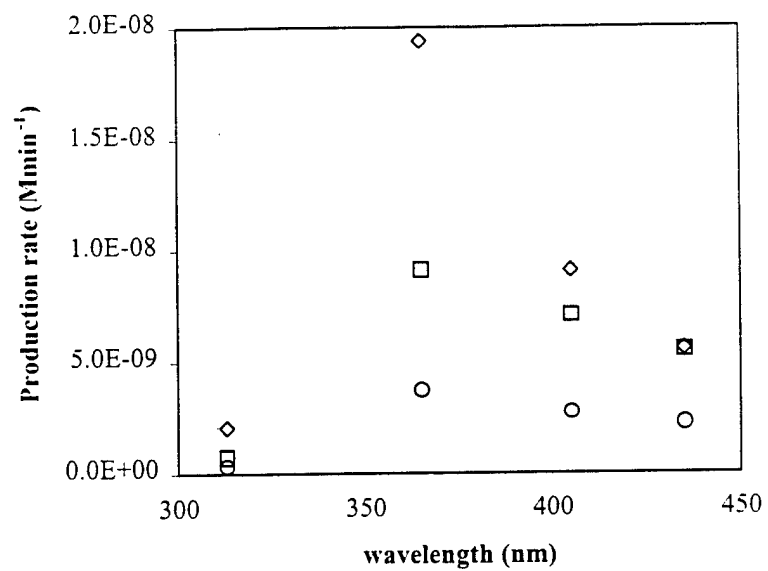


Figure 5.4. Wavelength dependence of modeled production rates of  $\text{HOO}/\text{O}_2^-$  for ( $\diamond$ ) Onondaga, ( $\square$ ) Cayuga, ( $\circ$ ) Ontario water using solar irradiation data for summer noon-time sun in Syracuse, NY.

# References:

1. Haag, W.R.; Mill, T., In Effects of Solar Ultraviolet Radiation on Biogeochemical Dynamics in Aquatic Environments; Blough, N.V.; Zepp, R.G., Eds.; Woods Hole Oceanographic Institution Technical Report, WHOI-90-09, 1990, pp 82 – 88.
2. Zepp, R.G.; Baugham, G.L.; Schlotzhauer, P.F. *Chemosphere*, **1981**, 10, 119.
3. Zepp, R.G.; Schlotzhauer, P.F.; Merritt Sink, R. *Environ. Sci. Technol.* **1985**, 19, 74.
4. Scully, N.M.; McQueen, D.J.; Lean, D.R.S.; Cooper, W.J. *Limnol. Oceanogr.* **1996**, 41, 540.
5. Zafiriou, O.C.; Voelker, B.M.; Sedlak, D.L. *J. Phys. Chem.* **1998**, 102, 5693.
6. Voelker, B.M.; Sedlak, D.L. *Mar. Chem.* **1995**, 50, 93.
7. Beretvas, M.K.; Hassett, J.P.; Burns, S.E. In preparation.
8. Beretvas, M.K.; Hassett, J.P. Basford, T.M. In preparation.
9. Hill, W.E.; Szechi, J.; Hofstee, C.; Dane, J.H. *Environ. Sci. Technol.* **1997**, 31, 651.
10. Burns, S.E. Personal communication.
11. Zepp, R.G.; Cline, D.M. *Environ. Sci. Technol.* **1977**, 11, 359.
12. Zepp, R.G.; Braun, A.M.; Hoigné, J.; Leenheer, J.A. *Environ. Sci. Technol.* **1987**, 21, 485.
13. Burns, S.E.; Hassett, J.P.; Rossi, M.V. *Environ. Sci. Technol.* **1996**, 30, 2934.

14. Murov, S.L. *Handbook of Photochemistry*; Dekker, M., Ed.; Wiley: New York, 1973.
15. Hatchard, C.G.; Parker, C.A. *Proc. Roy. Soc. (London)* **1956**, A235, 518.
16. Bielski, B.H.J.; Cabelli, D.E.; Arudi, R.L. *J. Phys. Chem. Ref. Data*, **1985**, 14, 1041.
17. Voelker, B.M. Preprints of Extended Abstracts, ACS, 1988.
18. Bloomfield, J.A. *Lakes of New York State, Volume 1: Ecology of the Finger Lakes*, Academic Press: New York, 1978.
19. The Great Lakes, An Environmental Atlas and Resource Book, 1988.
20. Effler, S.W.; Whitehead, K.A. In *Limnological and Engineering Analysis of a Polluted Urban Lake*; Effler, S.W., Ed.; Springer, New York, 1996; pp 97.
21. Baxter, R.M.; Carey, J.H. *Nature*, **1983**, 306, 575.
22. MacCarthy, P.; Malcolm, R.L. In *Aquatic Humic Substances: Influence on Fate and Treatment of Pollutants*; Suffett, I.H., MacCarthy, P., Eds.; Advances in Chemistry Series 219; American Chemical Society: Washington DC, 1989; pp 58-63.
23. Gao, H.; Zepp, R.G.; *Environ. Sci. Technol.* **1998**, 32, 2940.
24. Cooper, W.J.; Zika, R.G.; Petasne, R.G.; Plane, J.M.C. *Environ. Sci. Technol.* **1988**, 22, 1156.
25. Moffett, J.W.; Zafiriou, O.C. *Limnol. Oceanogr.* **1990**, 35, 1221.
26. Jacoby, M. *C&EN*, **1998**, 47.
27. Petasne, R.G.; Zika, R.G. *Nature*, **1987**, 325, 516.

## Conclusions

The photochemistry of two novel compounds was investigated with the purpose of describing their environmental fate in the case of a spill. Results derived thereof allowed alternate applications for both ammonium dinitramide and quadricyclane.

ADN could serve as an actinometer for light of wavelength up to 400nm. Advantages to its use are ease of detection, high solubility and stability. Possible drawbacks are high quantum yields (*circa* 0.1) and high absorptivity, dictating rapid reaction. Its slow degradation at depths greater than 1 m indicates that ADN is most suited to measure attenuated light at depth.

The indirect photolysis of quadricyclane is ascribed to the reaction with  $\text{HOO/O}_2^-$  produced by the interaction of excited DOM with dissolved oxygen. The basis for this conclusion is the reaction of quadricyclane with  $\text{HOO/O}_2^-$  produced through an alternative means. The retarded reduction of ferricytochrome in the presence of quadricyclane provides reliable results for the rate constant,  $k_Q$ . The variation of  $k_Q$  with pH supports the hypothesis that quadricyclane reacts with  $\text{HOO/O}_2^-$ . Furthermore, the simultaneous measurement of  $\text{HOO/O}_2^-$  production in an irradiated humic solution by ferricytochrome C and quadricyclane provides compelling evidence that quadricyclane is reacting with  $\text{HOO/O}_2^-$  in humic solutions.

However, at the high concentration of quadricyclane that is used, there are possible artifacts. For instance, at that level (2.5mM), quadricyclane may be reacting with all of the  $\text{HOO/O}_2^-$  as soon as it is formed, but an alternative mechanism may be

feasible at lower quadricyclane concentrations. The  $\text{HOO O}_2^-$  could react with other substrates, forming other reactive radicals (e.g. organic peroxy radicals) which could then react with quadricyclane. However, for the purposes of measuring  $\text{HOO O}_2^-$  production, using high concentrations of quadricyclane is effective.

Ideally, a similar study could be performed using lower concentrations of quadricyclane. This would serve to clarify the reaction chemistry of  $\text{HOO/O}_2^-$  in the situation where quadricyclane did not perturb the steady state. In such a case, quadricyclane could be deployed as a probe of the steady state concentration. In order to do this, an alternative analytical technique would be used; for example, GC-FID would certainly detect much lower concentrations of quadricyclane.

The wide range of detectable concentrations of quadricyclane adds to the appeal of this probe. The possible drawbacks (hydrolysis, reaction with  $\text{OH}$ ) have been described in the manuscripts and can easily be circumvented.

A study of the photochemistry of these two compounds has provided insight into some fundamental concepts. The extent of photolysis of ADN at different depths is directly related to the passage of light of different wavelengths through the water column. The apparent quantum yields for the production of  $\text{HOO/O}_2^-$  varies for different water samples and is related to the DOM composition. As it turns out, photolysis does indeed provide an important sink for both of these compounds, especially in shallow waters.



### Appendix 1

Values of extinction coefficient, quantum yield and associated margin of error for ADN for wavelengths 285 – 400 nm.

Wavelength (nm)	Extinction coefficient ( $M^{-1}cm^{-1}$ )	Quantum yield	Margin of error (95% C.I.)
280	5020	0.119	0.004
285	5150	0.104	0.003
290	4944	0.0955	0.004
295	4434	0.0832	0.005
300	3765	0.082	0.005
305	3184	0.0893	0.004
310	2793	0.0798	0.005
315	2562	0.0814	0.004
320	2431	0.0915	0.005
325	2321	0.0914	0.006
330	2193	0.0866	0.004
335	2032	0.101	0.005
340	1833	0.0977	0.005
345	1601	0.110	0.005
350	1341	0.113	0.005
355	1071	0.106	0.004
360	819.3	0.108	0.005
365	602.5	0.120	0.0055
370	398.0	0.102	0.0055
375	259.5	0.120	0.006
380	159.9	0.148	0.006
385	97.3	0.168	0.0065
390	55.6	0.130	0.008
395	31.2	0.104	0.01
400	17.1	0.086	0.01